Fall 2013

Dimensionless Criteria for Selecting Tidally-Influenced Advective-Dispersive Desalination Brine Mixing Plume Characterization Models

Alireza Shahvari
Old Dominion University

DIMENSIONLESS CRITERIA FOR SELECTING TIDALLY-INFLUENCED ADVECTIVE-DISPERSIVE DESALINATION BRINE MIXING PLUME CHARACTERIZATION MODELS

by

Alireza Shahvari
B.S. June 2004, Shiraz University
M.S. June 2007, Shiraz University

A Dissertation Submitted to the Faculties of Old Dominion University
in Partial Fulfillment of the Requirements for the Degree of

DOCTOR OF PHILOSOPHY

CIVIL/ENVIRONMENTAL ENGINEERING

Fall 2013

Approved by:

Jaewan Yoon (Director)

Yaohang Li (Member)

Gangfeng Ma (Member)

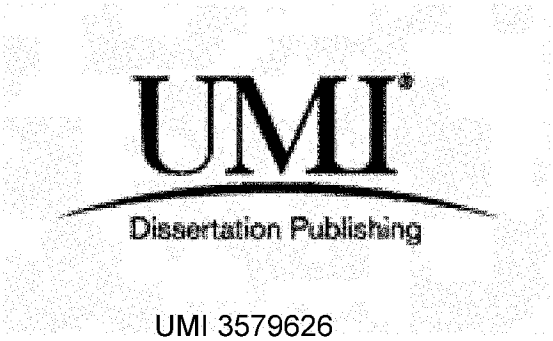

ProQuest LLC
789 East Eisenhower Parkway
P.O. Box 1346
Ann Arbor, MI 48106-1346

ABSTRACT

DIMENSIONLESS CRITERIA FOR SELECTING TIDALLY-INFLUENCED ADVECTIVE-DISPERSIVE DESALINATION BRINE MIXING PLUME CHARACTERIZATION MODELS

Alireza Shahvari
Old Dominion University, 2013
Director: Dr. Jaewan Yoon

The very nature of requirements for implementing a desalination process is highly spatial due to the need to secure both a source for the operation and sink for brine dilution. Thus, the applicable coastal location is bound to natural tidal mixing characteristics and subjected to a near- or a far-field availability for source and sink. Mixing characteristics of coastal waters are very different from one point to another due to the spatiotemporal tidal characteristic in loco in a manner that it can vary from being highly advective to completely dispersive dominant. Once a location is identified, estimation of corresponding water availability and demand and resultant adjective-dispersive mixing plume from desalination need to be evaluated. In this study, two different models, the steady-state Finite Segment Method (FSM) and the time-variant Analytical Method (AM), are proposed to simulate the brine plume dispersion process along with the tidally influenced flow with sloping seabed in near- and far-fields. Oscillating flow and flow reversals are also considered in the models using a harmonic function to reflect directional tidal currents. To select the most applicable model for a given site, a non-dimensional number for describing the in loco stability of advective-dispersive flux, the Shahvari-Yoon (SY) number, is proposed in this study to determine the range of applicability of FSM and AM models. Results from several comparative case studies of two implemented models indicate that the AM model can be applied for any SY number range of advective or advective-dispersive or dispersive dominant coastal region whereas the FSM model is found effective for a SY range equal to or less than zero which represents the advective or advective-dispersive dominant coastal region.

ACKNOWLEDGEMENTS

I would never have been able to finish my dissertation without the guidance of my committee members, help from friends, and support from my family.

I would like to express my deepest gratitude to my advisor Dr. Jaewan Yoon, a gracious mentor who demonstrates that rigorous scholarship can and must be accessible to everyone, that social change is central to intellectual work and, as such, scholars have a responsibility to use the privileges of academia to imagine and create a better world.

I would like to thank my committee members and professors, Dr. David Basco, Dr. Yaohang Li, Dr. Gangfeng Ma, Dr. Mujde Unal, and Dr. Seshadri Iyer, for guiding my research and for their encouraging words, thoughtful criticism, time and attention during busy semesters, and for helping me to develop my background to accomplish this research. My research would not have been possible without their help.

I would like to thank Mike Duffs who was always willing to help and gives his best suggestions.

And finally, I would also like to thank my lovely wife, Iris, my lovely parents, Reza and Azam, and my dearest sisters, Yalda and Negar, for their love, support and understanding during the long years of my education.

TABLE OF CONTENTS

Chapter page

LIST OF FIGURES

Figure page

Figure page

Figure page

LIST OF TABLES

Table page

Table

page

CHAPTER 1

SEAWATER DESALINATION PLANT AND THE ENVIRONMENTAL IMPACT OF BRINE DISCHARGE ON COASTAL WATERS

1-1- Introduction

In some arid regions seawater is the only reliable source of potable and agricultural water due to the lack of significant precipitation. In these areas, groundwater often contains high levels of salinity due to seawater intrusion and does not meet drinking water quality standards. Even if the groundwater is of quality, sources are very limited and unreliable due to extensive extraction of coastal aquifers in recent years due to rapid growth of cities and industry. As a result, desalination is usually the only feasible solution for meeting quality standards and required quantities for local citizens. To meet the expanding demands for drinking water, desalination plants have been constructed in many coastal locations around the world. In order to minimize the costs of conveying source and treated waters, it is standard practice to build desalination plants adjacent to coastlines. Furthermore, for large desalination operations with the capacity of 25 million gallons per day (MGD) and higher, it is absolutely optimal to discharge their concentrate waste back into the sea via outfalls at some distance from the beach [1].

Many industrialized and developing countries, however, have lately started to use desalination as a technique to increase and augment their water supply options. Desalinated water has become a commodity for these countries in order to satisfy the

increasing demand for water. For the pioneering countries, the driving factors were often a lack of surface waters and groundwater coupled with sufficient natural or economic resources to engage in energy-intensive and costly desalination projects. For the newly emerging desalination markets, driving factors are more diverse and multifaceted financial and demographic growth, development, droughts and climate change, or decreasing conventional water resources in terms of quality and quantity due to overuse and pollution. Moreover, as conventional water production costs have been rising in. many parts of the world and the costs of desalination, particularly seawater desalination, have been decreasing over the years, desalination has also become economically more competitive [14].

The combined capacity of all desalination plants worldwide increased by 30% from 28 million m^3 per day in 2007 to 36.4 million m^3 per day in 2009. While thermal distillation plants predominate in the Middle East, seawater reverse osmosis (SWRO) is the preferred process in many other countries. Desalination has become an increasingly feasible option to supplement the water supply for many coastal cities due to significant development in relevant methods and reduced costs of implementation and operation. The size of desalination plants has also grown noticeably over the years [5].

Meanwhile, the possible environmental impact caused by brine discharge into coastal waters has drawn growing consideration from government agencies and the desalination industry. The impact of brine discharge on coastal and marine environments is still generally unknown; however, it is commonly thought that the brines discharged must eventually be mixed and transported into the coastal waters to minimize sudden

shock to the receiving body of water. Thus, it is very important to recognize the optimum site location of water intakes and outfalls for desalination plants [2].

1-2- Desalination Technology and Reverse Osmosis (RO)

At this time, most seawater reverse osmosis (SWRO) desalination plants have the following key components:

1. Intake to collect seawater as the source of desalination process,
2. Pretreatment system to remove solid particulates from the seawater,
3. Reverse osmosis system to produce fresh water by isolating the salts from the seawater and permeate,
4. Post-treatment section to form fresh water for transmission and final use.

The main waste created by the desalination plant's salt isolation process is usually referred to as brine or concentrate. Along with concentrate, the discharge of the desalination plant may also contain other treatment procedure side-streams, such as spent pretreatment SWRO membrane rinsing water, filter backwash water, and treated membrane cleaning water (Fig. 1-1).

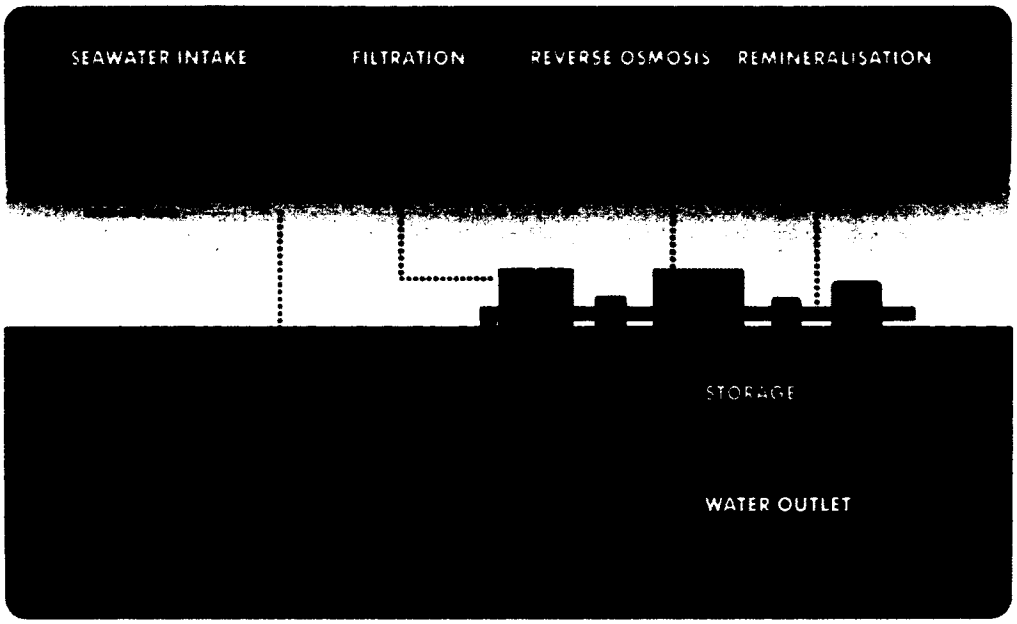

Fig. 1-1. Typical Discharge Components of Seawater Desalination Plant [19]

The resultant brine contains dissolved compounds (organic particles, minerals, metals, etc.) rejected by the reverse osmosis membranes. Backwash water is produced during the periodic cleaning of the pretreatment filters and consists of particles and other compounds removed from the source seawater. Brine and backwash water are first combined and then safely discharged to the coastal waters using outlets and a diffuser. Ocean currents with oscillating flow dilute the brine quite rapidly. [3]

The brine normally creates 90 to 95 percent of the entire brine discharge volume. This byproduct of the seawater isolation process consists of minerals and other substances eliminated from the pretreated source seawater. The percentage of the total volume of seawater converted into fresh water is referred to as desalination plant recovery. SWRO desalination plants are typically designed to recover 45 to 55 percent of

the seawater as fresh water. For example, a plant operating at 50% recovery needs two gallons of seawater to produce one gallon of potable water and one gallon of brine. The recovery of the source water will control how concentrated the final byproduct is. The recovery ratio, R, is defined as [13]:

$$R = \frac{Q_p}{Q_C + Q_F}$$

Eq. (1.1)

where Q_p represents the freshwater flow rate, Q_F is the seawater flow rate and Q_C is the brine waste flow rate [13].

The recovery rate varies based on the membrane process, and specifically is a function of the number of membrane elements in each vessel. Recovery rate of a desalination plant depends on many factors such as the number of membrane passes and stages per pass, the type of membrane used, and the quality of the final permeate [17]. With lower levels of total dissolved solids (TDS), brackish water systems are able to achieve higher recovery rates, as the brine is able to reach higher concentration levels. Brackish water desalination plants can achieve recoveries of between 40 to 65 percent which is approximately 10 percent higher than the average of seawater desalination plants [35].

Once the recovery rate is known, the TDS of the brine can be calculated using the following formula [13]:

$$TDS_{concentrate} = TDS_{feed}\left(\frac{1}{1-R}\right) - \frac{R \times TDS_{permeate}}{100(1-R)}.$$

Eq. (1.2)

In most cases the value of $TDS_{permeate}$ is very low and, consequently, can be estimated as zero; the above equation becomes [13]:

$$TDS_{concentrate} = TDS_{feed}\left(\frac{1}{1-R}\right).$$

Eq. (1.3)

The concentration factor, CF, of the brine, the ratio of the concentrate and feed concentrations can also be calculated [13]:

$$CF = \frac{TDS_{concentrate}}{TDS_{feed}} = \frac{1}{1-R}.$$

Eq. (1.4)

Using this formula, an operational throughput of a desalination plant can be designed. For example, a plant operating at a recovery ratio of 90% will have a concentration factor of 10. Fig. 1-2 shows the design chart which can assist the designer in determining the filter specifications as a function of ambient salinity and ideal recovery rate of the plant. For example for a location with ambient salinity of 32 Practical Salinity Units (PSU) and 55 PSU of desired brine concentration, the recovery rate is around 42%, and the designer should design the pressure cells to achieve 42% recovery rate [13].

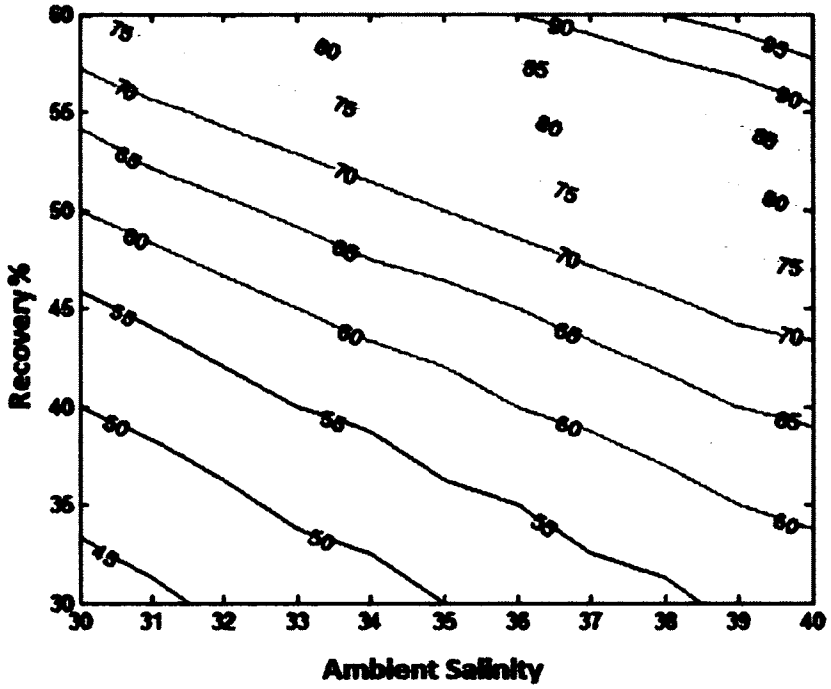

Fig. 1-2. Concentrate Salinity with Respect to Ambient Salinity and Recovery Rate of the Desalination Plant [13]

In terms of brine management, the design process often seeks to minimize the discharge volume and maximize the recovery rate. The more water that is removed, the smaller the volume of brine but the greater salinity becomes. This adjustment between concentration factor and recovery rate is shown in Fig. 1-3. As the figure shows, there is a sharp increase in the concentration factor as recovery rate approaches 100%; however, the volume of concentrate relative to the volume of source water decreases linearly [13].

In terms of brine management, some choices are more appropriate for disposing low volume and high concentration, while others are better suited to high volume with lower concentration. Eventually there is a relationship between the desalination performance and disposal suitability. Desalination plants with large recovery rates that

produce more concentrated brine must have the means to dispose of this concentrate in a safe and environmentally friendly manner. When suitable concentrate management is not achievable, the recovery efficiency of a plant may need to be adjusted [13].

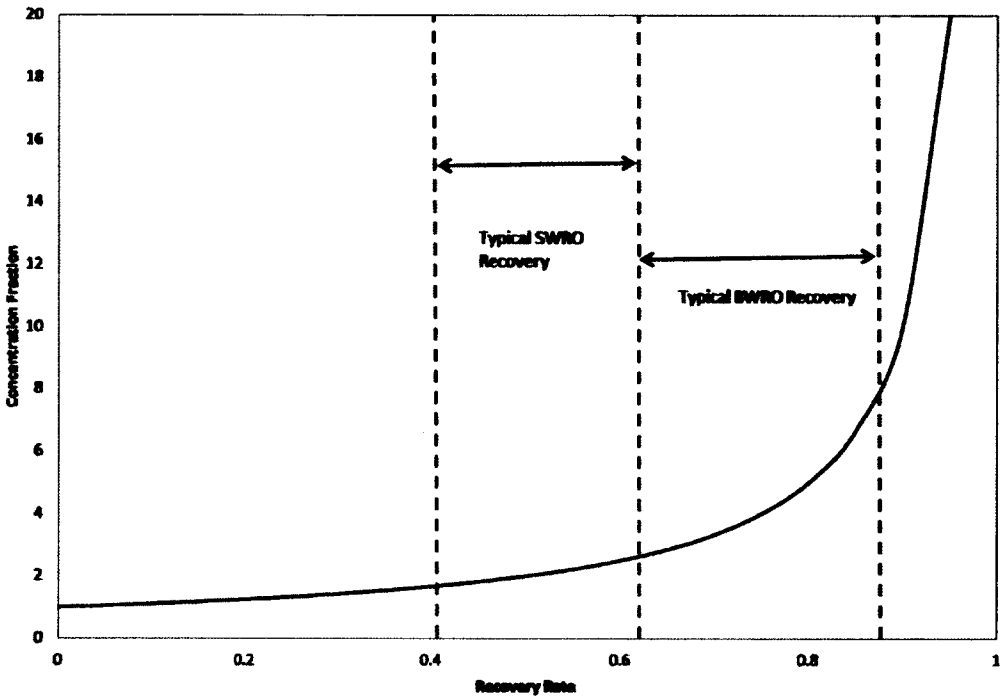

Fig. 1-3. Increases in Concentration Factor and Decrease in Concentrate Volume with Increasing Recovery Rate. The Shaded Regions Represent Typical Recovery Ranges for Typical Seawater Reverse Osmosis (SWRO) and Brackish Water Reverse Osmosis (BWRO) Processes [13]

1-3- The Brine Characteristics

The resulting fresh water produced during the desalination process usually has a very low mineral content, typically between 100 to 500 mg/L of salt in the form of TDS.

In over 99% of all seawater desalination plants, brine salt content is almost 1.5 to 2 times higher than the ambient seawater, which is in the range of 33 to 35 PSU. The brine produced from seawater desalination plants typically has the same color, odor, transparency and oxygen content. Therefore, brine discharge to coastal waters does not typically change its physical characteristics or aesthetic impact on the marine environment, except for its high salt content [13].

When a coagulant such as ferric chloride (FeCl3) or ferric sulfate ($Fe_2(SO_4)_3$) is used for seawater pretreatment, the spent pretreatment filter backwash will have a reddish color as a result of the increased concentration of ferric hydroxide ($Fe(OH)_3$) in the backwash water. If this backwash water is blended with the SWRO system brine, the brine and the entire desalination plant discharge will gain a red color. A good example of such coloration in the discharge is a 25 MGD seawater desalination plant in Tampa Bay, Florida, which uses ferric hydroxide in the desalination process. In order to remove the ferric hydroxide from the backwash water and remove the reddish color a pretreatment is done before discharging the brine into coastal waters. After the pretreatment process of the brine the discharge is no longer red and has the same color as that of the ambient seawater, i.e. the concentrate is transparent and does not have any aesthetic impact on coastal waters [13].

Levels of salinity and biological or chemical oxygen demand are two variables of the desalination brine and are independent variables. More than 80 percent of the brine minerals are sodium and chloride. These minerals are not nourishment sources or nutrients for marine organisms. The dissolved solids in the brine discharged from seawater desalination plants are not of anthropogenic origin as compared to contaminants

contained in discharges from manufacturing or municipal wastewater treatment plants [28].

The quantity of particles, total suspended solids and biochemical oxygen demand (BOD) in the brine are typically very low (5 mg/L) because these elements are removed during the desalination process. Normally in modern reverse osmosis seawater desalination plants, the filter backwash water is processed at the desalination plant site by settling. Hence, the treated backwash water, which is combined and discharged with the SWRO resulting brine, is also very low in terms of total suspended solids and biochemical oxygen demand. The organic minerals and solids eliminated from the feed seawater are usually disposed of in landfills as solid residuals. As a result, the total suspended solids content of the desalination plant discharge is lower than the solids content of the ambient feed seawater collected for desalination. Ambient seawater quality is usually very consistent with brine discharge. More than 98 percent of the brine salt content is composed of five dissolved minerals: sodium, chloride, sulphate, magnesium and calcium that are also consistently found in the receiving seawater[15].

1-4- Brine Management

There are four main management methods for desalination brine: (a) disposal to surface water, (b) deep well injection, (c) spray irrigation, and (d) evaporation ponds. While the cost of desalination using Reverse Osmosis technology has decreased exponentially during the last decade, the cost of brine disposal has remained fairly unchanged. Disposal expenses are unlikely to decrease in the future because of the simplicity and low-tech nature of the process [19].

In all four management methods the most important and significant cost is the cost of transporting the concentrate to the discharge location. This cost increases dramatically with increased distance between the plant and discharge location. As shown in Fig. 1-4, the cost of disposal is a function of concentrate flow rate. As concentrate flow rate increases, the management process costs increase as well. Evaporation pond, spray irrigation and deep well injection costs increase drastically with flow rate; however, the surface water discharge cost increases moderately with respect to the flow rate increase. Since the surface water discharge is the cheapest alternative, it has been used extensively around the world for years [19].

Other alternatives such as deep well injection are practical in the regions where surface water discharge is not an option due to the long distance of a desalination plant from the ocean. One such example is the El-Paso desalination plant in Texas where surface water discharge is not an option since the desalination plant is located inland. In this case, deep well injection has been used to dispose of the brine discharge [19].

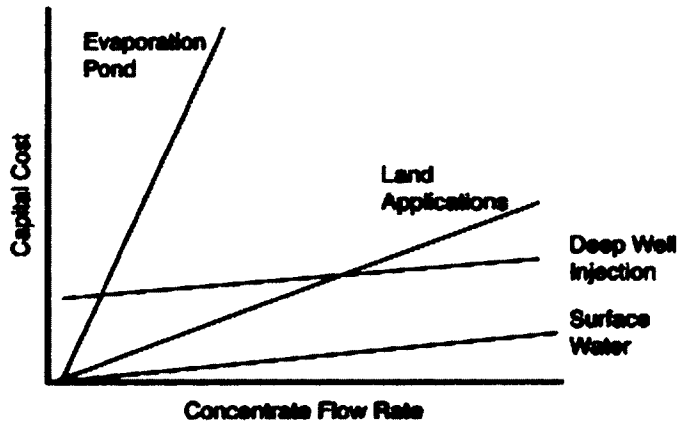

Fig. 1-4. Relative Capital Costs of Common Methods for Brine Disposal with Increasing Brine Flow rate [19]

Once surface water discharge is not feasible, land application and deep well injection are considered as competitive methods depending on the volume of the concentrate. For small amounts of brine, land application is preferable; however, for large amounts of concentrate deep well injection is more cost-effective. Since the majority of seawater desalination plants are located adjacent to coastal areas, surface water discharge is generally considered the most practical and economic brine management method [19].

1-5- Potential Environmental Impacts of Desalination Plants on Coastal Waters

The operation of desalination plants leads to a continuous discharge of brine, with twice the salinity content of the ambient water, as a by-product into the ocean. Discharge of the brine is typically through either surface outfalls at the coastline or submerged outfalls and diffusers at the seabed. Although the coastal inhabitants are used to saline, an excessive input of salinity can harmfully affect exposed marine ecosystems. This problem can be exaggerated as exposure time increases, which happens for continuous brine discharges. It is also known that a rise in the salt content of the ambient source waters at the intake location will decrease the proficiency of the desalination plant and increase the operation expenses in the long run. Another environmental concern is the release of chemicals into the coastal waters during the pretreatment procedures [8].

As previously mentioned, the desalination plants normally produce brine with a salt content of about 1.5 to 2 times greater than the salinity of the ambient seawater. Since coastal waters salt content in the United States usually varies between 33 to 35 PSU, the brine salinity is usually in the range of 52 to 70 PSU. While many aquatic organisms can adapt themselves to this salinity range, it is difficult and sometimes impossible for some

particular species to tolerate the exposure to elevated salinity concentrations. A very good example is gobies, a family of small fish which inhabit coastal regions with shallow water all around the world. Gobies are able to tolerate and survive high salt concentrations and famously reside in the Salton Sea of California with an ambient salinity of 45 PSU, which is significantly higher than average. However, there are some species such as sea urchins and abalone that have lower salinity resistance and are not able to survive high salinity [31].

As described, the consequences of elevated salt content in a marine environment and the corresponding environmental impacts are generally subjected to the nature of marine organisms residing in the brine release area as well as the exposure period. In order to understand the environmental impact of high salinity on coastal species, extensive research has been performed on the Carlsbad seawater desalination plant with brine discharge of 50 MGD in 2005. Over two dozen coastal species were exposed to high salt concentrations, and their responses and resistances to high salinity over time were studied accurately. The results showed that all the coastal species tested are able to survive and tolerate a salt content of 40 PSU, which was 19.4% above the ambient salinity [7].

Subsequent acute toxicity bioassay testing using standard top smelt test organisms (Atherinops affinis) was completed in conformance with the National Pollutant Discharge Elimination System (NPDES) permit requirements for the Carlsbad desalination project. The result of the test indicated four main points for the study area: (1) The No Observed Effect Concentration (NOEC) of the test occurred at 42 PSU of brine salt content; (2) The Lowest Observed Effect Concentration (LOEC) was found to be 44 PSU salinity; (3) The

plant was far below the related toxicity limit for salinity of 46 PSU or lower; (4) The No Observed Effect Time (NOET) for 60 PSU concentration was 2 hours, while the Lowest Observed Effect Time (LOET) for the 60 PSU concentration was 4 hours. This indicates that for a short period of time the species may be exposed to salinity as high as 60 PSU without any harmful impacts [7].

Other than the Carlsbad seawater desalination plant a large number of existing full-scale seawater desalination plants located in the Caribbean Sea were studied by researchers from the University of South Florida and the South Florida Water Management District in 1998. Their research findings indicated almost identical results to those observed from the Carlsbad coastal area study. They indicated that a salt content of 45 to 57 PSU did not cause statistically significant changes in the aquatic environment in the area of the brine release; however, they did not discuss the effect of exposure time in their research [4].

In order to study the biological influences of high salinity on coastal waters, hyper-salinity tests need to be performed at the study area. Hyper-salinity testing is a test that assesses harmful effects of both the degree of the increased salinity and the length of exposure time simultaneously. Results can then be combined with existing plume dispersion models to investigate the spreading and concentration of the brine plume over the seabed (benthic habitat) and in the water column (pelagic habitat) over time. Fig. 1-5 shows the two-day (48 hours) hyper-salinity test result in Huntington Beach, CA which studied three coastal species. The main goal of the Hyper-salinity test is to determine the salinity limit and corresponding exposure time in which 50% of the testing species can tolerate and survive, LC50 (Lethal Concentration 50%) using statically experimental

design. As shown in Fig. 1-5, 50% of bethic M.mysid shrimps were able to survive 40 PSU for a period of 48 hours. However, the same test shows that some of the shrimps begin to die when salt contents reach 36 PSU which is very close to the proposed 10% rule suggested by the state of California. In terms of the potential hyper-saline discharge effects in the water column, similar to M. mysid shrimp, 50% of the silverside minnows population that are a pelagic species, can tolerate and survive over 40 PSU for a duration of 48 hours, but some mortality happened at a lower salinity. In the pelagic environment, a fish that goes through a hyper-salinity brine plume is able to detect the changes in salinity and escape from the salinity zone by changing the direction of swimming. This behavior of fishes is called avoidance behavior which is not common in a benthic environment [9].

The long term effects of the hyper-saline on the coastal water inhabitants and the environmental impacts can be understood using models. These models are useful in quantifying long term effects of excessive salinity on the eggs and larvae of fish as well as other species and plankton. Fig. 1-6 illustrates modeling results performed for the Huntington desalination plant in 2005. The brine plume is discharged with the flow rate of 50 MGD to coastal waters. Fig. 1-7 shows the maximum exposure time allowed as a function of elevated salinity. The Huntington plant, as shown in Fig. 1-7, with a 126.7 MGD intake flow rate operating point (red line) discharges brine at 55.4 PSU. For example, the maximum exposure duration allowed for a salinity of 36 PSU is 4 hours; however, the allowable exposure time for 38 PSU is two hours. Thus, the exposure time decreases exponentially as the salinity value increases [9].

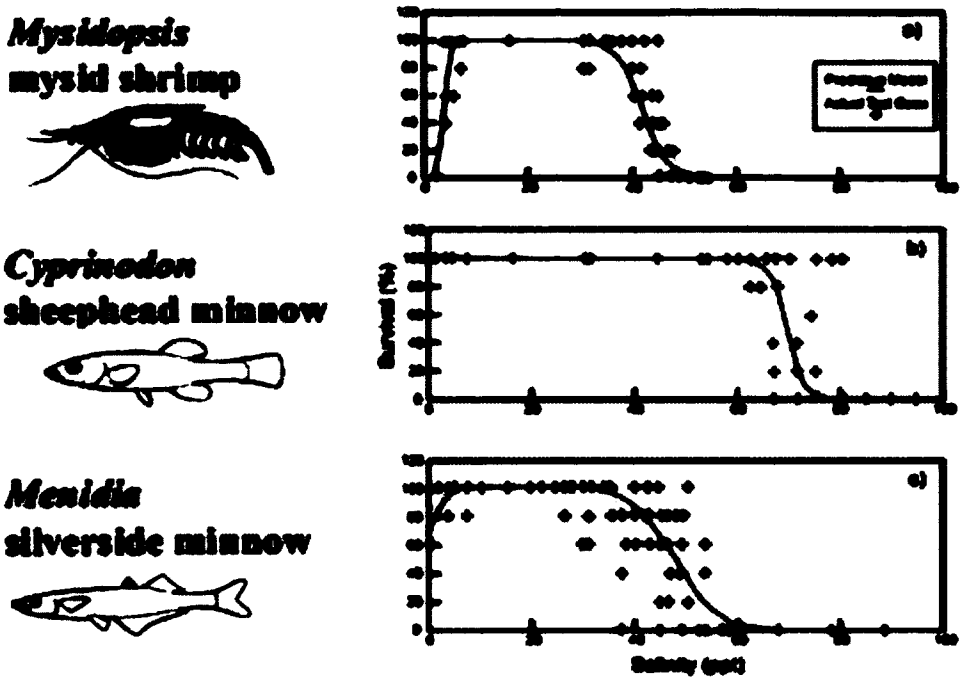

Fig. 1-5. Hyper-Salinity Test for Three Species: 1) Mysidopsis can Survive 40 PSU for 48-hours 2) Cyprinodon is able to Tolerate over 60 PSU for 48-hours 3) Menidia is able to Survive 40 PSU for a Period of 48 Hours [24]

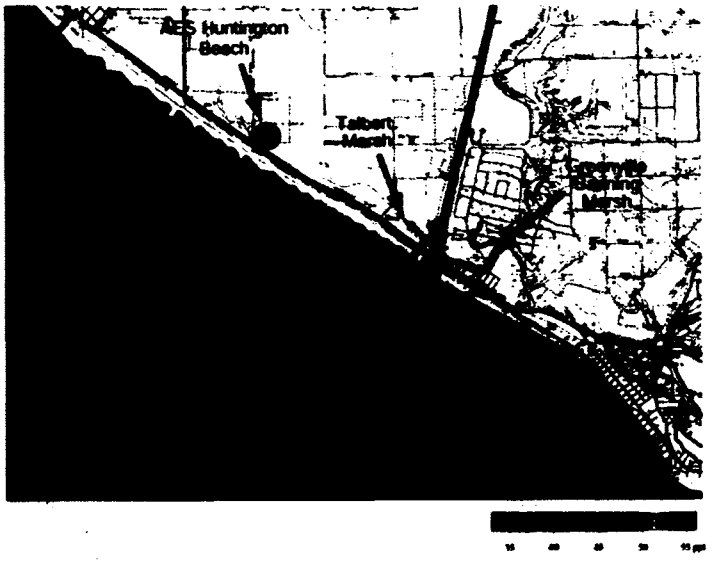

Fig. 1-6. Bottom Salinity Contour for Brine Dispersion (30 day average) for Huntington Beach Plant [9]

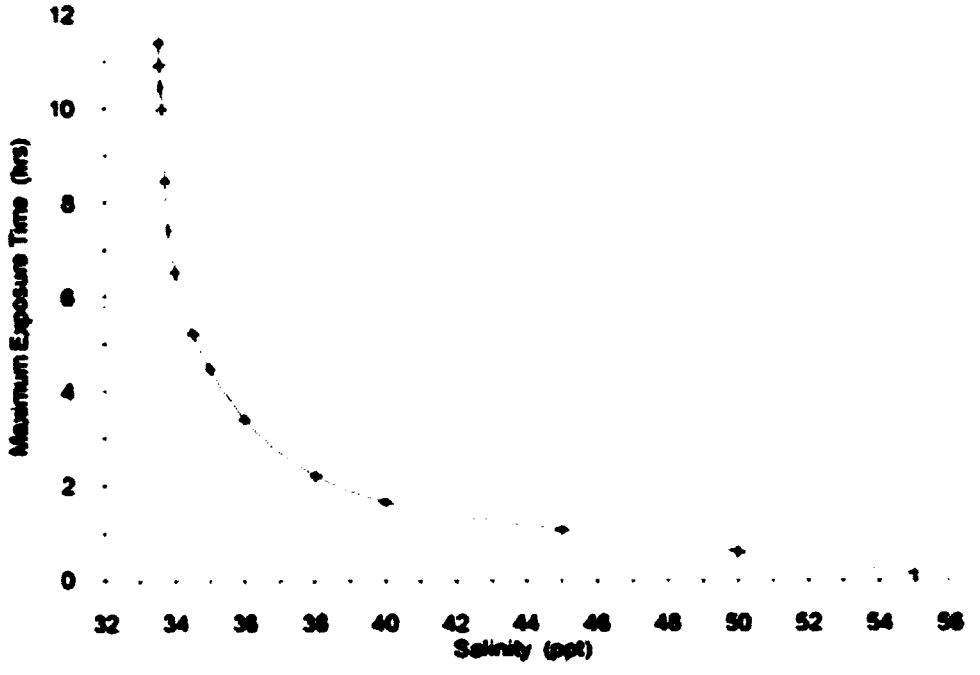

Fig. 1-7. Maximum Allowed Exposure Time as a Function of Salinity [9]

1-6- Regulations and Accomplished Researches on Brine Discharge

Currently and unfortunately, there are no federal or state laws that regulate brine discharge in the United States or throughout the world. However, there are some project-specific federal and state laws in one state such as California that control the brine discharge of a desalination plant by creating critical and long-lasting Whole Effluent Toxicity (WET) objectives. WET is more focused on controlling the environmental impact of different particles in seawater excluding salinity and does not necessarily emphasize salt content. Therefore, the motivation of WET is more on potential synergistic environmental impacts of the brine as a result of other constituents. However, the effect of increased salt content on the aquatic habitat in the area of the brine discharge is considered indirectly by studying the effect of total dissolved solids contained in the brine (e.g., metals, organics, and suspended solids). In other words, salinity is only a measure of the dissolved mineral (salt) content of the concentrate considered in WET rather than the complex chemistry of the discharge in relationship to the receiving body of water [29].

According to current regulations in the United States, if a desalination plant discharge meets all water quality objectives defined in the applicable federal state regulations as well as acute and chronic WET objectives, then the proposed discharge does not present a threat to aquatic life regardless of the actual salinity level of this discharge or what magnitude of increase above ambient salinity this discharge may cause because WET accounts for the salinity related environmental impacts of the concentrate [29].

The California Ocean Plan establishes a daily maximum acute toxicity receiving water quality objective of 0.3 TUa (acute toxicity units). Requirement III.C.4 (b) of the California Ocean Plan designates that this 0.3 TUa objective applies to ocean waters outside the acute toxicity mixing zone. Requirement III.C.4 (b) defines the acute toxicity mixing zone as follows:

> *"The mixing zone for the acute toxicity objective shall be 10 percent (10%) of the distance from the edge of the outfall structure to the edge of the chronic mixing zone (zone of initial dilution)."*

The state of California is considering a single state wide salinity limit for all ocean discharges of 10% above ambient salinity. So far this is the only existing semi-law that regulates the concentrate discharge in California, and other desalination plants around the world more or less try to follow this rule. This rule accepts the increase of up to 10% in ambient salinity in the zone of initial dilution. Now the question is whether one should design the outlet length based on 10% increase law. To answer this question many studies have been completed and considered this rule over-stringent or too conservative. Research shows that the increase of ambient salinity can be more than 10% without any detrimental impact on coastal environment. However, the allowable time of exposure has a reverse relationship with the elevated salinity value. The higher the elevated salinity, the less exposure time is allowable; in other words, the coastal water inhabitants, such as fishes, can resist higher salinities for a smaller period of time [29].

The California Ocean Plan defines the zone of initial dilution (ZID) as the zone in which the process of initial dilution is completed. Initial dilution is defined within Appendix I of the California Ocean Plan as follows:

"Initial Dilution is the process which results in the rapid and irreversible turbulent mixing of wastewater with ocean water around the point of discharge."

"For a submerged buoyant discharge, characteristic of most municipal and industrial wastes that are released from the submarine outfalls, the momentum of the discharge and its initial buoyancy act together to produce turbulent mixing. Initial dilution in this case is completed when the diluting wastewater ceases to rise in the water column and first begins to spread horizontally."

It should be noted that salinity tolerance of aquatic life is highly site specific and depends on the organisms inhabiting the area of the discharge as well as the nature of the discharge. Therefore, a single, non-site specific "blanket" narrative or numeric water quality objective (discharge limit) for salinity does not provide additional protection to the site specific marine environment in the area of a given discharge, beyond that which is already provided by the acute and chronic toxicity objectives. Despite the fact that environmental impacts associated with concentrate salinity are indirectly regulated through site-specific acute and chronic WET objectives, the discharge permits for some of the existing seawater desalination plants in the United States also contain specific numeric salinity limits as summarized in (Table 1-1) [29].

Table 1-1. Examples of Desalination Plant Discharge Limits [7, 9, 18]

Desalination plant	TDS (Avg.) (PSU)	TDS (Max.) (PSU)	Acute Toxicity TUa	Chronic Toxicity TUc	Mixing Ratio
Carlsbad 50 MGD 33.5 PSU (Ambient) 67.0 PSU (brine)	40 (daily) 19.4 % Above Ambient	44 (Maximum Hourly) 31.3 % Above Ambient	0.765	16.5	15.1:1
Huntington Beach 50 MGD 33.5 PSU (Ambient) 67.0 PSU (brine)	None	None	None	8.5	7.5:1 Min. Mixing 2.24:1
Tampa Bay 25 MGD 26 PSU (Ambient) 43 PSU (brine)	35.8 PSU 38% Above Ambient	35.8 PSU 38% Above Ambient	None	None	28:1 Min. Mixing 20:1

The Carlsbad Project NPDES discharge permit, for example, contains an effluent limitation for chronic toxicity at the edge of the zone of initial dilution concurrent with numeric limits for average daily and average hourly total dissolved solids (salinity) concentrations of 40 parts per thousand (PSU) and 44 PSU, respectively. These salinity limits were established based on a site specific Salinity Tolerance Study and chronic and acute toxicity testing completed for this project. The referenced limits are applicable to the point of discharge and reflective/protective of the acute toxicity effect of the proposed discharge [7].

The 50 MGD Huntington Beach SWRO Project NPDES permit also contains a limit for chronic toxicity but does not contain numeric limits for salinity. Instead, the potential acute toxicity effect of the discharge is limited by a ratio of the daily discharge flow from the desalination plant and the power plant intake cooling water flow, which describes a magnitudinal dilution to the concentrate. Such a dilution ratio requirement effectively provides a limit for the salinity discharge from the desalination plant of 40 PSU and is derived from site-specific analysis of the conditions of the discharge for this project [9].

Some state regulatory agencies in the United States (such as the State Water Resources Control Board in California) are considering the introduction of a single state-wide salinity limit for all ocean discharges of 10% above ambient ocean water salinity or other blanket numeric value, including disposal of concentrate from seawater desalination plants. However, this approach and reasoning are flawed because of several key considerations [29].

The salinity of the natural background varies by location, and therefore, the salinity limit derived from such objectives will differ and sometimes may exceed or underestimate the salinity tolerance of the site-specific aquatic environment in the area of the discharge. This is especially true for transient marine species. For example, a salinity tolerance study completed for the marine organisms living in the vicinity of the Carlsbad project can tolerate long-term exposure to salinities of 40 PSU and greater [29].

If the background salinity near Carlsbad (33.5 PSU) is examined for discussion purposes and a 10% increment is applied as a criterion, the salinity limit imposed at the edge of the zone of initial dilution would be 36.85 PSU, as opposed to the 40 PSU limit

set forth in the Carlsbad NPDES Permit. Both limits would be equally protective of the marine environment based upon the previously discussed WET testing results. However, if a limit of 36.8 PSU is used rather than 40 PSU, this limit would be overly restrictive for the project and would not have a scientific basis or precedence with respect to NPDES permitting requirements. This example shows that a blanket salinity limit may unduly hinder the implementation of desalination projects rather than protect marine environment. Moreover, the effect on the environment is associated with the actual tolerance of the marine organisms in loco, rather than with the value of the background salinity [29].

The variation in background ambient salinity may differ significantly from one location to another. Open-ocean salinity would naturally vary ± 10% from the average annual value (i.e., a total salinity variation bracket of 20%). However, in shallow areas along the shore or in shallow bays, this variation may be higher. An example is the source water quality variation documented during the desalination pilot testing completed by the Marin Municipal Water District in 2005/2006.

The average salinity concentration of the source water for this proposed desalination plant was 21.7 PSU; the maximum was 29.0 PSU (+34%), and the minimum was 2.5 PSU (-768%). If, for example, a typical open ocean salinity variation of 10% is chosen as a "blanket" narrative objective, then this numeric objective would be overly restrictive and completely unrealistic for the Marin County desalination project because the source water of the desalination plant will be more saline than the concentrate salinity limit. If the +34% salinity variation is chosen, then the maximum state limit for the salinity discharge of the Carlsbad desalination plant would be 44.6 PSU, which is higher

than the level established in the current Carlsbad NPDES permit. In both examples, however, the beneficial uses would be fully protected by the WET objectives applied to site-specific conditions in the vicinity of the discharge.

A similar observation can be made for the Tampa Bay desalination plant discharge where the ambient seawater salinity also varies in a very wide range of 16 PSU to 33 PSU and averages 26 PSU. In this case, because the 19 MGD of the desalination plant concentrate is diluted with 1.4 billion gallons of cooling water from the power plant with which the desalination plant is collocated, the actual salinity increment is within the level of accuracy of the salinity measurement instruments [18].

1-7- Motivation and Problem Conceptualization

According to the vast majority of previous research and case studies, understanding the environmental impact of brine waste discharge into the ocean is a difficult, if not impossible, and complex task. The difficulties arise from the diversity and variability of the mixing processes that significantly and subsequently dilute, spread and transport the brine plume, and the change in sea currents, temperature, salinity and density are highly site-specific. Moreover necessary generalization methods are either nonexistent or too complicated. Therefore, any generalization models that are capable of predicting brine mixing processes and subsequently the environmental impact with good accuracy and equally with ease of use should be valued, as they give scientific explanations related to the mixing processes and should be used as an aid in designing brine disposal operations from a coastal desalination plant.

In order to have a better understanding of the environmental impact of the brine plume discharge in coastal waters, modeling and simulation of the coastal area is essential. In this research two different generalization methods are proposed to model and simulate the brine dispersion in coastal waters under tidal currents. Two generalization methods, the Finite Segment Method (FSM) and the Analytical Method (AM), have been introduced and successfully modeled the brine propagation in a tidally influenced environment in this research. Advantages and disadvantages of each method have been identified. Both methods are scientifically sound and applicable, yet the site-specific characteristics of the receiving water are still key to dictating the method's applicability and subsequent accuracy of the model. For the selection of a proper method as well as generalizing the methodology for coastal waters all around the world, a non-dimensional criterion, Shahvari-Yoon (SY) number, has been developed and proposed in this research to represent the mixing characteristic of the study area as a function of current velocity and dispersion coefficient. Applicability and practicality of each method has been studied; as a result, the range of validity of each method with respect to the SY number has been investigated.

One of the most important issues that need more consideration is the lack of a nation-wide or worldwide regulation that regulates the brine discharge into coastal waters. All the studies that have been performed are based on a specific case study. The only existing regulation for brine discharge is the 10% law of the state of California which seems to be too conservative. In this research a risk analysis has been performed, and the 10% law has been studied in detail and revised in such a way to be applicable to optimize the design for the outlet length of a desalination plant.

CHAPTER 2

LITERATURE REVIEW

2-1- Introduction

As discussed in the previous chapter it is essential to understand how the brine propagates in coastal waters to minimize the potential environmental impact to the coastal inhabitants. Modeling and simulation of contamination transport in reversing and oscillating flow is a complicated task and was first studied by HARLEMAN, D. R. F *et al.* (1968). They developed a numerical model to simulate contamination transport in an estuary. The model was only capable of simulating one flow reversal. Later, Kay (1990) established an analytical method to solve the advection-diffusion equation for an oscillating flow. His model was able to simulate the effect of single reversal and was developed for constant water depth. He solved the following partial differential equation [11]:

$$\frac{\partial c}{\partial t} + u\frac{\partial c}{\partial x} + -D_x\frac{\partial^2 c}{\partial x^2} - D_y\frac{\partial^2 c}{\partial y^2} = Q\delta(x)\delta(y)$$

Eq. (2.1)

where c is the concentration of the contamination at time t at the location of (x, y), u is the current velocity, D_x and D_y are the longitudinal and lateral dispersion coefficients, and Q is the continuous brine discharge.

In order to reflect the oscillating flow velocity in the advection-diffusion equation, the velocity was defined as a linear time dependent function.

$$U(t) = At$$

Eq. (2.2)

This is the simplest way of simulating oscillating flow, which was first introduced by Pedley (1975). Later, Macdonald & Weisman (1977) represented oscillating current using a harmonic function [16, 23].

$$U(t) = V + U_0 \sin \omega t$$

Eq. (2.3)

2-2- Brine plume dispersion in shallow water with a constant depth

Kay solved Eq. (2.1) using boundary layer approximation originated from the characteristic elongation of plumes from continuous discharges first used by Fisher *et al.* (1979) in their research. Fisher *et al.* omitted the longitudinal diffusion due to the small value of the concentration gradient in the direction of the flow. However, they strongly recommended that the longitudinal diffusion should be considered during the flow reversal and stagnation points (zero velocities or velocity nulls). The result was highly accurate during the presence of advective-dominant flow. However, during the period with very low velocities of the current and over stagnation points the model encountered a large amount of error [25].

Kay (1990) calculated the observation time t_n as phase shifts to define the time before and after the flow reversal. The times with negative values represent the before

flow reversal condition, and the time equal to zero is the instance of flow reversal and positive values belong to the after flow reversal condition [11].

$$\begin{Bmatrix} t_n = -\left(t^2 - \frac{2x}{A}\right)^{0.5} & for\ x \le 0 \\ no\ solutions & for\ x > 0 \end{Bmatrix} when\ t < 0$$

$$\begin{Bmatrix} t_n = -\left(t^2 - \frac{2x}{A}\right)^{0.5} & for\ x \le 0 \\ t_n = \pm\left(t^2 - \frac{2x}{A}\right)^{0.5} & for\ 0 \le x \le \frac{1}{2}At^2 \\ no\ solutions & for\ x > \frac{1}{2}At^2 \end{Bmatrix} when\ t > 0$$

Eq. (2.4)

He solved equation (1) before and after flow reversal separately by substituting the above formulas.

Kay's solution before the flow reversal $t < 0$ [11]:

$$C = \frac{Q}{2A(\pi D_y)^{0.5}}\left[t + \left(t^2 - \frac{2x}{A}\right)^{0.5}\right]^{-0.5}\left(t^2 - \frac{2x}{A}\right)^{-0.5} exp\left(\frac{-y^2}{4D_y\left(t+\left(t^2-\frac{2x}{A}\right)^{0.5}\right)}\right) \quad for\ x < 0$$

Eq. (2.5)

$$C = 0$$

$$for\ x > 0.$$

Kay's (1990) Solution after flow reversal $t > 0$

$$C = \frac{Q}{2A(\pi D_y)^{0.5}}\left[t + \left(t^2 - \frac{2x}{A}\right)^{0.5}\right]^{-0.5}\left(t^2 - \frac{2x}{A}\right)^{-0.5} exp\left(\frac{-y^2}{4D_y\left(t+\left(t^2-\frac{2x}{A}\right)^{0.5}\right)}\right)$$

$$for\ x < 0$$

Eq. (2.6)

$$C = \frac{Q}{2A(\pi D_y)^{0.5}}\left[\left[t + \left(t^2 - \frac{2x}{A}\right)^{0.5}\right]^{-0.5}\left(t^2 - \frac{2x}{A}\right)^{-0.5} exp\left(\frac{-y^2}{4D_y\left(t + \left(t^2 - \frac{2x}{A}\right)^{0.5}\right)}\right)\right.$$

$$\left. + \left[t - \left(t^2 - \frac{2x}{A}\right)^{0.5}\right]^{-0.5}\left(t^2 - \frac{2x}{A}\right)^{-0.5} exp\left(\frac{-y^2}{4D_y\left(t - \left(t^2 - \frac{2x}{A}\right)^{0.5}\right)}\right)\right]$$

$$for\ 0 \leq x \leq \frac{1}{2}At^2$$

Eq. (2.7)

$$C = 0$$

$$for\ x > \tfrac{1}{2}At^2.$$

His solution is represented in Fig. 2-1. He used dimensionless x, y and concentration in his result. He defined dimensionless concentration as:

$$C^* = \frac{C}{\left(\frac{Q}{(D_y A^2 t^3)^{1/2}}\right)}.$$

Eq. (2.8)

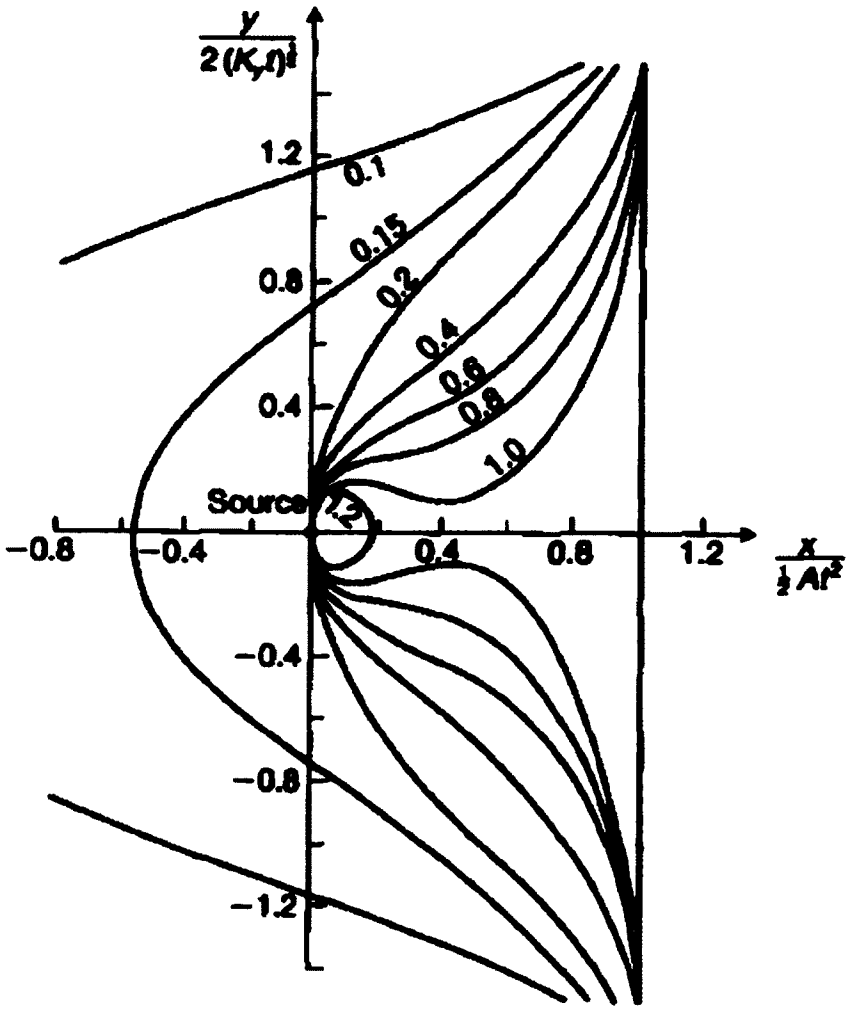

Fig. 2-1. Concentration distribution after the flow reversal, calculated using the boundary-layer approximation [11]

Kay (1997) updated his model from Pedley's approach (1975) (Eq. (2.2)) to Macdonald & Weisman's approach (1977) (Eq. (2.3)) by substituting the linear velocity function with a harmonic function. The advection diffusion equation was then solved for an estuary with oscillating tidal flows to consider multiple reversals in its cycle. Linear

superposition was used to superimpose the river velocity with tidal oscillations. It should be noted that his model was developed for a constant water depth condition [12].

Kay's (1994) solution of the advection-diffusion equation (equation 1) with multiple reversals and constant water depth:

$$C_c(x,y,t) = \frac{C_0 Q}{4\pi h_0 \sqrt{D_x D_y}} \int_0^t \left\{ exp\left[-\frac{(x-x_0)^2}{4D_x(t-t_0)} - \frac{\left[y - V(t-t_0) + \frac{U_0}{\omega}(cos\omega t - cos\omega t_0)\right]^2}{4D_y(t-t_0)} \right] + exp\left[-\frac{(x+x_0)^2}{4D_x(t-t_0)} - \frac{\left[y - V(t-t_0) + \frac{U_0}{\omega U_0}(cos\omega t - cos\omega t_0)\right]^2}{4D_y(t-t_0)} \right] \right\} \frac{dt_0}{t-t_0}$$

Eq. (2.9)

where D_x, D_y are longitudinal and the lateral dispersion coefficient, t_0, is the beginning of the simulation. U_0, ω represents tidal characteristics, (x_0, y_0) is the discharge location, h_0 is the water depth, V is the advective velocity, Q is the discharge flow rate, and C_0 is the discharge concentration [12].

Fig. 2-2 shows Kay's (1994) result for non-conservative contaminant distribution. He used dimensionless parameters to represent his results.

He defined dimensionless concentration as: $\frac{C}{\left(\frac{Q}{(D_y A^2 t^3)^{1/2}}\right)}$.

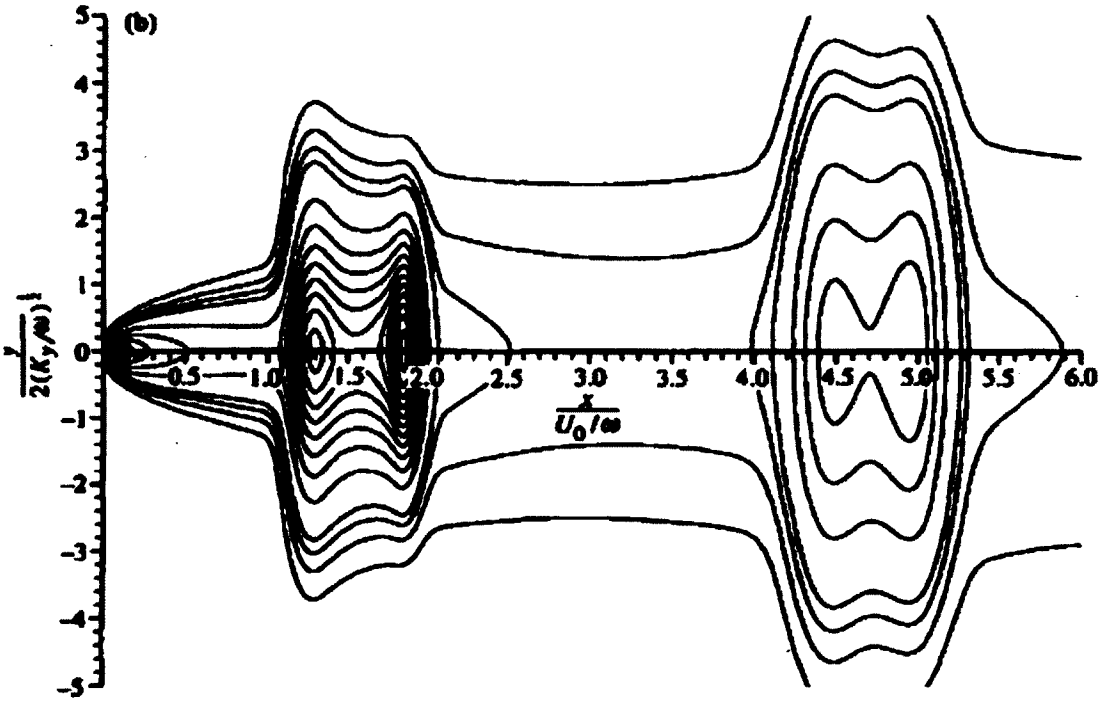

Fig. 2-2. Concentration Distribution after Multiple Reversals [12]

All analytical models discussed are developed to simulate the brine dispersion in coastal waters with a constant water depth. One of the most influential factors in contamination dispersion is the water depth. In deeper water the flow velocity has a tendency to be faster, and turbulent mixing is stronger. Hence, the effect of seabed topography and water depth on contamination dispersion has been investigated in much of the research. The first study was of cooling water dispersion and related dye study for

design of the Heysham nuclear power station outlet location in 1969 in the United Kingdom. An extensive dye study was performed in the study area to identify the mixing characteristic around the power station (Fig. 2-3). The dye study's result showed that the water depth has a significant influence on the dilution and spread of the contaminant [11].

Fig. 2-3. Dye Study Performed to Select Outlet Location for Heysham Nuclear Power Station Located in United Kingdom, Showing Concentrate Dispersion Two Hours Before Low Tide [11]

Fig. 2-4 shows the topography of the seabed in the Heysham harbor. Comparing Fig. 2-3 and Fig. 2-4 it becomes evident that as soon as the dye reaches the deeper area, it

spreads very rapidly. On the other hand, in shallower water the concentration tends to maintain its homogeneity within the flow. The maximum concentration happened in shallow water with less than 10 ft. depth. The dye plume disappears rapidly while it reaches a steep slope between 10ft contour and 30ft contour. Results from the Heysham power plant research motivated many researchers to study the effect of slope and water depth on plume dispersion in coastal waters.

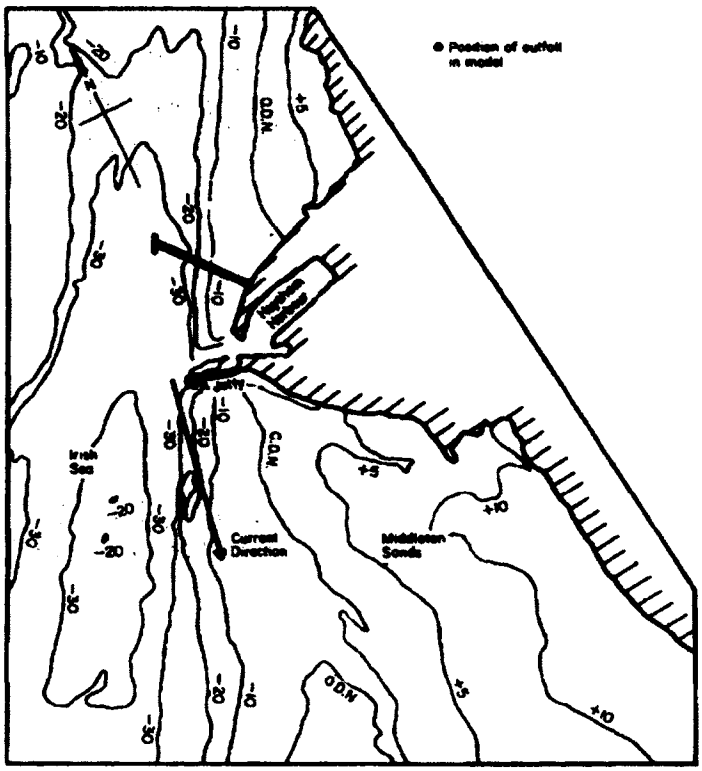

Fig. 2-4. Topography of Seabed at Heysham around the Outlet [11]

2-3- Brine plume dispersion on a sloping beach

Purnama and Barwani (2003) studied the brine discharge on a sloping beach. They assumed the seabed depth profile is as shown in Fig. 2-5. They defined the seabed as follow

$$h = \begin{cases} my & 0 < y < lh_0 \\ h_0 & y > lh_0 \end{cases}$$

Eq. (2.10)

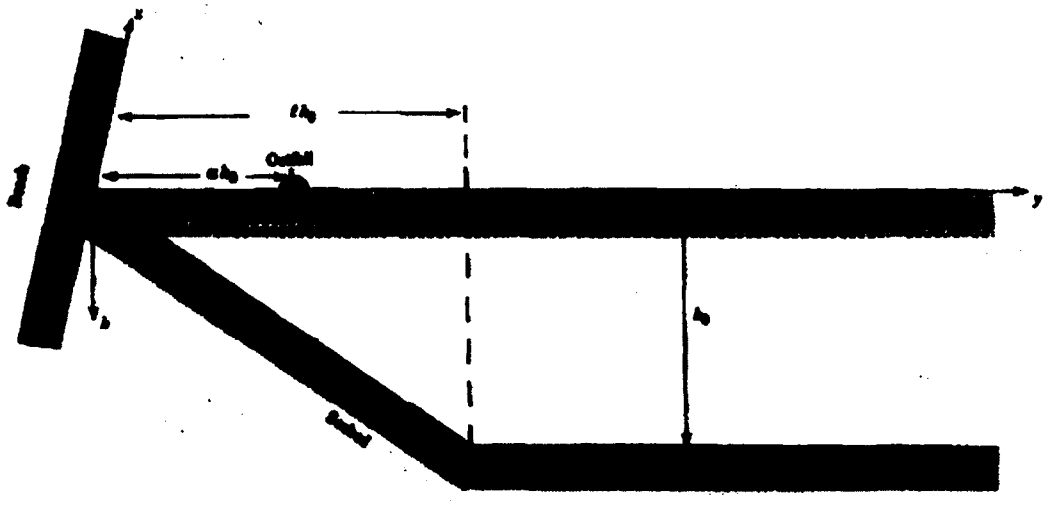

Fig. 2-5. Seabed Depth Profile of a Sloping Beach [27]

They assumed that the outfall is located at a distance of αh_0 from the coastline and rearranged advection-diffusion equation (equation 1) with respect to equation 10 as follows:

$$\frac{\partial}{\partial x}(hUc) - \frac{\partial}{\partial y}\left(hD\frac{\partial c}{\partial y}\right) = Q\delta(x)\delta(y + lh_0)$$

Eq. (2.11)

with the boundary conditions of:

$$hD\frac{\partial c}{\partial y} = 0 \quad at \quad y = 0$$

Eq. (2.12)

where δ is the Dirac delta function.

Then the governing equation was solved at the slope and after the slope separately using Laplace transforms, and then they superimposed the resultant concentrations.

Purnama and Barwani's (2003) Solution [27] becomes:

$$C_1 * = \frac{1}{mx*}\frac{1}{(\alpha y*)^{3/4}}\exp\left(-\frac{y*+\alpha}{x*}\right)I_{3/2}\left(\frac{2\sqrt{\alpha y*}}{x*}\right)$$

$$C_2 * = \frac{f}{\sqrt{4\pi x*}}\left[\exp\left(-\frac{(y*-\alpha)^2}{4x*}\right) + exp\left(-\frac{(y*+\alpha)^2}{4x*}\right)\right]$$

Eq. (2.13)

${}_wC_2 *$ is the concentration after the slope, x= $\frac{x*U_0h_0^2}{D_0}$, $C_1 = \frac{C_1*Q}{U_0h_0^2}$, $C_2 = \frac{C_2*Q}{U_0h_0^2}$, $U = U_0y*^{1/2}$,

$C_2 *$ is the concentration after the slope, x= $\frac{x*U_0h_0^2}{D_0}$, $C_1 = \frac{C_1*Q}{U_0h_0^2}$, $C_2 = \frac{C_2*Q}{U_0h_0^2}$, $U = U_0y*^{1/2}$,

and the factor f was given as:

$$f = \frac{1}{m}\sqrt{\frac{4\pi}{x*}}\frac{1}{(\alpha l)^{3/4}} I_{3/2}\left(\frac{2\sqrt{\alpha l}}{x*}\right)\frac{\exp\left(-\frac{l+\alpha}{x*}\right)}{\exp\left(-\frac{(1-\alpha)^2}{4x*}\right)+exp\left(-\frac{(1+\alpha)^2}{4x*}\right)}.$$

Eq. (2.14)

Fig. 2-6 shows Purnama and Barwani's (2003) resultant concentration with $m = 0.2, \alpha = 0, l = 5$. As shown in Fig. 2-6, the concentration disperses at a faster rate at the sloped location than at the flat part.

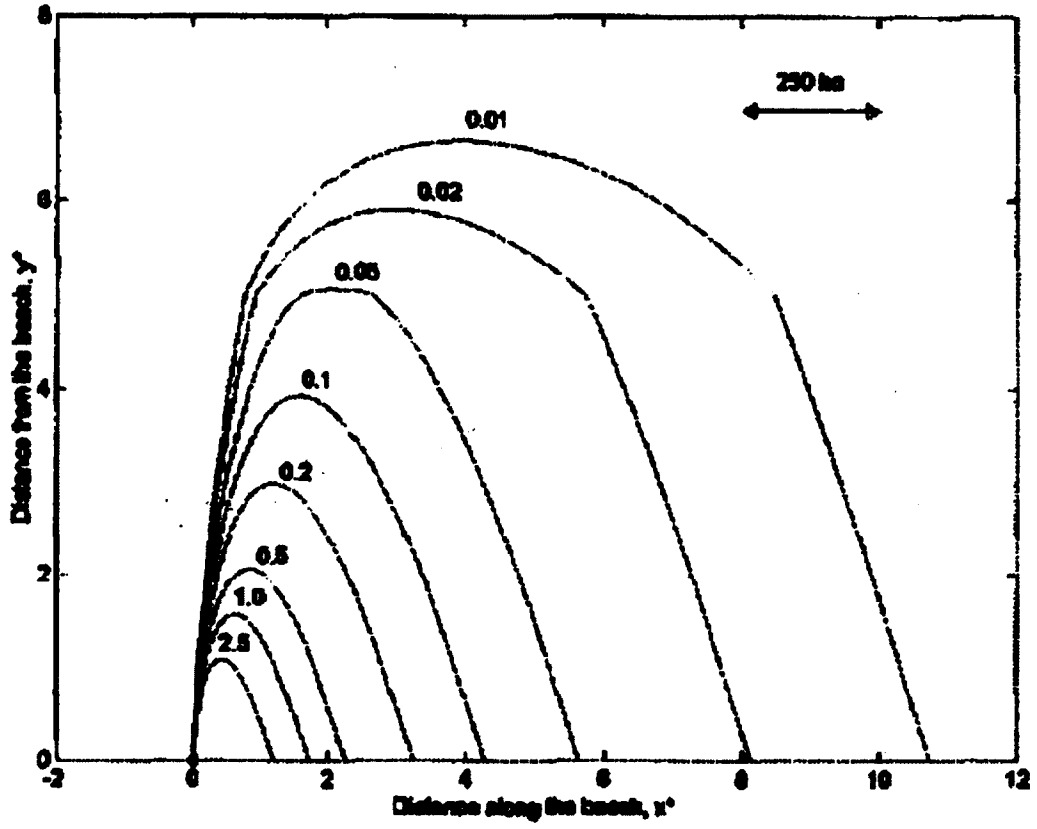

Fig. 2-6. Resultant Concentration with $m = 0.2, \alpha = 0, l = 5$ [27]

2-4- The effect of depth variation on brine dispersion

Most previous works in the literature have focused on the seabed with constant slope. In some cases the seabed topography is very complex, and it becomes inadequate to simulate the seabed with the forced constant slope assumption. Kay (1987) reported the effect of depth variation in a vertically well-mixed current. The contamination transport was modeled using the advection diffusion equation. The Fickian diffusion equation was applied to model turbulent diffusion. Method of images was used to obtain the general solution for the partial differential equation. It was assumed that [31]

$$U \propto h^{\frac{1}{2}} \quad and \quad D_y \propto h^{\frac{3}{2}}$$

Eq. (2.15)

where h is the water depth, U is the current speed and D_y is the eddy diffusivity.

Study area was partitioned into two different sections as shown in Fig. 2-7. The first section has a shallower depth of h_1, and the second section has a deeper depth of h_2.

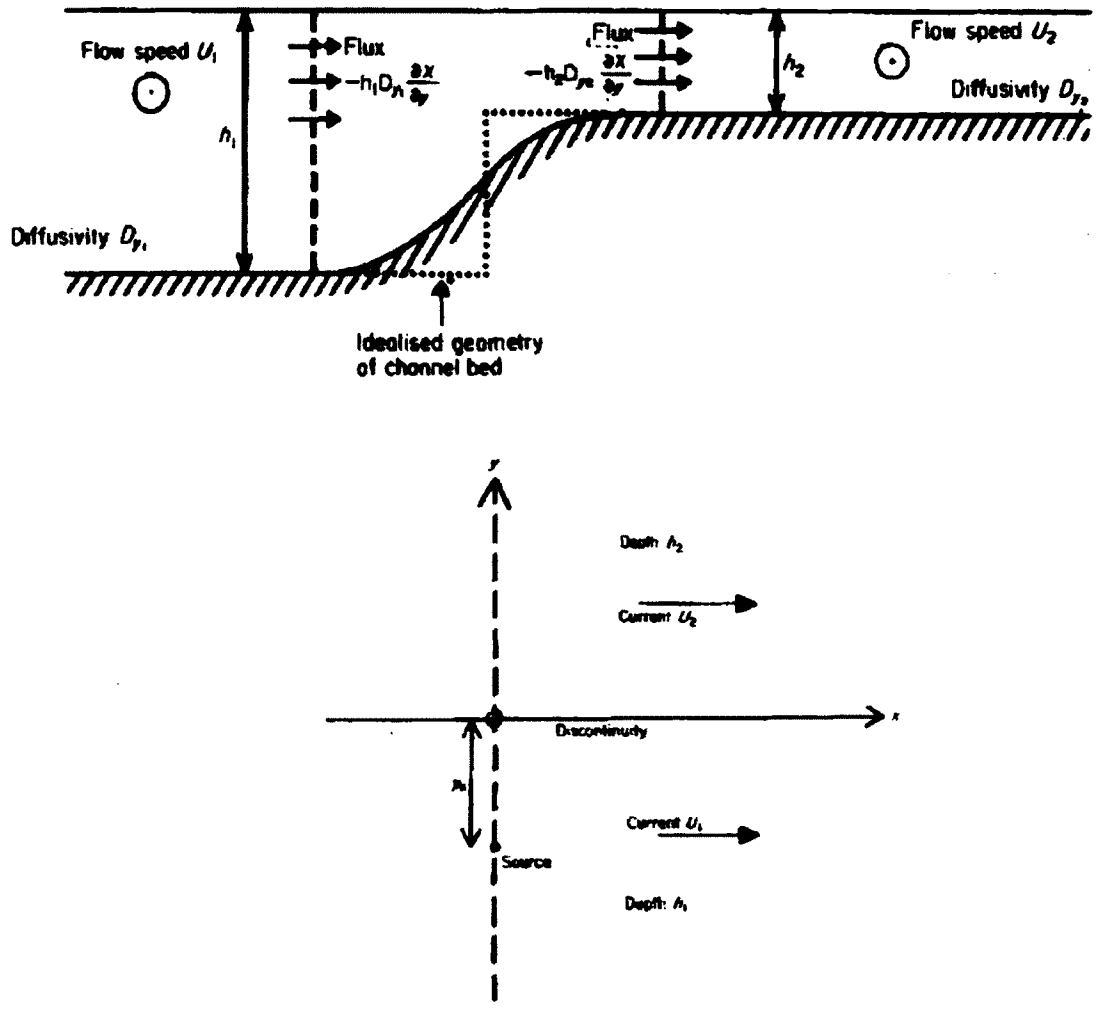

Fig. 2-7. The Sharp Depth Change: Cross Sectional View and Plan View [10]

The outlet is located at the deeper section with the distance of y_0 from the depth discontinuity location. The resultant advection-diffusion equation comes within the region with $y < 0$ since we have discharge [10]:

$$U_1 \frac{\partial c}{\partial x} - D_{y1} \frac{\partial^2 c}{\partial y^2} = Q\delta(x)\delta(y + y_0).$$

Eq. (2.16)

In the region $y > 0$

$$U_2 \frac{\partial c}{\partial x} - D_{y2} \frac{\partial^2 c}{\partial y^2} = 0$$

Eq. (2.17)

with the following boundary conditions:

$$\lim_{y \to 0^-} c(x,y) = \lim_{y \to 0^+} c(x,y)$$

$$\lim_{y \to 0^-} h_1 D_{y1} \frac{\partial c}{\partial y} = \lim_{y \to 0^+} h_2 D_{y2} \frac{\partial c}{\partial y}.$$

Eq. (2.18)

Thus, Kay's (1987) solution of the advection-diffusion equation for variable seabed depth becomes:

$$C = \frac{Q}{2\sqrt{\pi U_1 D_{y1} x}} \left[exp\left(-\frac{U_1 (y + y_0)^2}{4 D_{y1} x} \right) + \frac{h_1 \sqrt{U_1 D_{y1}} - h_2 \sqrt{U_2 D_{y2}}}{h_1 \sqrt{U_1 D_{y1}} + h_2 \sqrt{U_2 D_{y2}}} exp\left(-\frac{U_1 (y - y_0)^2}{4 D_{y1} x} \right) \right]$$

$for\ y < 0,$

Eq. (2.19)

and

$$C = \frac{Q}{2\sqrt{\pi U_1 D_{y1} x}} \frac{h_1\sqrt{U_1 D_{y1}}}{h_1\sqrt{U_1 D_{y1}} + h_2\sqrt{U_2 D_{y2}}} exp\left(- \frac{U_2\left(y + y_0 \left({}^{U_2}/_{U_1}\right)^{-1/2} \left({}^{D_{y2}}/_{D_{y1}}\right)^{1/2}\right)^2}{4D_{y2}x} \right)$$

$for\ y > 0.$

Eq. (2.20)

Smith (1976) simplified the above equation more

$$C = \frac{Q}{2\sqrt{\pi U_1 D_{y1} x}} \left[exp\left(- \frac{U_1 (y + y_0)^2}{4D_{y1}x} \right) + \frac{{h_1}^2 - {h_2}^2}{{h_1}^2 + {h_2}^2} exp\left(- \frac{U_1 (y - y_0)^2}{4D_{y1}x} \right) \right]$$

$for\ y < 0,$

Eq. (2.21)

and

$$C = \frac{Q}{\sqrt{\pi U_1 D_{y1} x}} \frac{{h_1}^2}{{h_1}^2 + {h_2}^2} exp\left(- \frac{U_2\left(y + y_0 \left({}^{h_2}/_{h_1}\right)^{1/2}\right)^2}{4D_{y2}x} \right).$$

$for\ y > 0$

Eq. (2.22)

Fig. 2-8 demonstrates the resultant contours, and Fig. 2-9 shows the flux gradient. As showed when the water depth increases the plume disperses faster, and in shallower water contaminants tend to accumulate in higher concentrations. As part (a) shows, the

conservative contamination scatters faster in the region with $y < 0$ since the water depth in this region (h_1) is larger than the other region with $y > 0$ ($h_2 = \frac{h_1}{2}$). The contours in part (b) are the same in both parts since there is no depth discontinuity. Part (c) shows increase of the dispersion rate with increased water depth. As shown, the contamination in the region with double depth propagates much faster than the zone with $y < 0$.

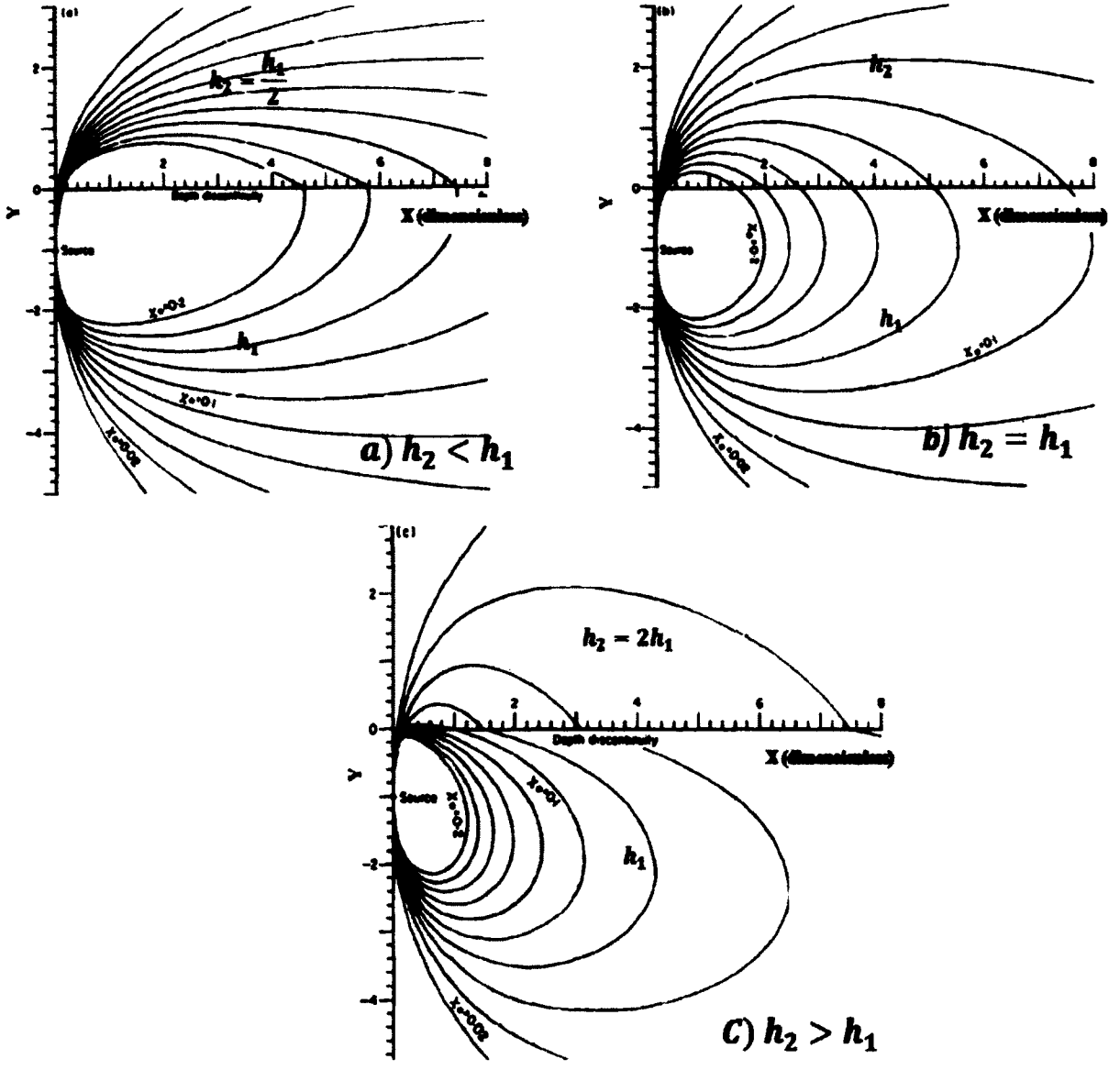

Fig. 2-8 Contours of Non-Conservative Concentration in Coastal Waters with Variable Depth: a) $h_2 = \frac{h_1}{2}$; b) $h_2 = h_1$; C) $h_2 = 2h_1$ [10]

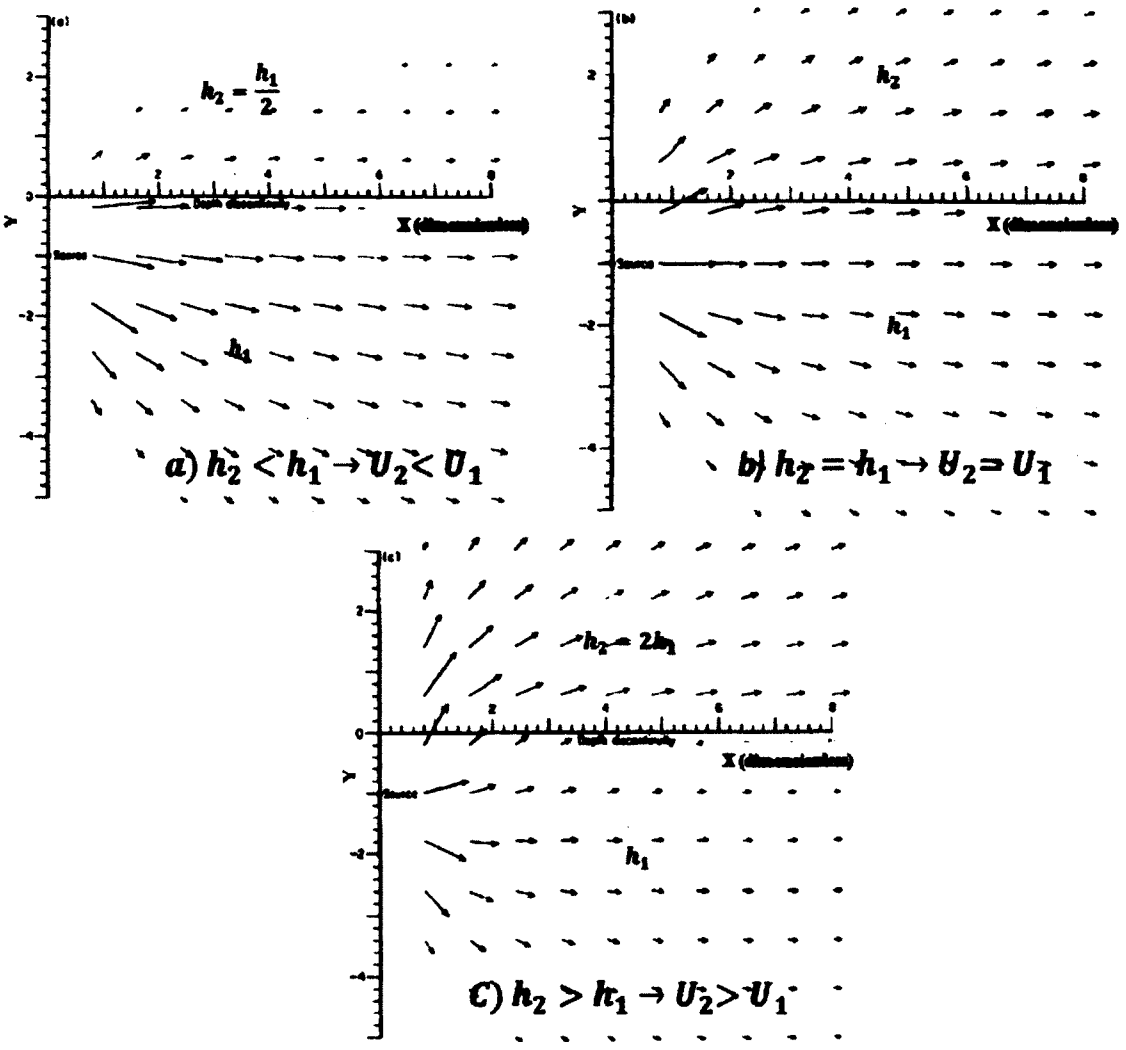

Fig. 2-9. Contamination Flux in Coastal Waters with Variable Depth: a) $h_2 = \frac{h_1}{2}$; b) $h_2 = h_1$; C) $h_2 = 2h_1$ [10]

CHAPTER 3

IMPLEMENTATION OF FINITE SEGMENT METHOD (FSM) & ANALYTICAL METHOD (AM) TO SIMULATE BRINE DISPERSION IN COASTAL REGIONS

3-1- Introduction

In this chapter, two common approaches proposed in this research for simulating plume dispersion will be discussed. The first method is the Finite Segment Method (FSM), which is a numerical approach based on a steady state assumption. This method is capable of simulating brine dispersion with any complex seabed geometry. The Finite Segment discretization scheme is one of the simplest forms of discretization and does not include the topological nature of partial differential equations. FSM is easy to implement and is capable of simulating spatial and temporal brine dispersion in coastal waters. The second method is the Analytical Method (AM), which is developed based on the analytical solution of the advection-diffusion equation for a sloping seabed. This method is capable of simulating temporal and spatial brine dispersion efficiently for the sloping seabed.

3-2- Finite Segment Method (FSM)

The finite segment method is a technique that signifies and evaluates partial differential equations in the form of algebraic equations. Similar to the finite difference or finite element methods, values are calculated at discrete places on a meshed geometry. "Finite segment" refers to the small segment surrounding each node point on a mesh. In

the finite segment method, volume integrals in a partial differential equation that contain a divergence term are converted to surface integrals, using the divergence theorem. These terms are then evaluated as fluxes at the surfaces of each finite segment [20].

Fig. 3-1 shows the segmentation scheme of a typical estuarine area. Moving toward the ocean the segment depth increases due to a constant slope toward the coastline. It is assumed that each segment is completely well mixed; therefore, the concentration gradient is only along the x and y axes, and the concentration gradient in the z dimension is neglected. FSM is capable of modeling and simulating point loads, distributed loads, and multiple point loads. Since the bottom topography is reflected in segment size while calculating a segment volume, FSM is able to simulate the estuaries with complex bottom topography without any difficulty [33].

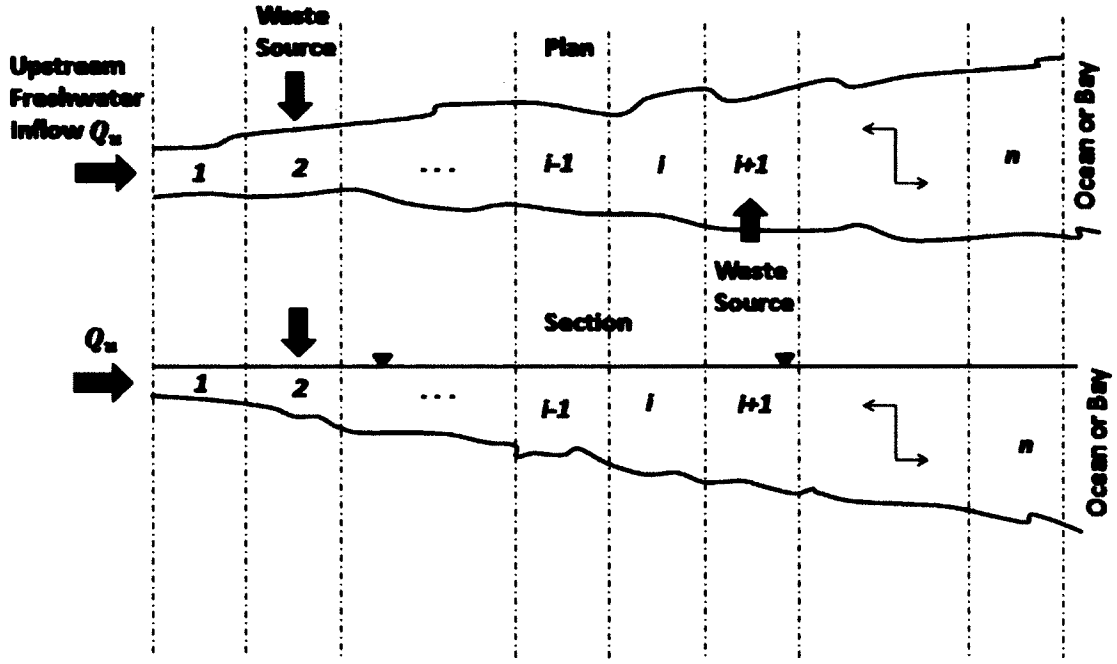

Fig. 3-1. Demonstration of the Estuary Segmentation [34]

With faster and more efficient computers available today, the segment size is no longer a big concern as long as it satisfies all the stability conditions and avoids numerical dispersion. However, as the number of segments used in the simulation increases, the more measured data will be required and the more expensive the simulation will be in form of data collection for these additional segments. As a general guideline, Thomann and Mueller (1987) suggested that a segment size of 2 miles would be acceptable to represent a typical estuary. The number of segments normally depends on the number of point loads and the gradient of salinity change. Later in this chapter, the requirements to avoid numerical dispersion are also discussed to identify the best segment size used in this research [33].

The FSM is based on the mass balance around each segment. In order to govern the mass balance for a segment, it is necessary to consider three mechanisms: (1) mass transport due to advection, (2) mass transport due to dispersion (in both X and Y directions), and (3) loss of mass as a result of decay as illustrated in (Fig. 3-2). Since salinity is measured as a conservative substance, the decay part can be eliminated from the mass balance equation that governs each segment in case of the brine discharge. The resultant concentration will describe the salinity at the center of the segment, and it is assumed that all other points inside of the segment will have the same concentration.

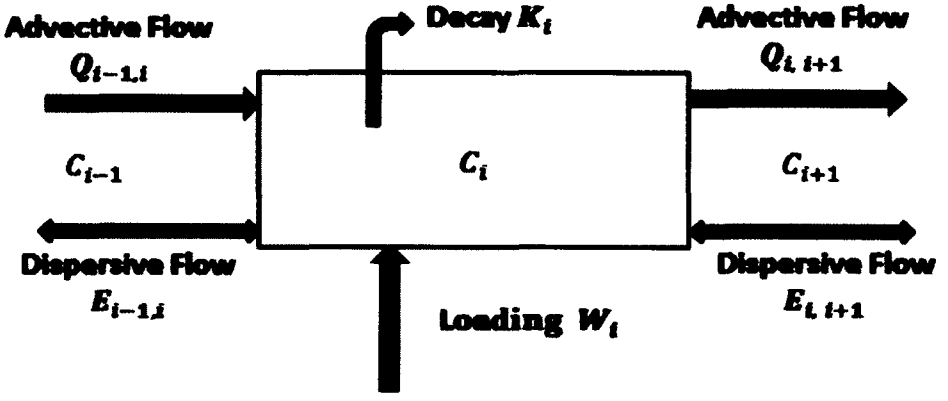

Fig. 3-2. Notation for *i*th Segment Showing Advective Flow, Tidal Dispersion, and Decay of Substance *Ci*

To generalize and estimate the dispersive salinity tidal plume of brine discharge concentrations from a reverse osmosis (RO) desalination system in X (parallel to shoreline) and Y (perpendicular to shoreline) directions from the shoreline, the finite

segment model is developed from the following second-order differential flux equations [34].

$$V\frac{\partial C}{\partial t} = -Q\frac{\partial C}{\partial x}\Delta x - \Delta QC + \frac{\partial}{\partial x}\left(EA\frac{\partial C}{\partial x}\right)\Delta x - kCV$$

$$V\frac{\partial C}{\partial t} = -Q\frac{\partial C}{\partial y}\Delta y - \Delta QC + \frac{\partial}{\partial y}\left(EA\frac{\partial C}{\partial y}\right)\Delta y - kCV$$

Eq. (3.1)

where C represents the salinity concentration of brine discharged and mixed over time, and E is a combined coefficient term for rate of diffusive and dispersive flux. This flux relationship can be further generalized to reflect spatially invariant flows/discharges and dispersion coefficients in the receiving shore water [34].

$$\frac{dC}{dt} = E_x\frac{d^2C}{dx^2} - U\frac{dC}{dx} - kC$$

$$\frac{dC}{dt} = E_y\frac{d^2C}{dy^2} - U\frac{dC}{dy} - kC$$

Eq. (3.2)

With a constant volume, discretized mass balance components that are representative of substance or salinity flux, transport and fate in a segment then can be expressed by incorporating forward, backward and central components for space and time [34].

$$V_i\frac{\partial C_i}{\partial t} = Q_{i-1,i}C_{i-1} - Q_{i,i+1}C_i + E'_{i-1,i}(C_{i-1} - C_i) + E'_{i+1,i}(C_{i+1} - C_i) - k_iC_iV_i \pm W_i$$

Eq. (3.3)

At the beginning a boundary segment under a steady state becomes

$$0 = Q_{u,i}C_u - Q_{1,2}C_1 + E'_{2,1}(C_2 - C_1) - k_1C_1V_1 \pm W_1$$

Eq. (3.4)

Correspondingly, the mass balance at the last, nth segment can be then expressed by

$$0 = Q_{n-1,n}C_{n-1} - Q_{n,b}C_n + E'_{n-1,n}(C_{n-1} - C_n) + E'_{n,b}(C_b - C_n) - k_nC_nV_n \pm W_n$$

Eq. (3.5)

Further rearranging the above expression for concentration C_i yields the following n-simultaneous equation matrix referred to as the Steady-State Response Matrix (SSRM). This SSRM approach will be used to estimate the dispersive salinity tidal plume [34].

$$\left(-Q_{i-1,i} - E'_{i-1,i}\right)C_{i-1} + \left(Q_{i,i+1} + E'_{i-1,i} + E'_{i,i+1} + k_iC_iV_i\right)C_i + \left(-E'_{i,i+1}\right)C_{i+1} = W_i$$

Eq. (3.6)

The n number of simultaneous equations can be written in matrix form:

$$[A]_{n\times n} \times [C]_{n\times 1} = [\mathrm{W}]_{n\times 1}$$

Eq. (3.7)

where A represents the matrix of coefficients; C is the matrix of unknowns and represents the salinity concentration in each segment, and W is the loading matrix which shows the location and value of the brine plume discharge. In order to obtain the steady state

resultant concentration in each segment, all n linear equations are required to be solved simultaneously.

$$[C]_{n\times 1} = [A]_{n\times n}{}^{-1} \times [\mathrm{W}]_{n\times 1}$$

Eq. (3.8)

The consequent C matrix demonstrates the salinity concentration in each segment. In order to apply this FSM approach the study area around the discharge location is divided into 20 segments of the equal volume. The use of 20 segments is based on ensuring a tridiagonal formation for SSRM. A Δx of 0.4 mi and Δt of six minutes has been chosen for this research based on the stability check result for the selected segment size and corresponding time step. A detailed discussion of the stability check will be given next.

3-2-1- Stability Criteria and Numerical Dispersion Condition

The numerical dispersion would occur in FSM because the method uses the difference approximations rather than continuous spatial derivatives in the mass balance differential equation. The nature of the error can be explained by expanding the first and second orders of a Taylor series.

The function u(x,t) can be approximated on a regular grid as shown in Fig. 3-3.

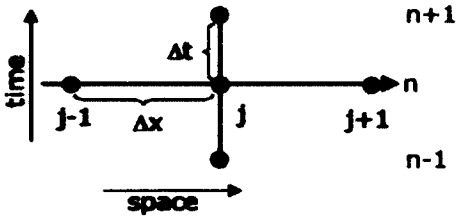

Fig. 3-3. Finite Difference Mesh in Time and Space [20]

In time:

$$u_j^{n+1} = \sum_{m=0}^{\infty} \frac{\Delta t^m}{m!} \left[\frac{\partial^m u}{\partial t^m}\right]_j^n .$$

Eq. (3.9)

In space:

$$u_{j+1}^n = \sum_{m=0}^{\infty} \frac{\Delta x^m}{m!} \left[\frac{\partial^m u}{\partial t^m}\right]_j^n .$$

Eq. (3.10)

Expanding yields:

$$u_{j+1}^n = u_j^n + \Delta x \left[\frac{\partial u}{\partial x}\right]_j^n + \frac{\Delta x}{2} \left[\frac{\partial^2 u}{\partial x^2}\right]_j^n + 0(\Delta x^2) .$$

Eq. (3.11)

Based on this approximation the first order derivatives can be obtained by rearranging the above equation [32]:

$$\left[\frac{\partial u}{\partial t}\right]_j^n = \frac{u_{j+1}^n - u_j^n}{\Delta t} - \frac{\Delta t}{2}\left[\frac{\partial^2 u}{\partial t^2}\right]_j^n + 0(\Delta t^2)$$

$$\left[\frac{\partial u}{\partial x}\right]_j^n = \frac{u_{j+1}^n - u_j^n}{\Delta x} - \frac{\Delta x}{2}\left[\frac{\partial^2 u}{\partial x^2}\right]_j^n + 0(\Delta x^2)\,.$$

Eq. (3.12)

In FSM, only the first term $\left(\frac{u_{j+1}^n - u_j^n}{\Delta t}\right)$ is used to calculate the derivatives and the rest of the equation is neglected, therefore:

$$\left[\frac{\partial u}{\partial t}\right]_j^n = \frac{u_{j+1}^n - u_j^n}{\Delta t}$$

$$\left[\frac{\partial u}{\partial x}\right]_j^n = \frac{u_{j+1}^n - u_j^n}{\Delta x}\,.$$

Eq. (3.13)

Using the same approximation the second order derivatives are [32]:

$$\left[\frac{\partial^2 u}{\partial t^2}\right]_j^n = \frac{u_{j+1}^n - 2u_j^n + u_{j-1}^n}{\Delta t^2}$$

$$\left[\frac{\partial^2 u}{\partial x^2}\right]_j^n = \frac{u_{j+1}^n - 2u_j^n + u_{j-1}^n}{\Delta x^2}.$$

Eq. (3.14)

Substituting these approximations in the advection-diffusion equation we have a Forward Time-Central Difference Space (FTCS) scheme:

$$\frac{u_{j+1}^n - u_j^n}{\Delta t} + v\frac{u_{j+1}^n - u_{j-1}^n}{2\Delta x} - D\frac{u_{j+1}^n - 2u_j^n + u_{j-1}^n}{\Delta x^2} = 0 \ .$$

Eq. (3.15)

By replacing the derivative terms with the Taylor series expansions, it is found that the truncation error is $(\Delta t, \Delta x^2)$. This indicates that FTCS will be consistent if very small time steps and grid spacing are used [32].

There are two criteria to avoid numerical dispersion in FSM. One is focused on advection and is called Courant criterion. The other one focused on diffusion and is called Neumann Criterion. Courant criterion guarantees that the concentration in the segment does not go over the mass dispersed in the advective inflows. Expressly, advective mass from segment 1 to segment 2 has to be the same as mass storage in segment 2 or less, as shown in (Fig. 3-4).

$$Co = \frac{v\Delta t}{\Delta x} \leq 1$$

$$\frac{v\Delta t}{\Delta x} = \frac{\Delta C_2}{C_1} \leq 1$$

Eq. (3.16)

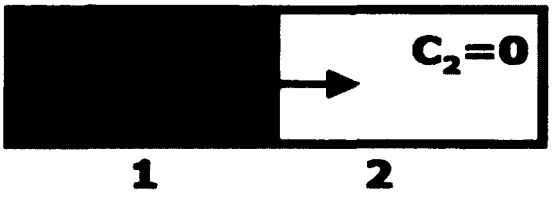

Fig. 3-4. Courant Criterion $\frac{v\Delta t}{\Delta x} = \frac{\Delta C_2}{C_1} \leq 1$

Neumann criterion guarantees that the dispersive mass input from adjacent segments into the segment is less or equal to the segment storage (as illustrated in Fig. 3-5):

$$Ne = \frac{D\Delta t}{(\Delta x)^2} \leq \frac{1}{2}.$$

Eq. (3.17)

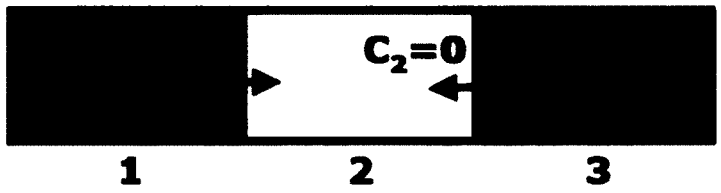

Fig. 3-5. Neumann Criterion $\frac{D\Delta t}{(\Delta x)^2} = \frac{\Delta C_2}{2\Delta C} \leq \frac{1}{2}$

Based on these two criteria the stability of the FSM based on FTCS scheme is guaranteed if:

$$\Delta t \leq \frac{(\Delta x)^2}{2\alpha v} \quad and \quad \Delta x \leq 2\alpha$$

$$Co \leq \frac{1}{2} Pe \quad and \quad Pe \leq 2$$

Eq. (3.18)

where $Pe = \frac{vL}{D}$ and $\alpha = \frac{D}{v}$. Fig. 3-6 shows the zone of the stable FD scheme.

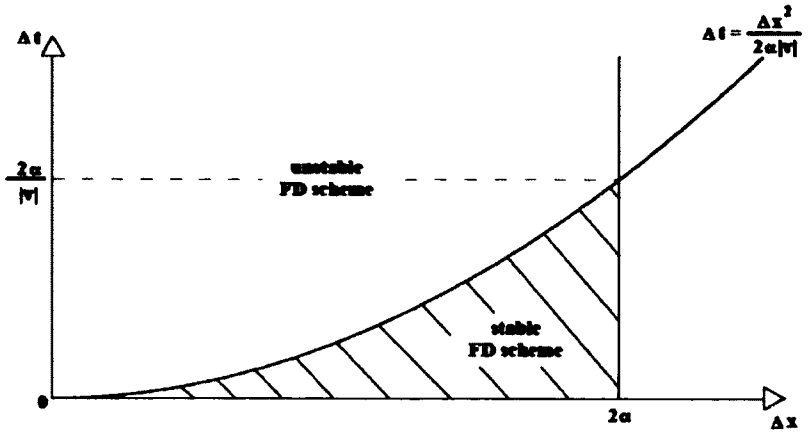

Fig. 3-6. Stability of FTCS Scheme for FSM [20]

In order to use FSM for different locations with different mixing characteristics $\Delta x, \Delta t$ must be chosen from the stable zone shown in Fig. 3-6. For example, for the desalination plant located in the U.S. Virgin Islands, the stable FD scheme based on the value of velocity and dispersion coefficient is shown in Fig. 3-7. As shown, the selected segment size of 0.4 mi with a time step of 6 minutes satisfies the stability conditions to avoid the numerical dispersion in the computation process and fit in the stable FD scheme. The first step in using FSM is to make sure that the selected segment size fits in the stable zone. As a result, for all desalination plant locations simulated in this research, the stability of the segment size of 0.4 mi and time step of 6 minutes has been checked and verified [20].

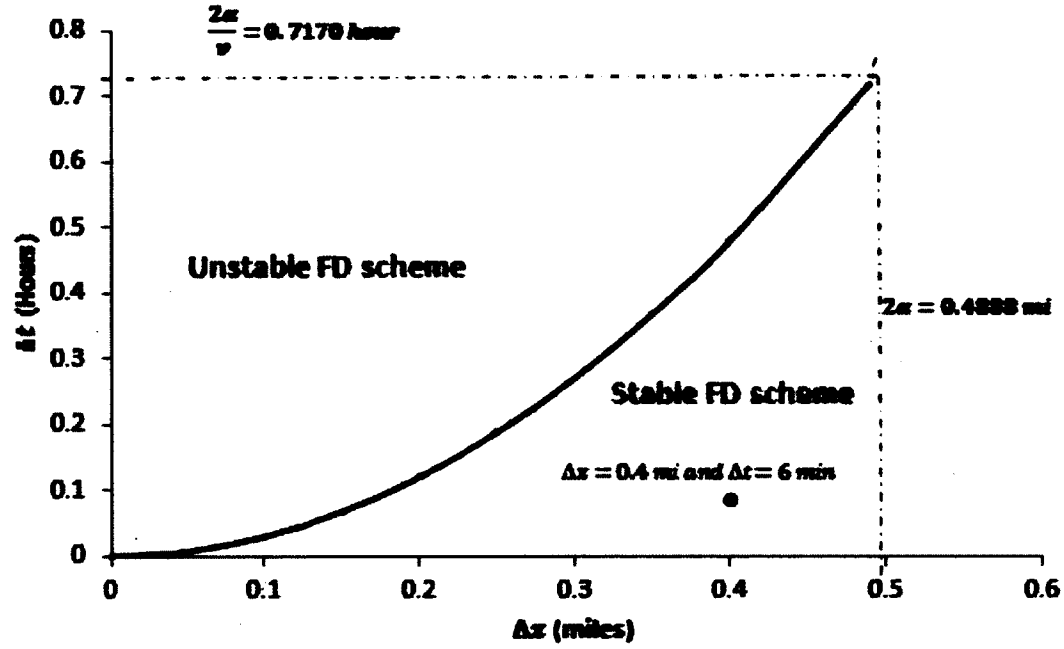

Fig. 3-7. Stability Check of FTCS Scheme for FSM for US-Virgin Islands

Table 3-1 shows the dispersion coefficients and velocity ranges in five different coastal areas studied in this research. As shown, for all the locations the segment size of 0.4 mi and time step of 6 minutes has satisfied the stability conditions to avoid numerical dispersion and subsequently used in case studies for this research.

Table 3-1. Stability Control of the Model for Different Locations with Respect to Designated Segment Size (0.4 mi) and Time Step (6 minutes)

Location	Dispersive Coefficient (mi/d)	Velocity (miles/day)	Δx (miles)	Δt (minutes)	Stability
Caribbean Sea	4 to 6	16	0.4	6	✓
Mediterranean Sea	5.7 to 6	8	0.4	6	✓
Persian Gulf	6 to 9	7	0.4	6	✓
Tampa Bay	2.5	32	0.4	6	✓
California	2	28	0.4	6	✓

In addition to the numerical dispersion concern, the segment volume is another important constraint which dictates the segment size. Since the segments must have equal volume and the water depth is increasing as we move away from the coastline, the segment dimension is variable from one segment to another. Therefore a stable domain must be defined rather than a single value. For example, as shown in Fig. 3-8, the stable range for the U.S. Virgin Islands has been determined by selecting a rectangle from the stable domain as follows:

$$0.32\,mi < \Delta x < 0.48\,mi$$

$$0min < \Delta t < 18min\ ,$$

Eq. (3.19)

or by assuming the constant time step of 6 minutes, we can choose Δx from the following range:

$$0.2\,mi < \Delta x < 0.48\,mi\,.$$

Eq. (3.20)

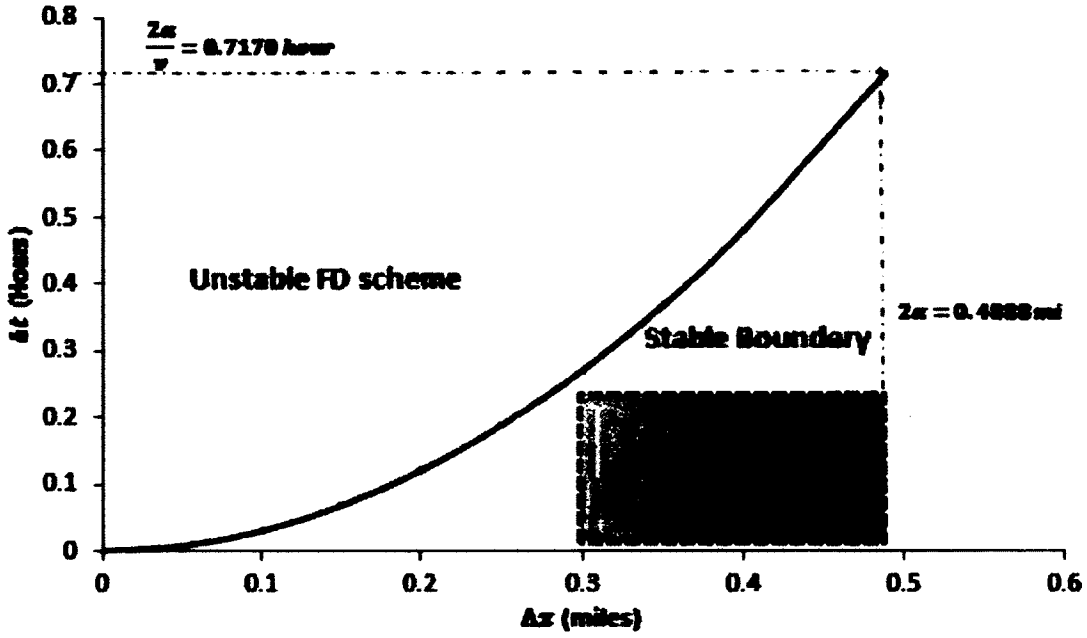

Fig. 3-8. Defining the Stable Boundary for U.S. Virgin Island

3-2-2- Segmentation of the study area

In this section a method has been developed for the segmentation of coastal waters with complex seabed topography. The study area has been divided into 20 segments of equal volume (5 segments parallel × 4 segments perpendicular to the coastline).

The segmentation process starts from the last row which has the longest distance from the coastline. It then moves towards the coastline row by row. To obtain the final segment size a constrained optimization problem has been formulated and solved. There are two main constraints considered in the segmentation process which guarantees a unique solution. The first one requires that all the segments must have an equal volume,

and the second constraint requires that the stability conditions avoid numerical dispersion. The following equation shows the formulation of the optimization problem.

Objective: Minimize the error defined as follows

$$E = \sum_{i=1}^{20} (V_{avg} - V_i)^2$$

Eq. (3.21)

subjected to:

$$V_{avg} - V_i \leq 10m^3$$

$$\Delta x_{min} \leq \Delta x \leq \Delta x_{max}$$

Eq. (3.22)

where V_{avg} represents the volume of the entire study area divided by 20, and V_i is the volume of i^{th} segment. The current optimization problem has been solved using the MATLAB optimization toolbox. Fig. 3-9 shows the resultant optimized segmentation for a case study site located in the U.S. Virgin Islands in the Caribbean Sea.

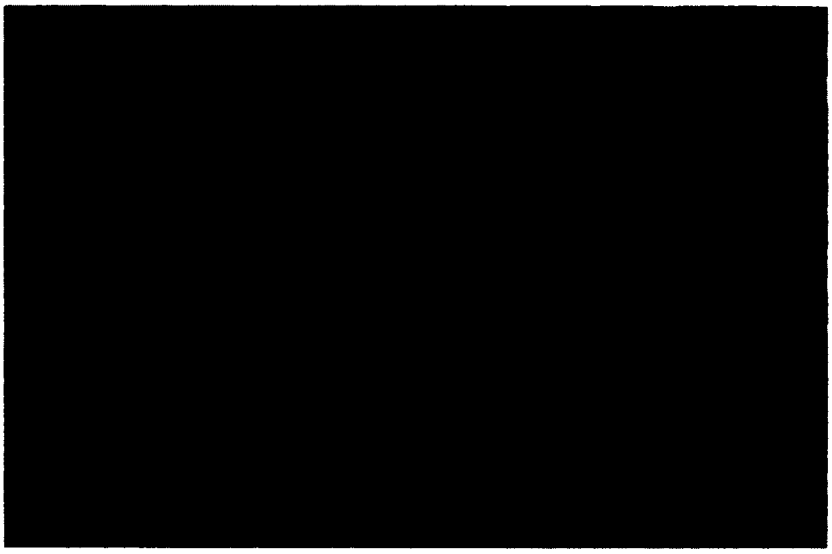

Fig. 3-9. Segmentation of the Study Area Using Optimization Approach

3-2-3- Application of FSM Brine Plume Dispersion Simulation in Coastal Waters

As described in Section 3-2-2, for the segmentation process, the study area is divided into 20 segments of an equal volume. Fig. 3-9 shows the segmentation of the coastal area for a desalination plant located in the U.S. Virgin Islands. As shown in the figure, there are five segments in each row and four segments in each column. All the segments have an equal volume. The brine plume is discharged to the first row and third column which is the location of the third segment (the green segment).

Rearranging the mass balance equations for each segment and representing them in matrix form (Eq. (3.7)) leads to a series of twenty simultaneous equations (Fig 3-10). Each row of these matrix-form equations represents the mass balance equation for the corresponding segment number. For example, the fifth row represents the mass balance equation for segment 5. As previously described, matrix A is called the matrix of coefficients and contains all the constant parameters such as dispersion coefficient and

velocity. Matrix S is called the matrix of unknowns and contains all the concentration values for each segment. Matrix W contains all the loading values, and since there is only one point of discharge (segment 3) other than w_3 all the other components of this matrix are equal to zero. By calculating the inverse of matrix A and substituting it in Eq. (3.8), all the unknown concentrations will be obtained. Since A^{-1} is computed based on a steady state assumption, it is called steady state response matrix (SSRM).

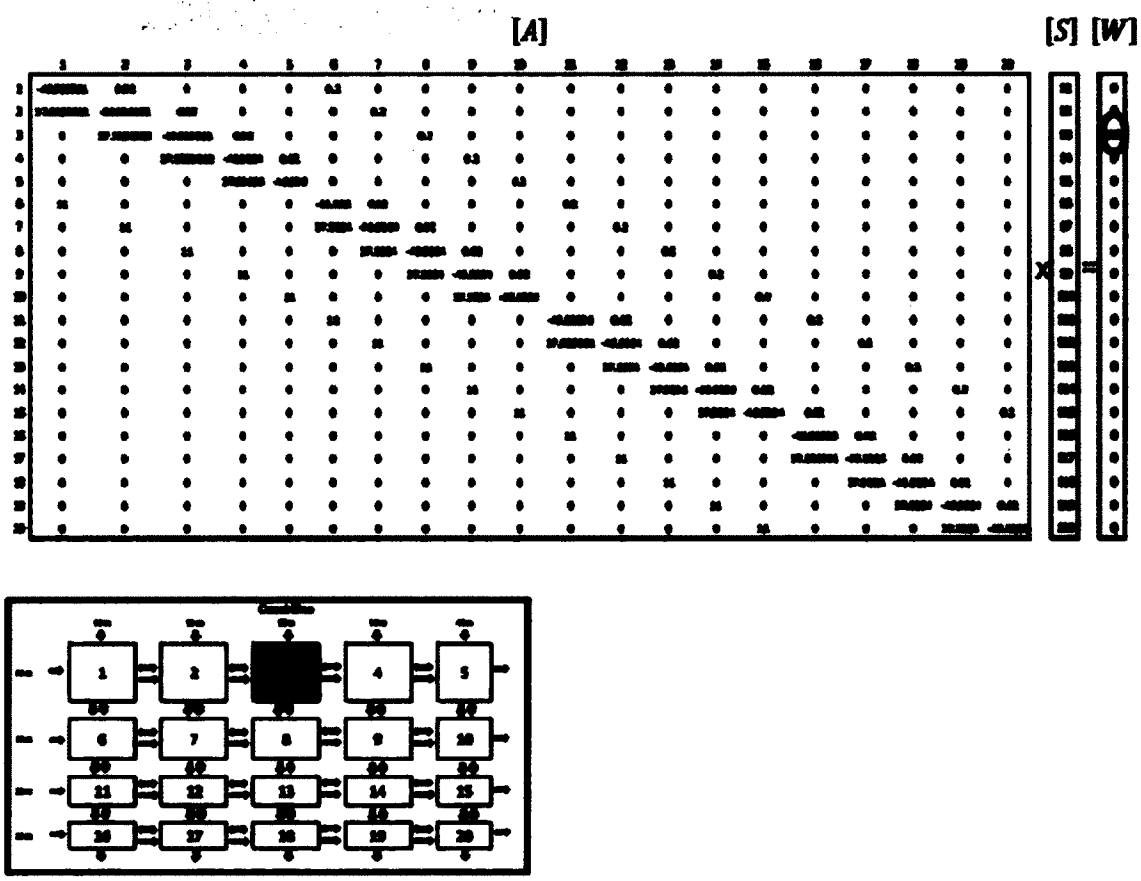

Fig 3-10. Segmentation and 20 Linear Equations in Matrix Form

Although FSM is developed based on a steady state assumption, and its solution is a steady state response; it is still applicable to time dependent and transient problems. The key element to convert the steady state analysis to the transient one is to update the matrix of coefficients with time dependent parameters. Since the only time dependent parameter is the velocity of tidal current, by updating the matrix of coefficients with the corresponding velocity the updated concentration will be calculated for that time step. In order to update the matrix of coefficients, the velocity of the current can be defined as a linear or harmonic function. In this research the velocity is defined using a harmonic function as shown in Fig. 3-11.

$$v = V + A\cos(\omega t)$$

Eq. (3.23)

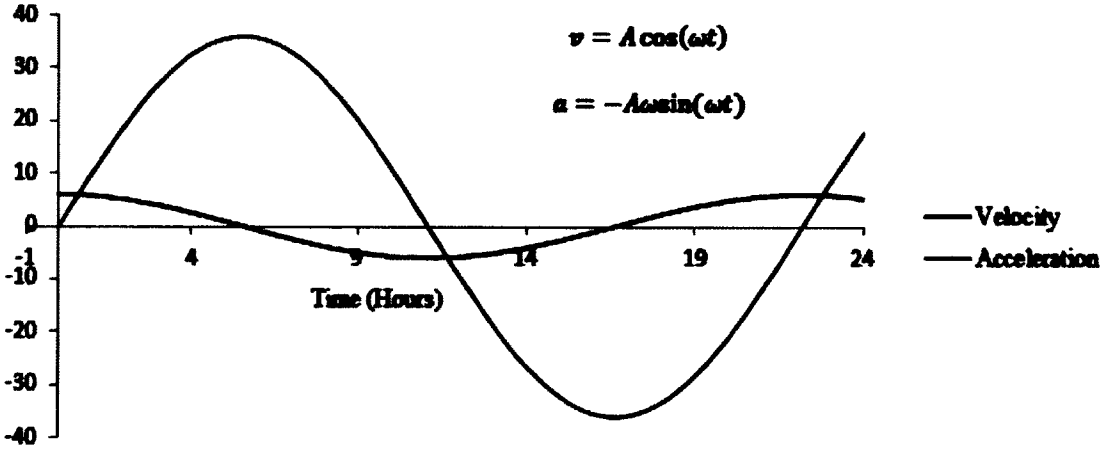

Fig. 3-11. Defining the Velocity Using a Harmonic Function

This harmonic function approach facilitates simulation of the oscillating and tidally influenced flow. In some coastal regions where the velocity profile is more complicated the velocity can be represented with a combination of multiple harmonic functions (Fig. 3-12). As shown in Fig. 3-11, the velocity is changing from a positive value (ebb) to zero value (stagnation point) and then to a negative value (flood) as a function of time. This provides a relatively accurate representation of temporal tidal conditions.

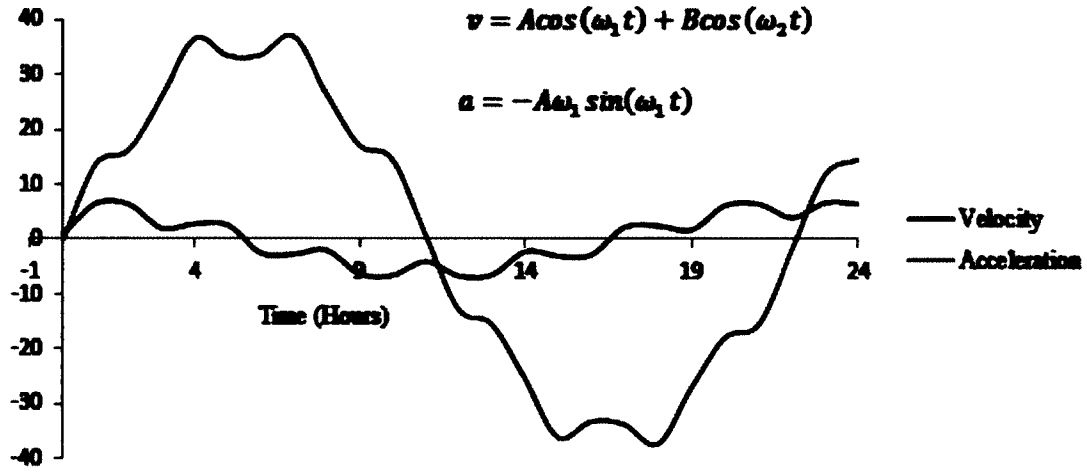

Fig. 3-12. Defining the Velocity Using Multiple Harmonic Functions

By computing the velocity value for each time step and creating the system of mass balance equations in matrix form for corresponding velocity and solving for C, the resulting concentrations will demonstrate the brine dispersion with respect to the time. This quasi steady state method is a flexible and efficient way to study and evaluate the

temporal brine dispersion in coastal waters. As discussed, a time step of six minutes has been selected to avoid numerical dispersion. Therefore, the velocity as well as the matrix of coefficients has been updated every six minutes. The system of mass balance equations has been solved with updated values to calculate the salinity concentrations with respect to time. Fig. 3-13 shows the resulting brine dispersion for the Kish Island desalination plant in the Persian Gulf using FSM.

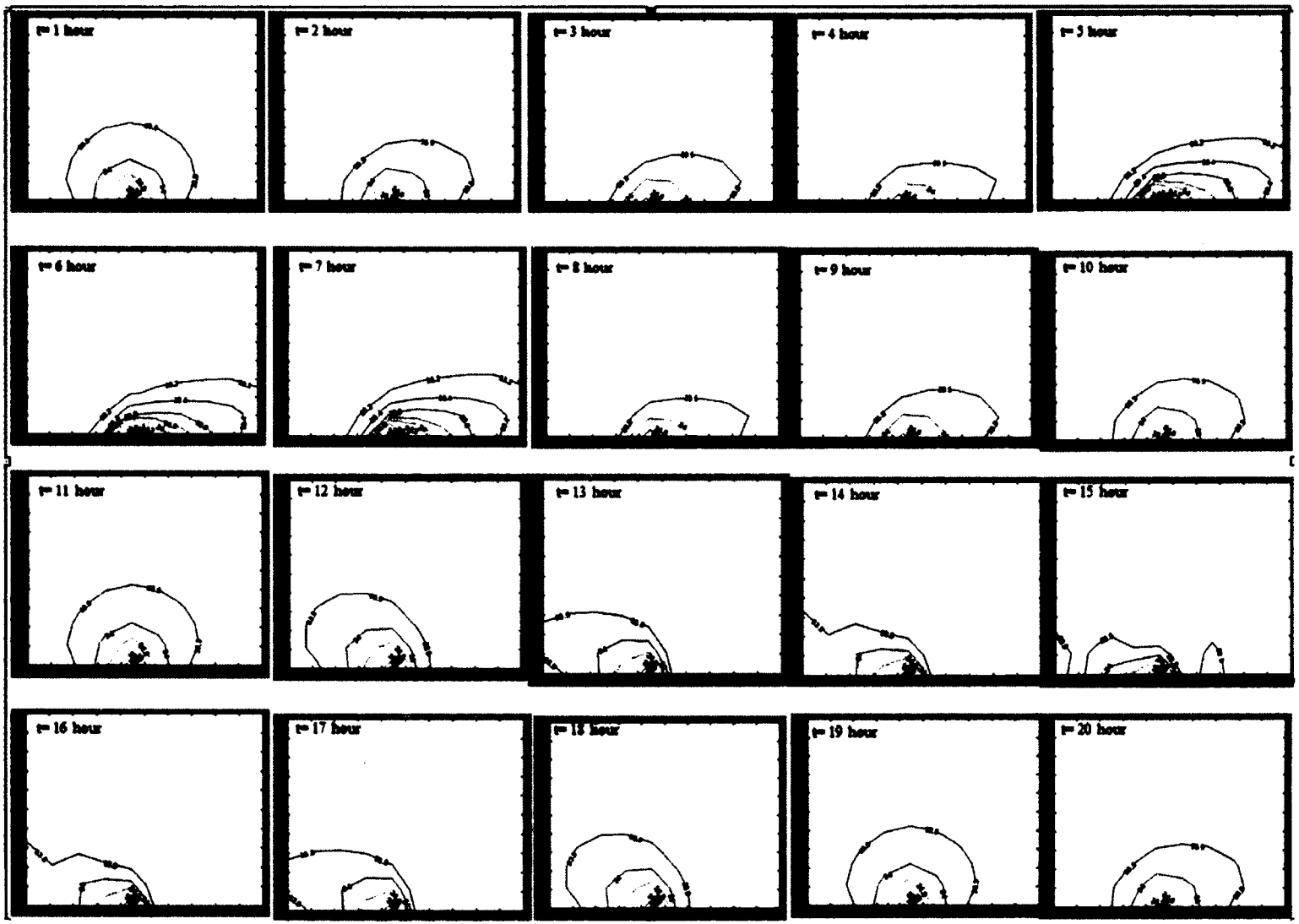

Fig. 3-13. Brine Dispersion Simulation Using FSM (Kish Island, Persian Gulf)

3-2-4- Advantages and disadvantages of FSM

FSM is a very capable method of simulating brine dispersion in tidally influenced environments. This method is capable of simulating brine dispersion with any complex seabed geometry. The Finite Segment discretization scheme is one of the simplest forms of discretization and does not include the topological nature of partial differential equations. FSM is easy to implement and is capable of simulating spatial and temporal brine dispersion in coastal waters. Its ability to simulate the time dependent response to the brine discharge as well as its simplicity to simulate multiple point loads and diffusers make it a very applicable method in modeling and simulating plume dispersion in coastal areas. As shown in Fig. 3-14, FSM can simply model vertical, horizontal or any combination of multiple loading scenarios without any additional computation. The only difference in expressing multiple loads and single point load in FSM formulation is in formation of the loading matrix itself. As an example, Fig. 3-15 shows the segmentation of a coastal area for two different loading scenarios. The general FSM formulation for these four segments will be:

$$[A] \times [C] = [W]$$

$$\begin{bmatrix} A_{11} & A_{12} & A_{13} & A_{14} \\ A_{21} & A_{22} & A_{23} & A_{24} \\ A_{31} & A_{32} & A_{33} & A_{34} \\ A_{41} & A_{42} & A_{43} & A_{44} \end{bmatrix} \times \begin{bmatrix} C_1 \\ C_2 \\ C_3 \\ C_4 \end{bmatrix} = \begin{bmatrix} W_1 \\ W_2 \\ W_3 \\ W_4 \end{bmatrix}$$

Eq. (3.24)

where $[A]$ is the matrix of coefficients, $[C]$ is the matrix of unknowns (concentrations), and $[W]$ is the loading matrix. For single point load (part A of Fig. 3-15) we have

$$\begin{bmatrix} A_{11} & A_{12} & 0 & 0 \\ A_{21} & A_{22} & A_{23} & 0 \\ 0 & A_{32} & A_{33} & A_{34} \\ 0 & 0 & A_{43} & A_{44} \end{bmatrix} \times \begin{bmatrix} C_1 \\ C_2 \\ C_3 \\ C_4 \end{bmatrix} = \begin{bmatrix} w_1 \\ 0 \\ 0 \\ 0 \end{bmatrix}.$$

Eq. (3.25)

In solving multiple-load problems (part B of Fig. 3-15), the matrix of coefficients (A) and matrix of unknowns (C) will remain unchanged compared to the single load problem. The only changing matrix is the loading matrix (w). In the loading matrix there are more non-zero values.

$$\begin{bmatrix} A_{11} & A_{12} & 0 & 0 \\ A_{21} & A_{22} & A_{23} & 0 \\ 0 & A_{32} & A_{33} & A_{34} \\ 0 & 0 & A_{43} & A_{44} \end{bmatrix} \times \begin{bmatrix} C_1 \\ C_2 \\ C_3 \\ C_4 \end{bmatrix} = \begin{bmatrix} w_1 \\ w_2 \\ w_3 \\ 0 \end{bmatrix}$$

Eq. (3.26)

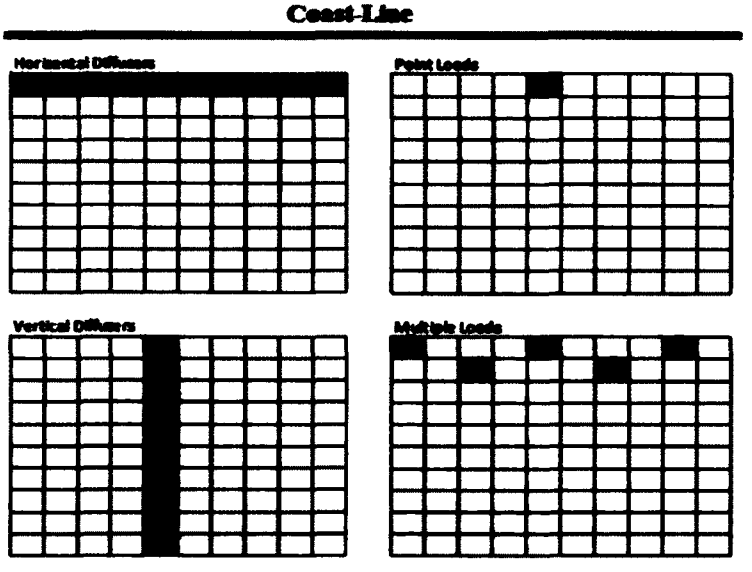

Fig. 3-14. Proficiency of FSM in Modeling Different Loading Scenarios (Plan View)

As shown, multiple loading does not add any additional complexity and computational time to the problem in FSM. Unlike FSM, in other analytical methods, modeling multiple loading requires extra effort and sharply increases the complexity of the problem and consequently, the computational time.

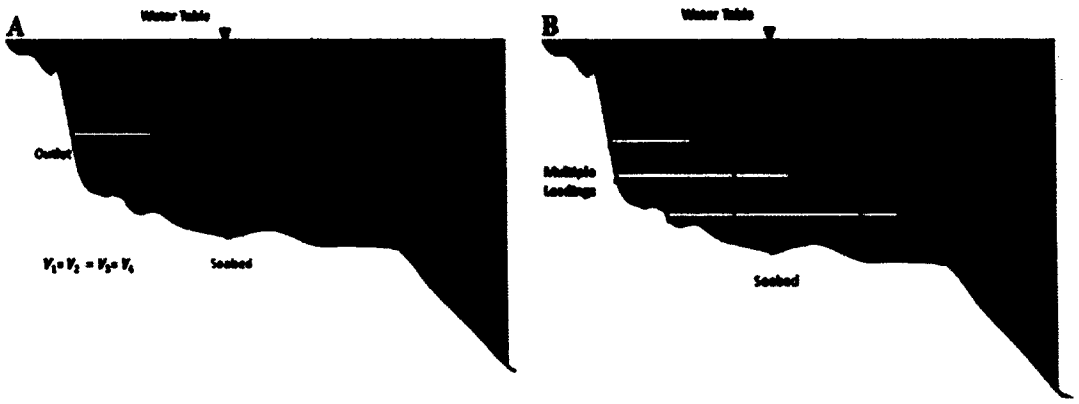

Fig. 3-15. Point Load (A) Vs. Multiple Loading (B) in FSM (Section View)

Although FSM is a very practical method, applicable to solving very complicated plume dispersion problems with complex loading scenarios and seabed geometry, the range of its applicability and limitation must be recognized. Since this method is based on the assumption of a steady state condition and the resultant concentration vector expresses the steady state response, it is necessary to verify whether the steady state assumption is valid for its application. While FSM is applicable for the majority of coastal areas, in some cases with high dispersive characteristics in addition to very low advective characteristics, FSM is not the ideal methodology. The steady state condition is

not a valid hypothesis in these regions. The model encounters a large amount of error; hence, the result would be unreliable.

Since FSM is a very useful method in simulating plume dispersion in coastal areas, it is essential to understand the range of its applicability. In the following chapters a method, a dimensionless criteria for selecting tidally-influenced advective-dispersive brine mixing plume characterization models, namely a non-dimensional number, Shahvari-Yoon (SY) number, has been developed to identify the applicability of FSM.

3-3- Analytical Model (AM)

The analytical model (AM) presented in this research was based on the assumptions of incompressible flow, Fickian diffusion and uniform diffusivities. With respect to these assumptions the advective-diffusive equation is [26]:

$$\frac{\partial c}{\partial t} + u\frac{\partial c}{\partial x} + v\frac{\partial c}{\partial y} + w\frac{\partial c}{\partial z} - D_x\frac{\partial^2 c}{\partial x^2} - D_y\frac{\partial^2 c}{\partial y^2} - D_z\frac{\partial^2 c}{\partial z^2} + Kc = Q\delta(x)\delta(y).$$

Eq. (3.27)

Since the brine plume is considered a conservative substance and it does not decay with respect to time the above equation can be simplified as [26]:

$$\frac{\partial c}{\partial t} + u\frac{\partial c}{\partial x} + v\frac{\partial c}{\partial y} + w\frac{\partial c}{\partial z} - D_x\frac{\partial^2 c}{\partial x^2} - D_y\frac{\partial^2 c}{\partial y^2} - D_z\frac{\partial^2 c}{\partial z^2} = Q\delta(x)\delta(y).$$

Eq. (3.28)

Based on the brine loading characteristics we can rewrite the above equation and solve it analytically. Substituting the oscillating flow using the following harmonic equation we have

$$U(t) = V + u_0 \sin \omega t$$

$$\frac{\partial c}{\partial t} + U(t)\frac{\partial c}{\partial y} - D_x \frac{\partial^2 c}{\partial x^2} - D_y \frac{\partial^2 c}{\partial y^2} = 0$$

Eq. (3.29)

where c is the salinity increase above the ambient salinity and D_x and D_y are dispersive coefficients in the x and y directions. Applying the following boundary conditions,

$$c \to 0 \; as \; x \to \infty \; or \; y \to \pm\infty$$

$$\frac{\partial c}{\partial x} = 0 \; @ \; x = 0, for \; all \; y.$$

Eq. (3.30)

The first boundary represents that the salinity increase contributed by the brine discharge approaches a zero very far from the discharge location, and the second boundary means that the coastline behaves as a solid boundary without any flux.

The solution for this partial differential equation will be [30]

$$C_c(x,y,t) = \frac{C_0 Q}{4\pi h_0 \sqrt{D_x D_y}} \left\{ \int_0^t exp\left[-\frac{(x-x_0)^2}{4D_x(t-t_0)} - \frac{\left[y - V(t-t_0) + \frac{U_0}{\omega}(cos\omega t - cos\omega t_0)\right]^2}{4D_y(t-t_0)} \right] + exp\left[-\frac{(x+x_0)^2}{4D_x(t-t_0)} - \frac{\left[y - V(t-t_0) + \frac{U_0}{\omega}(cos\omega t - cos\omega t_0)\right]^2}{4D_y(t-t_0)} \right] \right\} \frac{dt_0}{t-t_0}$$

Eq. (3.31)

where C_0 is the discharge concentration, and Q is the brine discharge flow rate.

Equation 25 can be written in dimensionless form as follow s [30]:

$$C_c^*(\xi,\eta,\tau) = \int_0^\tau \frac{d\tau_0}{\tau_0} \left\{ exp\left[-\lambda\alpha^2 \frac{(\xi-\xi_0)^2}{\tau_0} \right] + exp\left[-\lambda\alpha^2 \frac{(\xi+\xi_0)^2}{\tau_0} \right] \right\} \times exp\left[-\lambda \frac{[\eta - \upsilon\tau_0 + cos\tau - \cos(\tau-\tau_0)]^2}{\tau_0} \right]$$

Eq. (3.32)

Where $\upsilon = \frac{V}{U_0}, \lambda = \frac{U_0^2}{4\omega D_y}, \alpha^2 = \frac{D_y}{D_x}$.

υ represents the advective aspect, and λ, α^2 signifies the dispersive feature of the mixing process.

These solutions (Eq. (3.31) and Eq. (3.32)) have been used for coastal regions with constant depth. For a variable seabed the following equation has been solved:

$$\frac{\partial c}{\partial t}+\frac{\partial}{\partial x}(hUc)-\frac{\partial}{\partial y}\left(hD\frac{\partial c}{\partial y}\right)=Q\delta(t)\delta(x)\delta(y+lh_0).$$

Eq. (3.33)

As described in chapter two, for impulse loading the solution is [27]:

$$C_1*=\frac{1}{mx*}\frac{1}{(\alpha y*)^{3/4}}\exp\left(-\frac{y*+\alpha}{x*}\right)I_{3/2}\left(\frac{2\sqrt{\alpha y*}}{x*}\right)$$

$$C_2*=\frac{f}{\sqrt{4\pi x*}}\left|\exp\left(-\frac{(y*-\alpha)^2}{4x*}\right)+exp\left(-\frac{(y*+\alpha)^2}{4x*}\right)\right|$$

Eq. (3.34)

where $I_{3/2}$ is a modified Bessel function of the first kind, C_1* is the concentration at the slope location, C_2* is the concentration after the slope, x= $\frac{x*U_0h_0^2}{D_0}$, $C_1=\frac{C_1*Q}{U_0h_0^2}$, $C_2=\frac{C_2*Q}{U_0h_0^2}$, $U=U_0y*^{1/2}$.

where factor f is equal to

$$f=\frac{1}{m}\sqrt{\frac{4\pi}{x*}}\frac{1}{(\alpha l)^{3/4}}I_{3/2}\left(\frac{2\sqrt{\alpha l}}{x*}\right)\frac{\exp\left(-\frac{l+\alpha}{x*}\right)}{\exp\left(-\frac{(l-\alpha)^2}{4x*}\right)+exp\left(-\frac{(l+\alpha)^2}{4x*}\right)}.$$

Eq. (3.35)

For continuous loading the resulting concentration will be [27]:

$$C_1*=\left\{\int_0^t\frac{1}{mx*}\frac{1}{(\alpha y*)^{3/4}}exp\left(-\frac{y*+\alpha}{x*}\right)I_{3/2}\left(\frac{2\sqrt{\alpha y*}}{x*}\right)\right\}\frac{dt_0}{t-t_0}$$

$$C_2 *= \left\{ \int_0^t \frac{f}{\sqrt{4\pi x *}} \left[exp\left(-\frac{(y* - \alpha)^2}{4x*} \right) + exp\left(-\frac{(y* + \alpha)^2}{4x*} \right) \right] \right\} \frac{dt_0}{t - t_0}.$$

Eq. (3.36)

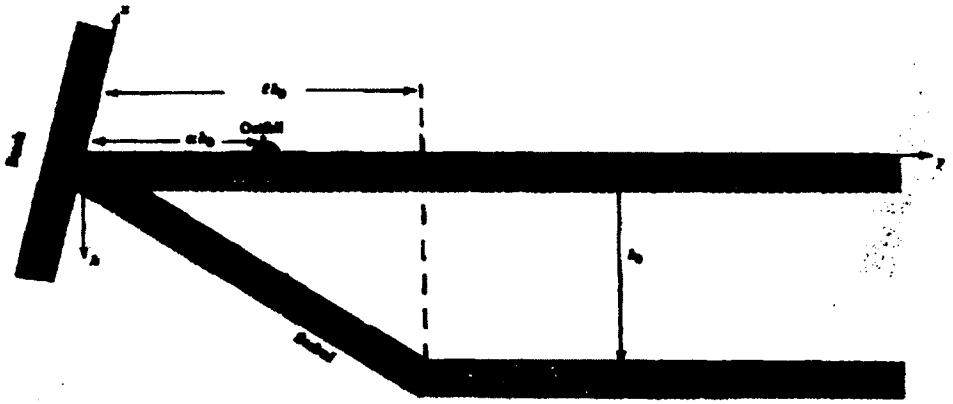

Fig. 3-16. Seabed Depth Profile of a Sloping Beach (Purnama and Barwani .2003) [27]

3-3-1- Application of AM Brine Plume Dispersion Simulation in Coastal Waters

AM is a very suitable approach for simulating transient brine dispersion in coastal waters. To demonstrate the proficiency of this method, the brine dispersion in four different locations has been simulated. Since this method is formulated to simulate brine dispersion for a single seabed slope, the slope is roughly assumed to be 1% for all four regions. Table 3-2 shows the dispersion coefficient's range as well as the velocity value for these locations. The duration of the simulation for all the case studies is 100 days.

Table 3-2. Stability Control of the Model for Different Locations with Respect to Designated Segment Size (0.4 mi) and Time Step (6 Minutes)

Name of Desalination	Location	Mixing Characteristics	$D\left(\frac{mi^2}{d}\right)$	$V\left(\frac{mi}{d}\right)$	$\tau = 400\pi$	Maximum Concentration (PSU)
Huntington Beach	West Coast	Advective-Dispersive	2	28	100 days	34.1
Tampa Bay	Florida	Advective	2.5	32	100 days	37
Maspalomas	Canary Island	Dispersive	5.7-8	5	100 days	38
Kish Island	Persian Gulf	Dispersive	6-9	7	100 days	38.5

Fig. 3-17 demonstrates the brine propagation at the end of simulation (100 days). The ambient salinity for all case studies is assumed to be 33 PSU. As expected, the brine propagates much faster in Tampa Bay as a result of high flow velocity. The maximum concentration of salinity around the outlet is 34.1 (1.1 PSU above the ambient salinity). In Huntington Beach, where flow velocity and tidal range are intermediate, the brine propagates fairly fast. The maximum concentration achieved is 37 PSU which is 2.9 PSU more than Tampa Bay. In Canary and Kish Islands, as a result of small tidal range and flow velocity, the coastal area is high dispersive dominant. In these cases, the brine spreads slowly, and the concentrations of above 38 have been simulated around the outlet location. The radius of influence of the brine discharge is also larger compared to those of Huntington Beach and Tampa Bay.

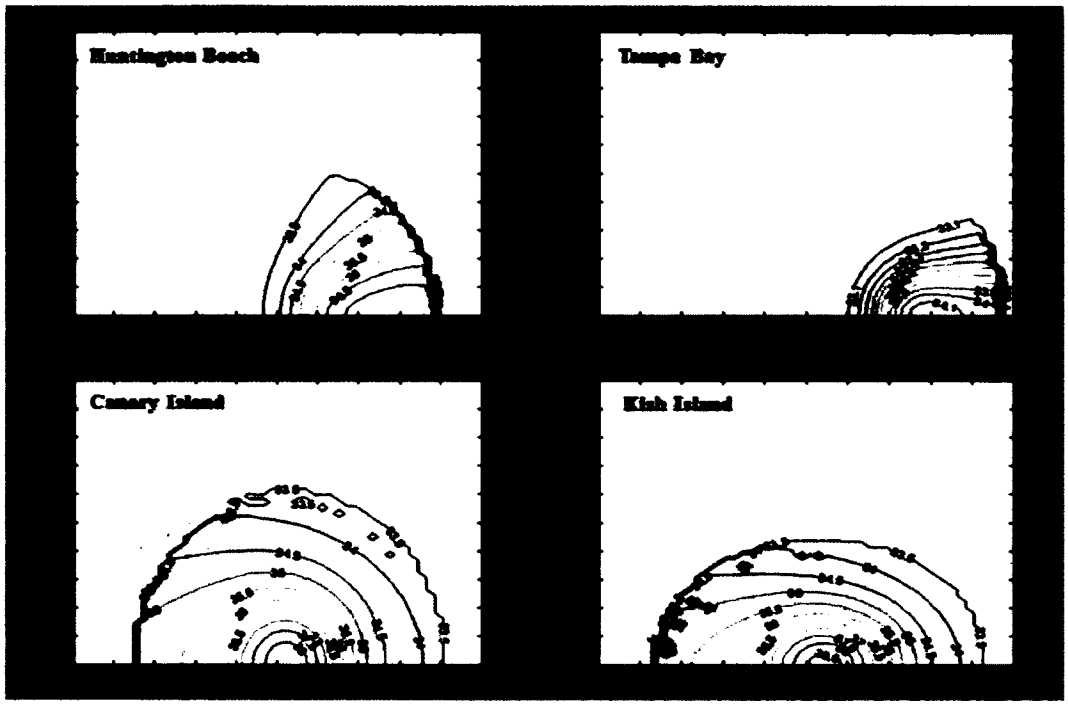

Fig. 3-17. Brine Dispersion Simulation for 4 Locations with Different Mixing Characteristics

As shown, AM facilitates a powerful and practical way to study brine dispersion in coastal waters. Due to the time-variant nature of this method, it is an excellent way to study the brine propagation as a function of time in a tidal cycle. It can simply simulate the outlet length by determining the discharge location as a function of x and y. Fig. 3-18, Fig. 3-19, and Fig. 3-20 illustrate the brine dispersion for a simulation period of 24 hours and the outlet length of 100 meters, showing the brine plume movement with tide and ebb in a detailed and accurate manner. Maximum concentration occurred during the stagnation points when the tidal cycle is changing from flood to ebb and vice versa. For example t = 1hr is one of the stagnation points.

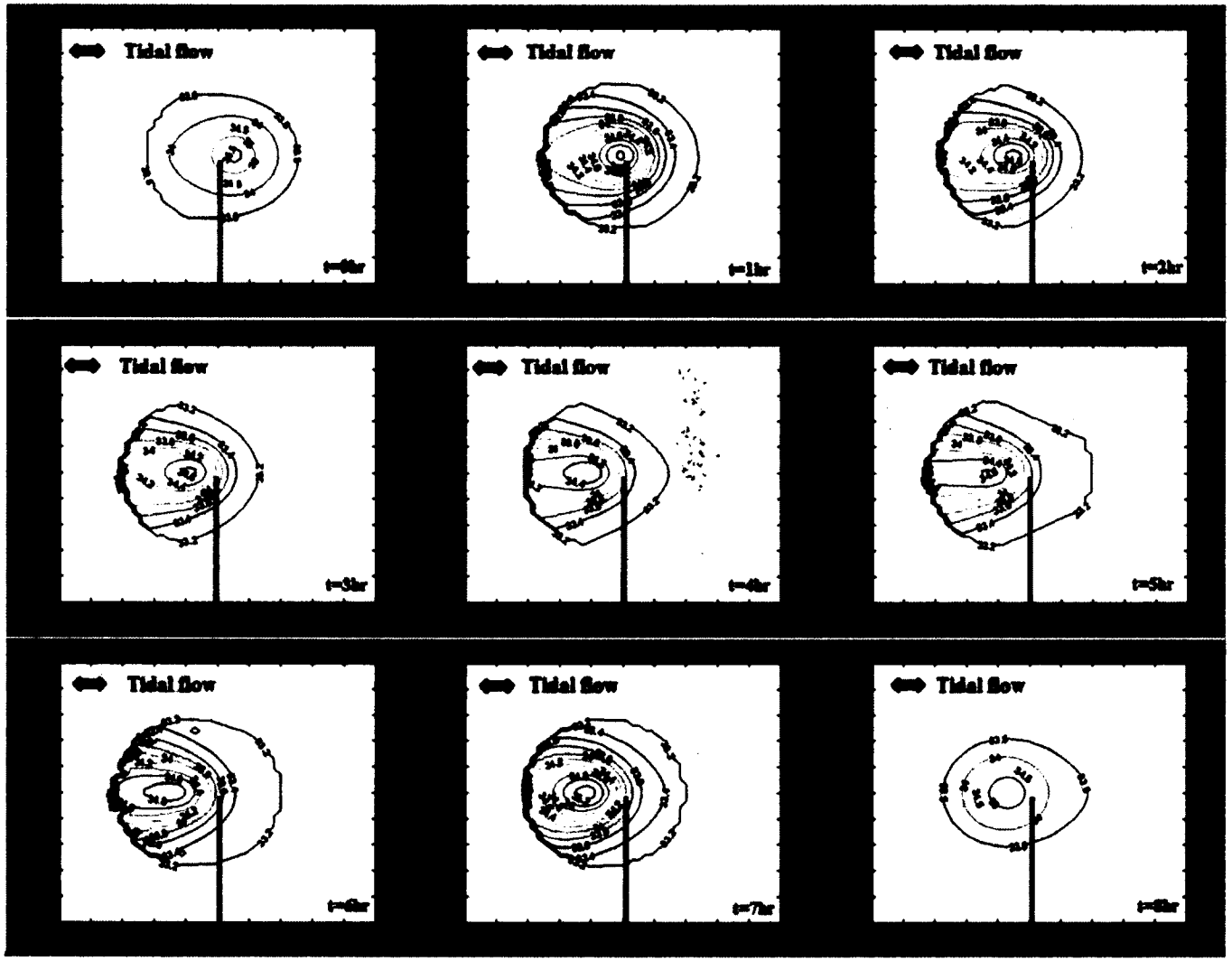

Fig. 3-18. Brine Dispersion with an Outlet Length of 100 Meters (t= 1 hour to 9 hour)

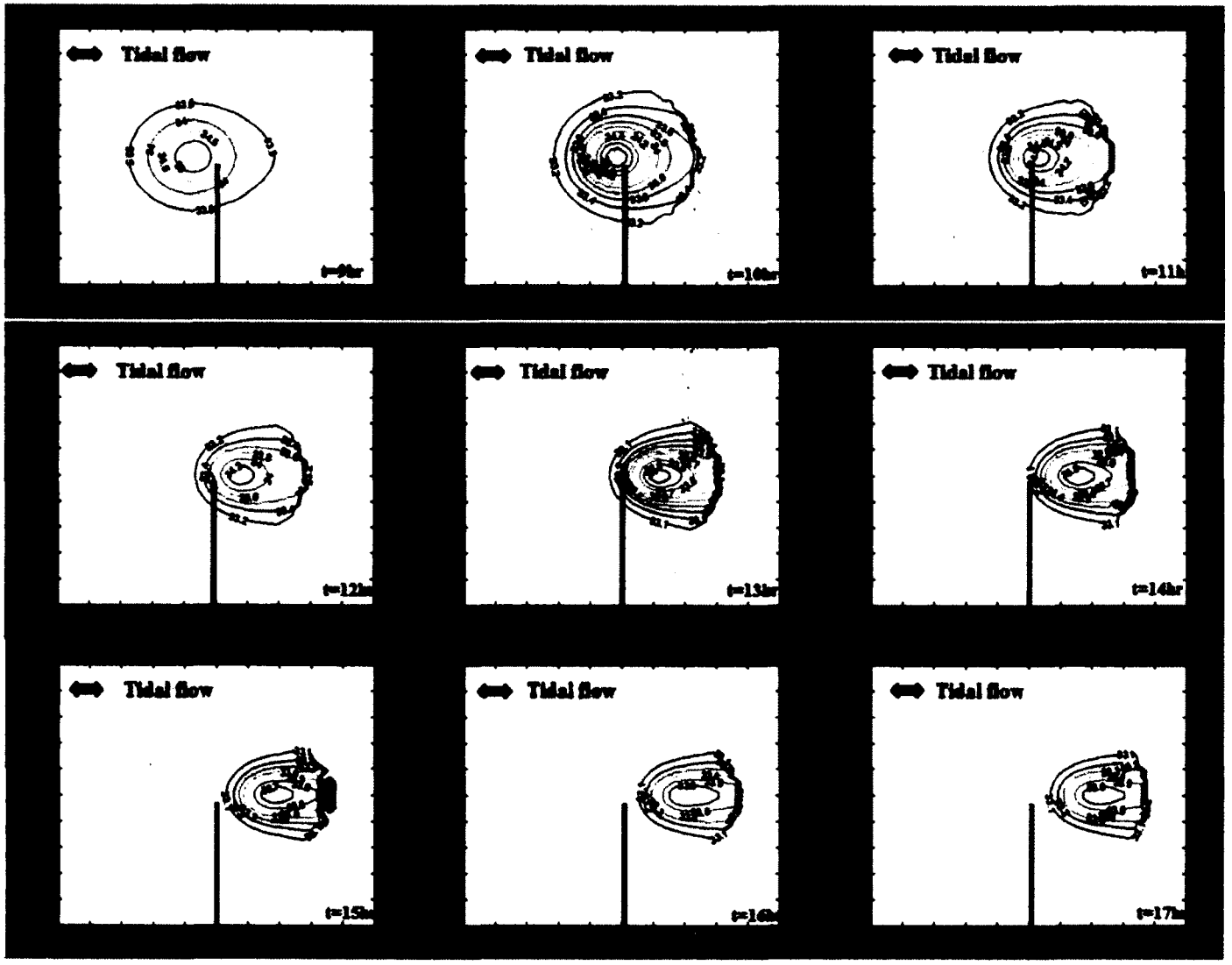

Fig. 3-19. Brine Dispersion with an Outlet Length of 100 Meters (t= 10 hour to 17 hour)

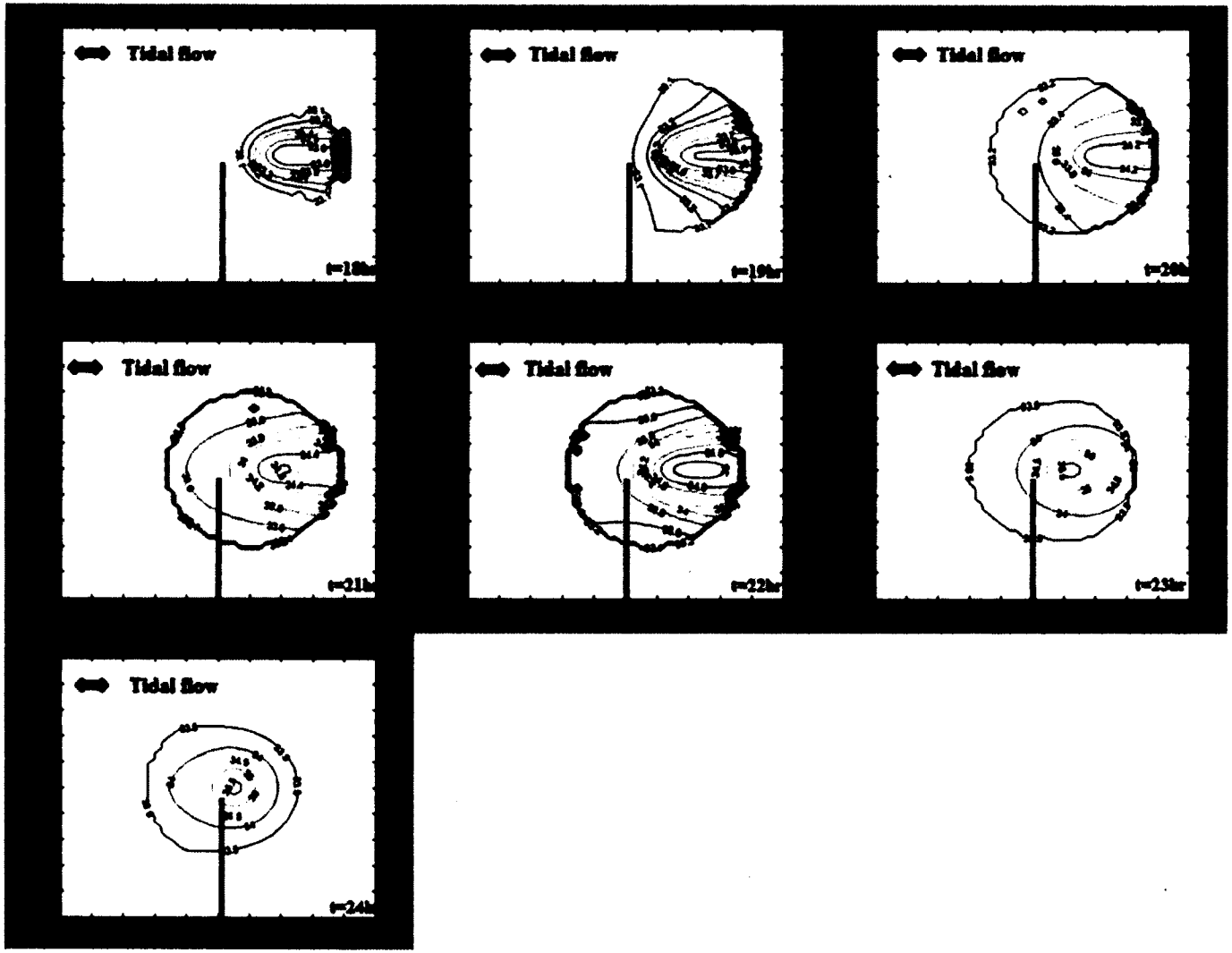

Fig. 3-20. Brine Dispersion with an Outlet Length of 100 Meters (t= 18 hour to 24 hour)

3-3-2- Advantages and disadvantages of AM

AM is a very powerful method that is able to simulate transient plume dispersion with the presence of oscillating flow. It can simply simulate a single outlet of any length. The seabed topography is also reflected by being approximated with a constant slope. Although this method is very easy to use in places with simple topography, which is the case for most coastal areas, it cannot be applied in locations with a complex, locally varying seabed profile. For example, Fig. 3-21 shows a good example of a complex seabed shape near the outlet location. It would be difficult to simulate such a seabed profile using a constant slope approximation. In order to obviate such localized topographic variations of seabed shape, the study area needs to be divided into seven zones with different slopes. Thus, seven separate models need to be developed to simulate the plume dispersion in this location. The resulting concentration will be obtained by superimposing all seven models. Dividing the model into seven models because of the complexity of the seabed shape not only increases the computation time but also increases the degree of complexity of the problem since separate boundary conditions have to be defined for each model.

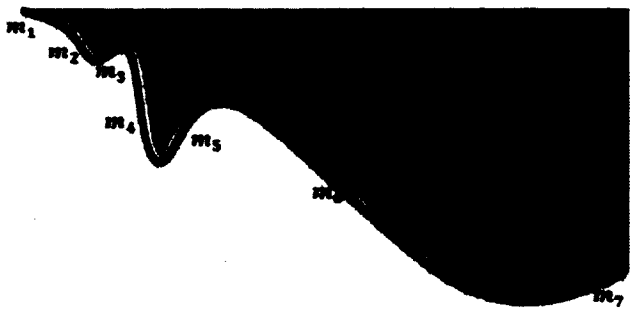

Fig. 3-21. Complex Seabed Topography with Changing Seabed Slope

The other disadvantage of AM is the difficulty in simulating the complex loading scenarios. Although modeling of a single point load with any outlet length is not a problem in AM, simulating multiple point loads and diffusers is not an easy process and increases the complexity of the problem. Fig. 3-22 shows an example of modeling multiple outlets in AM. As shown, there are three outlets with lengths of 20, 40 and 60 meters from the coastline that have been designed to discharge the brine in coastal waters. AM is formulated in a way that can simulate one point load at a time. To simulate this problem, three models with three single point loads have been developed. To calculate the resulting concentration of all three outlets, the method of superposition has been used.

In summary, AM is a very powerful and accurate method for simulating time variant brine dispersion problems on a sloping seabed. While this method is an efficient way of simulating brine dispersion in coastal waters with a simple seabed profile and single outlet, this method becomes less practical as the complexity of the problem increases.

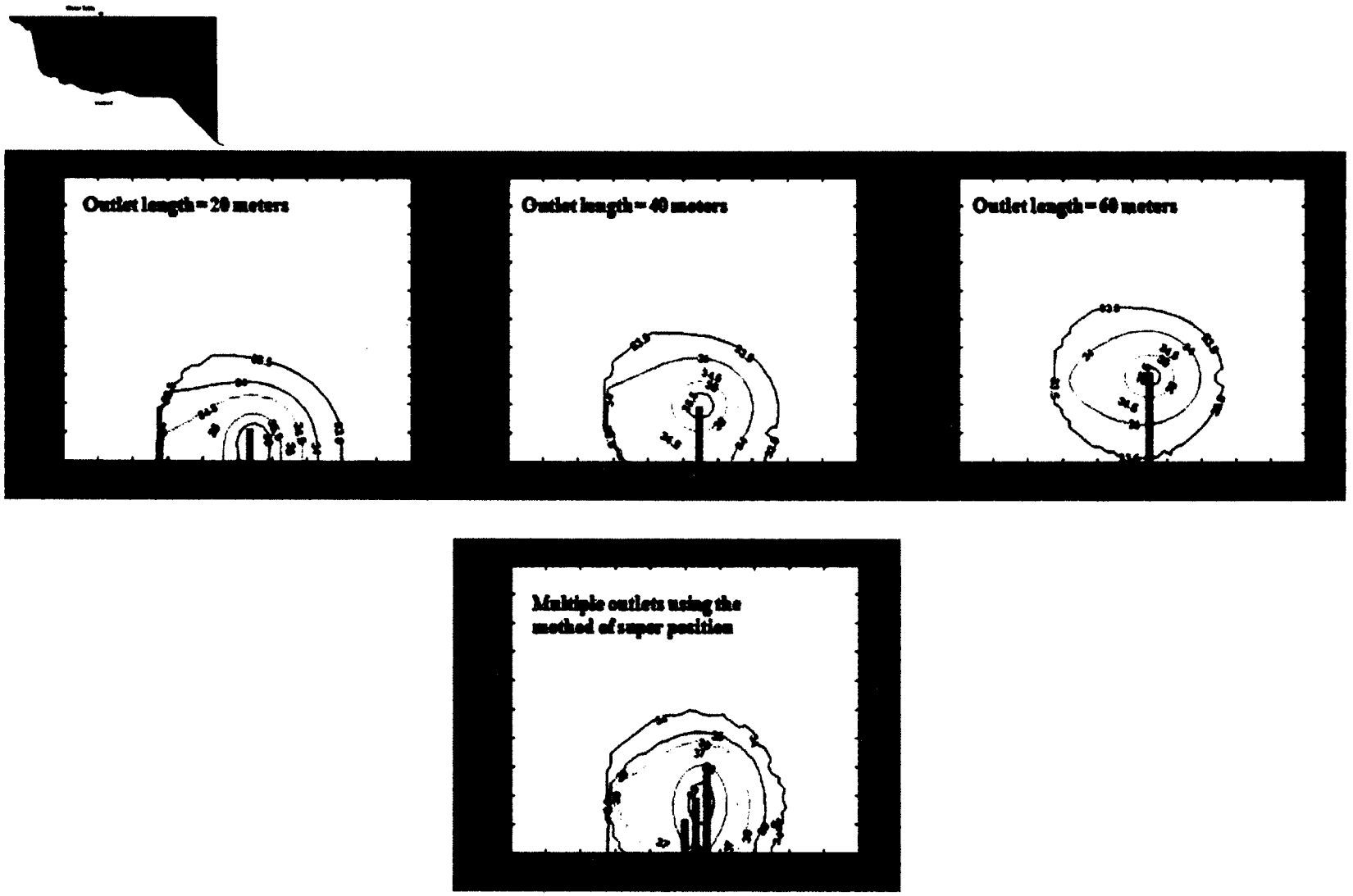

Fig. 3-22. Multiple Outlet Simulation in AM and Method of Superposition

CHAPTER 4

DIMENSIONLESS CRITERIA FOR SELECTING TIDALLY-INFLUENCED ADVECTIVE-DISPERSIVE BRINE MIXING PLUME CHARACTERIZATION MODELS

4-1- Introduction

As described in previous chapters, the environmental assessment of the brine plume dispersion in coastal waters requires the simulation and modeling of the coastal area. Mixing characteristics of coastal waters are very different from one point to another, and depend on the magnitude of tidal range and wind speed of the coastal location. As a result, the coastal water mixing characteristics can vary from being highly advective to completely dispersive. In order to simulate the brine dispersion in coastal regions, the right model needs to be selected based on the mixing characteristics of the study area. Although AM and FSM are capable models for simulating brine dispersion in tidally influenced environments, their limitations and the range of their proficiency are relatively dependant on given site specifics.

In this chapter, a non-dimensional number, Shahvari-Yoon (SY), has been proposed and derived to define the FSM and AM applicable domain. To define this domain, we started from the very beginning steady state assumption in developing the FSM formulation. If the mixing characteristics of the coastal region force the brine dispersion process to reach a steady state fairly fast, the FSM results are reliable and thus

can be used as a tool in the design procedure. However, if the steady state condition is practically inaccessible, then the FSM might not be considered as a proper and realistic method to obtain the solution for the advection-diffusion equation. The following sections describe a technique to find the convergence time to a steady state and verify the applicability of FSM.

4-2- Computation of the time duration to reach steady state

FSM is developed based on a steady state assumption. If the case study converges to the steady state condition after a long period of time, then the FSM might not be considered as a suitable choice to be applied. In some regions the steady state condition is not even attainable because of the special mixing features of the area. In such cases the FSM model encounters a large amount of error which makes it impractical. To avoid this situation, it is essential to determine how fast the case study converges to the steady state condition. If the steady state condition dominates the study area, the FSM would perform effectively and efficiently with accuracy.

In order to test the validity of FSM, the time to reach a steady state has to be computed. The smaller the convergence time, the more efficient and applicable the FSM will be. To calculate the convergence time, the advection diffusion equation can be solved and the solution can be represented using dimensionless factors as follow s [30]:

$$C_c^*(\xi,\eta,\tau) = \int_0^{\tau} \frac{d\tau_0}{\tau_0}\left\{exp\left[-\lambda\alpha^2\frac{(\xi-\xi_0)^2}{\tau_0}\right] + exp\left[-\lambda\alpha^2\frac{(\xi+\xi_0)^2}{\tau_0}\right]\right\}$$

$$\times\, exp\left[-\lambda\frac{[\eta - v\tau_0 + cos\tau - \cos(\tau-\tau_0)]^2}{\tau_0}\right]$$

Eq. (4.1)

where $\upsilon = \frac{V}{U_0}, \lambda = \frac{U_0^2}{4\omega D_y}, \alpha^2 = \frac{D_y}{D_x}$.

υ represents the advective aspect, and λ, α^2 signifies the dispersive feature of the mixing process.

Since the brine tends to accumulate in shallower water, we investigate the salinity accumulation near the coast-line by substituting $\xi = 0$ in equation (1); therefore, the resulting salinity concentration along the shoreline will be [30]:

$$C_c^*(\eta,\tau) = 2\int_0^{\tau} \frac{d\tau_0}{\tau_0} exp\left[-\frac{\lambda\alpha^2{\xi_0}^2}{\tau_0}\right].exp\left[-\lambda\frac{[\eta - \nu\tau_0 + cos\tau - cos(\tau-\tau_0)]^2}{\tau_0}\right].$$

Eq. (4.2)

As seen, the resulting concentration is a function of time (τ) and the distance from the brine source (η). By substituting a η value in Eq. (4.2), the salt concentration can be determined as a function of time for the specific location. For the case of Oman Gulf with $\upsilon = 0.4, \lambda = 10$, and $\alpha^2 = 20$ with the outlet length of 50 meters, Eq. (4.2) has been solved for two locations. Fig. 0-1 part a) shows the resultant excessive salinity concentration as a function of time at 30 meters from the shoreline. As shown, the steady state will be attained in less than a day for this location. Fig. 0-1 part b) shows the resultant concentration 150 meters from the coastline. The steady state will be dominant in almost four days. Comparing these two results demonstrates that convergence to the steady state can be achieved significantly faster near the plume source. As the brine travels further from the outlet, the steady state will be attained with a delay [30].

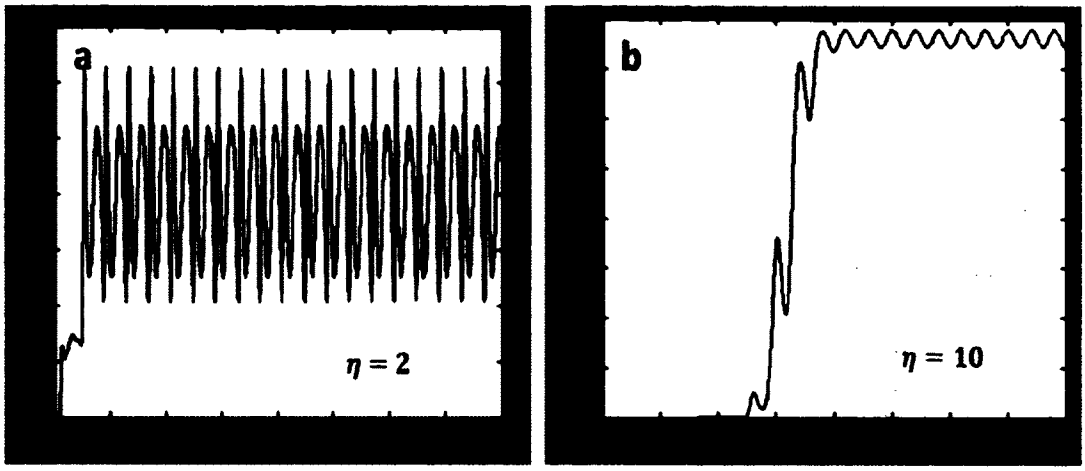

Fig. 0-1. Eq. (4.2) Solution for a) 30 Meters from the Brine Source Location and b) 150 Meters from the Brine Source Location- The Steady State Response Achieved in Less Than a Day Close to the Outlet and After 4 days at a Further Distance

4-3- Identify the contributing factors in mixing process

As previously discussed, υ, λ, and α^2 are contribution factors that help the mixing process reach the steady state and are the initial factors that were considered in this research. υ represents the advective aspect, and λ, α^2 signifies the dispersive feature of the mixing process. In order to determine the possibility of these parameters' contribution in convergence to the steady state condition, 144 random variables have been uniformly generated from the predefined domain for each parameter. The corresponding convergence time has been obtained using Eq. (4.2) at a distance of 200 meters ($\eta = 14$) from the outlet location. The Regression Model and ANOVA have been applied to find any possible correlation between these parameters and the resulting convergence time. Five different analyses have been performed in this part. In the first model all three

parameters were considered. As shown in Table 4-1 the resulting p-value for the model indicates that the model is invalid due to the fact that the p-values exceed $\alpha = 0.05$. As a result, it can be concluded that none of these parameters contribute to reaching a steady state.

Table 4-2, Table 4-3 and Table 4-4 show the model results that investigate the effect of each parameter independently. Table 4-2 illustrates the regression model of convergence time as a function of λ. This model is valid since the p-value is small, and it can be concluded that λ is significant in reaching a steady state. Table 4-3 shows that υ also has a significant role in reaching the steady state, and Table 4-4 indicates that α^2 does not have any contribution to reach the steady state since the model is invalid based on the p-value. Since the substantial roles of λ and υ to reach the steady state are verified, the regression model is developed based on these two parameters together as shown in Table 4-5, and the result shows that the model is valid based on the p-value

Table 4-1. Regression Model- Convergence Time to Steady State as a Function of υ, λ, and α^2; The Model is Invalid Due to p-values of Greater Than 0.05; Conclusion: Not all the Three Parameters Contributes to Reach Steady State $\alpha = 0.05$

Regression Statistics	
Multiple R	0.78819116
R Square	0.62124531
Adjusted R Square	0.51794857
Standard Error	54.6549308
Observations	144

ANOVA					
	df	SS	MS	F	Significance F
Regression	3	53895.99322	17965.3311	6.0141815	0.01115207
Residual	140	32858.77611	2987.16146		
Total	143	86754.76933			

	Coefficients	Standard Error	p-value	Lower 95%	Upper 95%	Lower 95.0%	Upper 95.0%
Intercept	178.727188	106.8026092	0.1224085	-56.343769	413.798146	-56.343769	413.798146
λ	5.98465937	2.423284459	0.0311409	0.65104623	11.3182725	0.65104623	11.3182725
υ	-163.97609	58.07671197	0.0165654	-291.80207	-36.150111	-291.80207	36.1501114
α^2	-2.5432006	6.599307023	0.7073084	-17.068177	11.9817762	-17.068177	11.9817762

Table 4-2. Regression Model- Convergence Time to Steady State as a Function of λ; The Model is Valid Due to p-values of Less Than 0.05; Conclusion: λ Contributes to Reach Steady State $\alpha = 0.05$

Regression Statistics	
Multiple R	0.51313479
R Square	0.26330731
Adjusted R Square	0.20663864
Standard Error	70.1161697
Observations	144

ANOVA					
	df	SS	MS	F	Significance F
Regression	1	22843.1649	22843.1649	4.64643545	0.05044148
Residual	142	63911.6044	4916.27726		
Total	143	86754.7693			

	Coefficients	Standard Error	p-value	Lower 95%	Upper 95%	Lower 95.0%	Upper 95.0%
Intercept	92.8400223	22.049942	0.00101953	45.2040187	140.476026	45.2040187	140.476026
λ	-0.6076899	0.28191754	0.05044148	-1.2167357	0.00135587	-1.2167357	0.00135587

Table 4-3. Regression Model- Convergence Time to Steady State as a Function of υ; The Model is Valid Due to *p*-values of Less Than 0.05; Conclusion: υ Contributes to Reach Steady State $\alpha = 0.05$

Regression Statistics	
Multiple R	0.57873188
R Square	0.33493059
Adjusted R Square	0.28377141
Standard Error	66.6205922
Observations	144

ANOVA					
	df	SS	MS	F	Significance F
Regression	1	29056.8263	29056.8263	6.54683204	0.02379857
Residual	142	57697.943	4438.30331		
Total	143	86754.7693			

	Coefficients	Standard Error	*p*-value	Lower 95%	Upper 95%	Lower 95.0%	Upper 95.0%
Intercept	101.272189	22.1155106	0.00051686	53.4945328	149.049845	53.4945328	149.049845
υ	-17.098809	6.68267365	0.02379857	-31.535847	-2.66177	-31.535847	-2.66177

Table 4-4. Regression Model- Convergence Time to Steady State as a Function of α^2; The Model is Invalid Due to *p*-values of Greater Than 0.05; Conclusion: α^2 Doesn't Have Any Contribution to Reach Steady State $\alpha = 0.05$

Regression Statistics	
Multiple R	0.02315852
R Square	0.00053632
Adjusted R Square	-0.0763455
Standard Error	81.6692397
Observations	144

ANOVA					
	df	SS	MS	F	Significance F
Regression	1	46.5280474	46.5280474	0.00697586	0.93470921
Residual	142	86708.2413	6669.86471		
Total	143	86754.7693			

	Coefficients	Standard Error	*p*-value	Lower 95%	Upper 95%	Lower 95.0%	Upper 95.0%
Intercept	74.4726555	107.052104	0.49888538	-156.79935	305.744665	-156.79935	305.744665
α^2	-0.5692201	6.81524217	0.93470921	-15.292656	14.1542155	-15.292656	14.1542155

Table 4-5. Regression Model- Convergence time to Steady State as a Function υ and λ Together; The Model is Valid Due to *p*-values of Less Than 0.05; Conclusion: υ and λ Does Have Contribution to Reach Steady State Condition $\alpha = 0.05$

Regression Statistics	
Multiple R	0.78494055
R Square	0.61613167
Adjusted R Square	0.55215361
Standard Error	52.6801738
Observations	144

ANOVA					
	Df	SS	MS	F	Significance F
Regression	2	53452.3608	26726.1804	9.63035945	0.00319959
Residual	141	33302.4085	2775.20071		
Total	143	86754.7693			

	Coefficients	Standard Error	*p*-value	Lower 95%	Upper 95%	Lower 95.0%	Upper 95.0%
Intercept	138.477997	21.5243272	3.2379E-05	91.5805172	185.375478	91.5805172	185.375478
λ	5.39998612	1.82131336	0.01181292	1.4316852	9.36828704	1.4316852	9.36828704
υ	-150.90419	45.4383478	0.00609803	-249.90584	-51.902533	-249.90584	-51.902533

4-4- Derivation of Shahvari-Yoon (SY) number

The result of all the six analyses agrees that unlike α^2, the two other parameters, λ and υ, play significant roles in converging to a steady state condition. As a result, in order to develop a non-dimensional number which represents the mixing characteristics of the study area, these λ and υ parameters are used, and the α^2 is eliminated from the computations.

In this part 200 random numbers for λ and υ have been generated from a predefined domain to represent a very diverse range of mixing characteristics of coastal waters. These random values are created to represent a wide range of mixing characteristics, from highly dispersive locations such as the Caribbean Sea to highly advective places such as the East Coast. These generated values are imported to the

MATLAB code, and the related convergence time has been computed. The corresponding convergence time has been obtained using Eq. (4.2) at a distance of 200 meters ($\eta = 14$) from the outlet location. In some cases, the steady state condition has been attained in less than a day. However, in some other cases reaching the steady state is next to impossible. As discussed, the rate to attain the steady state can be employed as a tool to validate the FSM performance. The result shows that the FSM has very accurate results when the convergence to the steady condition occurs in less than 5 lunar days which represents a highly advective driven environment. The FSM performance is still fairly reasonable when the convergence is achieved in 5 to 15 lunar days which represents the advective-dispersive environment. For convergence times of greater than 10 days the FSM results encounter a large amount of error and are no longer applicable. Fig. 4-2 shows some examples of convergence to the steady state for different values of λ and υ.

In order to check the validity of FSM, the nonparametric comparison has been performed to compare the results of FSM and AM to the measured salinity data in five different locations with very diverse mixing characteristics. The nonparametric analysis is performed to evaluate whether there is a statistically significant difference between the observed and simulated data. The null hypothesis, H_0, assumes that there is no significant difference between the observed and simulated data, and the alternative hypothesis, H_a, assumes that there is a significant difference between them. The observed significance level, or p-value, is the probability of assuming H_0 is true. If the p-value exceeds the α, which is the probability of committing a type I error, we have insufficient evidence to reject H_0.

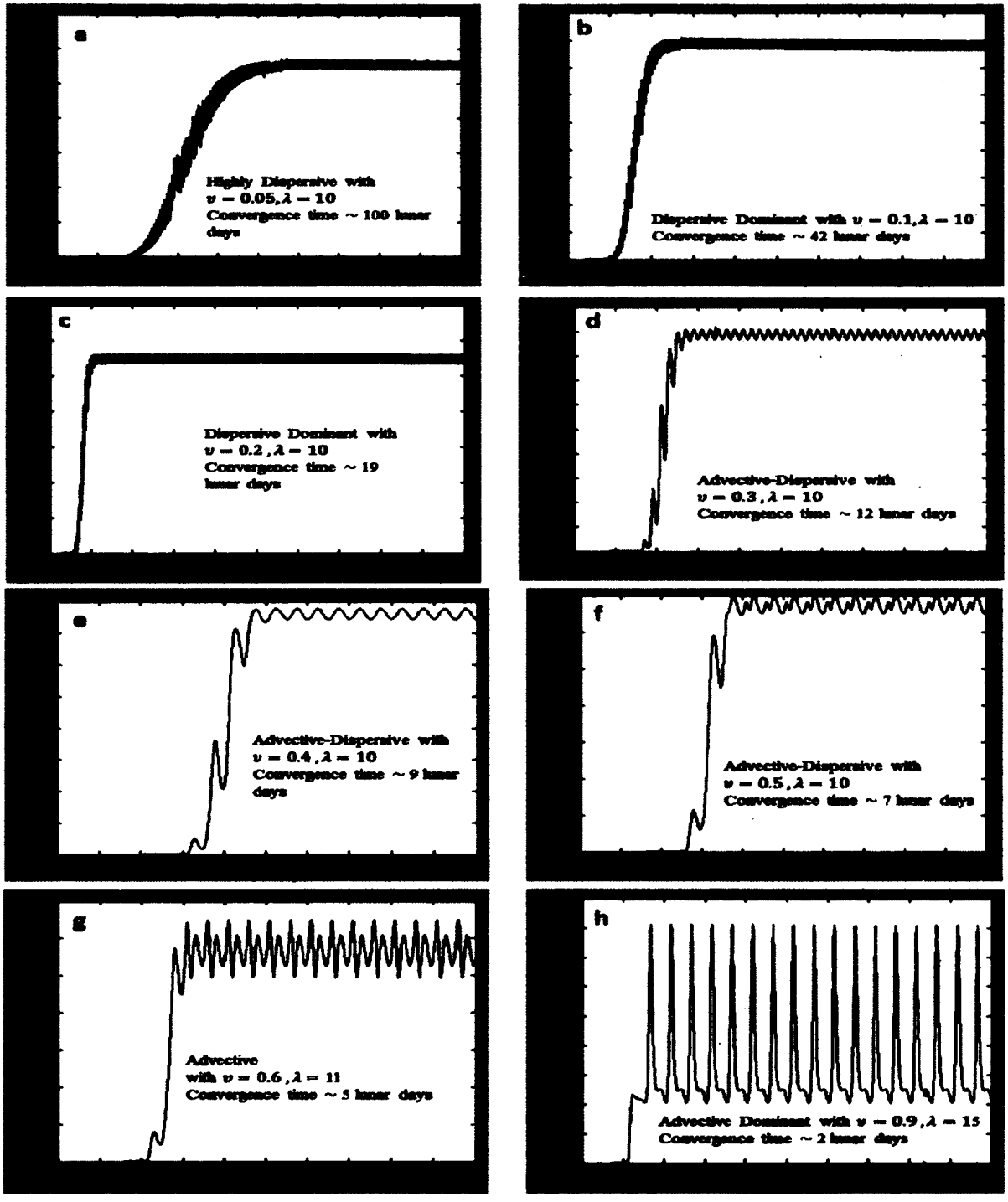

Fig. 4-2. Computation of Convergence Time to Steady State (t); a) Highly Dispersive with $t = 100$ days, b,c)Dispersive Dominant with $t = 42, t = 19$ days, d,e,f) Advective-Dispersive with $t = 12, t = 9, t = 7$ days and g,h) Advective Dominant with $t = 5, t = 2$ days

Table 4-6 summarizes the result of nonparametric comparison. As shown, in Tampa bay, Huntington Beach, and the U.S. Virgin Islands, both FSM and AM work well, and the corresponding *p*-values support the validity of the models. The *p*-values for AM are all greater than α at 0.05 in this analysis. Therefore, it can be concluded that the AM can be applied to any coastal location regardless of the mixing features of the region and decent results can be attained. On the other hand, as we expected, comparison results indicate that the performance of FSM is a function of mixing characteristics of the study area. In advective and advective-dispersive driven locations, FSM becomes a reliable simulation method with reliable results. However, the model is no longer valid in dispersive dominant environments.

Fig. 4-3 shows a sample comparison of simulated and observed salinity data in Tampa Bay. Part a) shows the salinity value 30 meters from the outlet while part b) represents the salinity 150 meters from the outlet. Since Tampa Bay is considered as an advective driven environment, all the *p*-values are greater than 0.05, thus, both models have reliable and valid results. In other words, there is no significant difference between the measured data and simulated data.

Table 4-6. Check the Validity of FSM and AM by Comparing the Result of the Models with Measured Data for Five Locations with Very Diverse Mixing Characteristics

Name of Desalination	Location	Mixing Characteristics	P-Value (FSM)	P-Value (AM)	Validity
Huntington Beach	West Coast	Advective-Dispersive	0.3123	0.4432	✓
Tampa Bay	Florida	Advective	0.5198	0.5413	✓
Maspalomas	Canary Island	Dispersive	0.0488	0.4723	×
Kish Island	Persian Gulf	Dispersive	0.0459	0.3893	×
US virgin Island	Caribbean Sea	Advective-Dispersive	0.2788	0.5142	✓

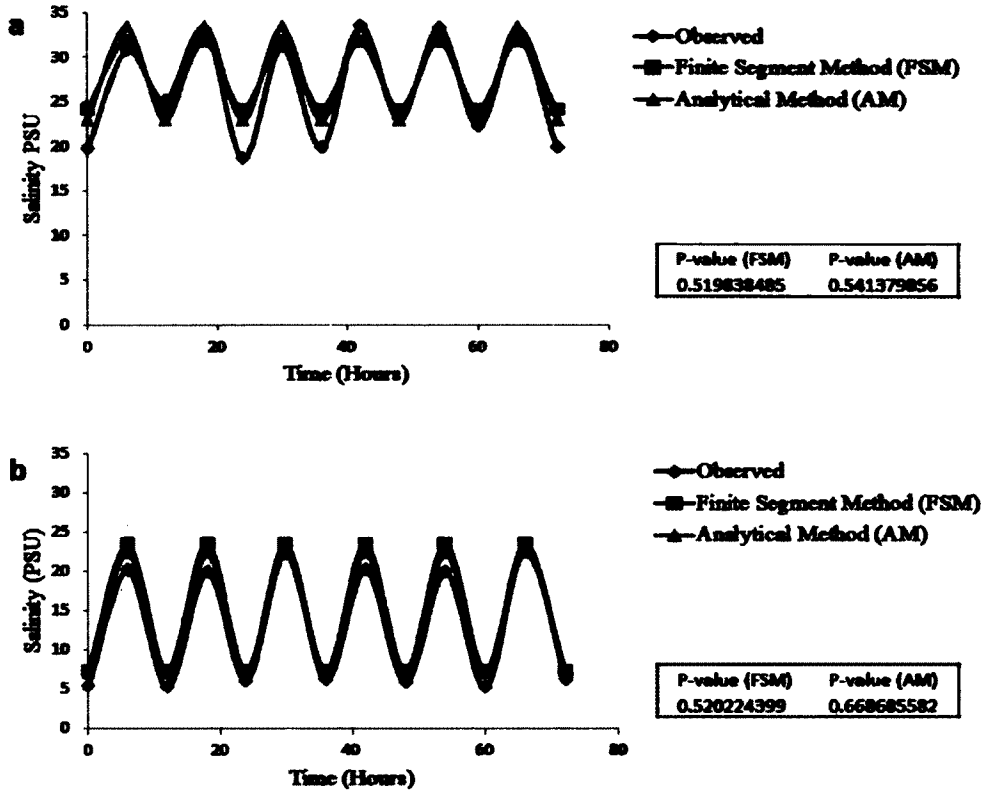

Fig. 4-3. Comparing AM, FSM, and Measured Data in Two Locations in Tampa Bay a) 30 Meters from Outlet and b) 150 Meters from Outlet

After understanding the significant role of the mixing characteristic in FSM performance, it is time to define the valid domain for this method. The objective of this section is to divide the coastal regions into three categories: advective, advective-dispersive and dispersive. These three categories are obtained based on the rate of reaching a steady state. The coastal area is considered advective driven if the steady state is attained in less than 5 lunar days. If the steady condition is obtained in 5 to 15 days, the study area is considered to be advective dispersive. The critical condition is when the steady state is attained after more than 15 lunar days; this describes the dispersive

dominant environment. For the Maspalomas desalination plant in the Canary Islands and Kish Island desalination plant in the Persian Gulf, the steady state was attained after 24 and 27 days. Based on these criteria, the Shahvari-Yoon (SY) number has been derived in terms of influential parameters of λ and υ.

The SY number is set to be zero for the convergence time of 5 days which is assumed to be the boundary of an advective and advective-dispersive driven environment. Therefore, the SY number has been calculated as follows:

$$SY = -\upsilon - 0.0611 \times \lambda + 4.0981 .$$

Eq. (4.3)

The SY number is completely capable of representing the mixing characteristics of the coastal waters. As shown, the SY number contains both advective and dispersive aspects of mass transport phenomenon as well as the tidal characteristics of the study area. By using the SY number, describing the mixing features of the study area is straightforward and succinct. The convergence time of 15 days, which separates the advective-dispersive category from dispersive driven environments, is equal to a SY number of 0.12. We categorize the three different mixing characteristics as a function of SY as follows:

$$\begin{cases} Advective\ Dominant & SY < 0 \\ Advective - Dispersive & 0 < SY < 0.12 \\ Dispersive\ Dominant & SY > 0.12 \end{cases} .$$

Eq. (4.4)

Fig. 4-4 shows the classification of coastal regions as a function of the SY number. As shown, the SY number is effective for describing the mixing features in a succinct and clear way. Regions with high tidal ranges have a negative or small SY number whereas as the tidal range decreases the SY number increases. For example, in the Persian Gulf and the Mediterranean Sea, with tidal range of 0.5 ft. and less, the SY number is greater than 0.12. The average SY number for Kish Island in the Persian Gulf, with a tidal range of 0.5 ft., is 0.16 which represents a highly dispersive condition.

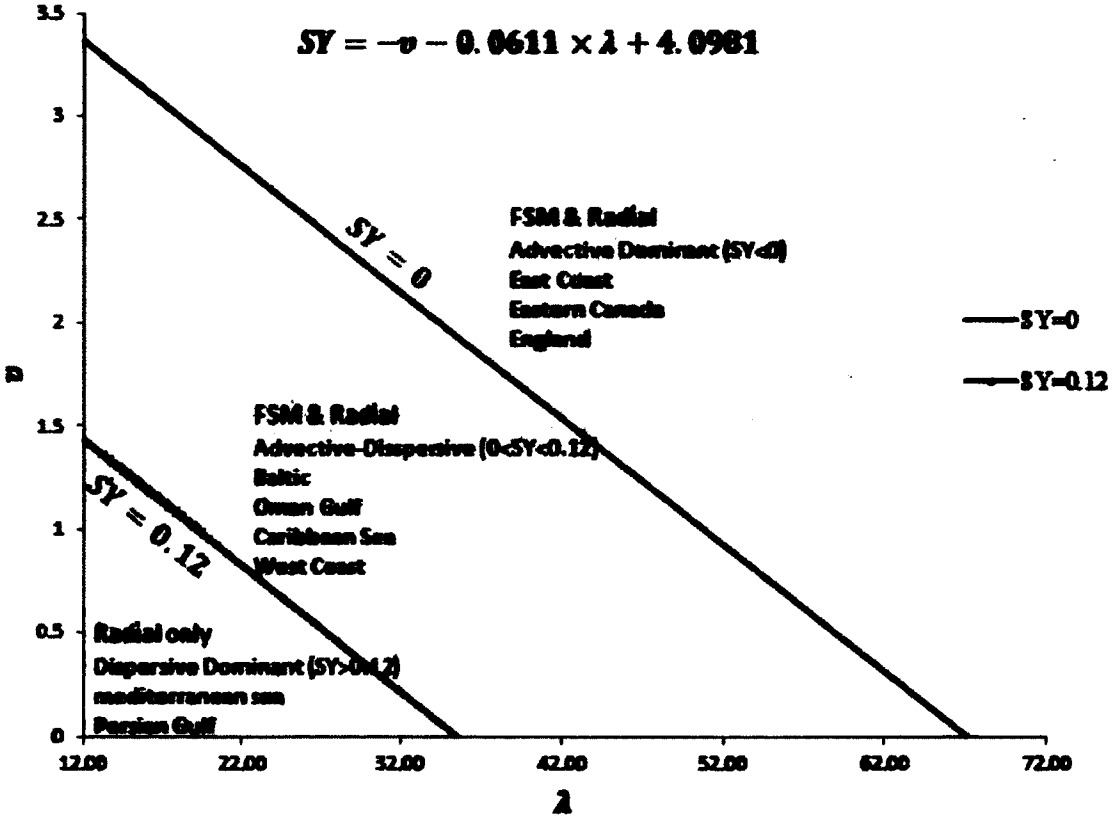

Fig. 4-4. Classification of Mixing Characteristics in Coastal Waters Using SY Number

Comparison of the two implemented models indicates that AM can work efficiently for any SY number range. However, the AM method is more complicated and needs more input data to simulate the seabed as well as boundary conditions. FSM, on the other hand, works for a SY range of equal to and less than zero which represents the advective dominant coastal regions. Though FSM is considered to be a deficient method for simulating dispersive dominant locations, as a result of its steady state nature, it still can be considered a very competitive approach due to its practicality and high level of efficiency especially in advective or advective-dispersive regions where most typical desalination brine discharge operation takes place.

4-5- Application of (SY) number in design of desalination plant outlet

As described in Chapter 1, due to economic reasons, it is common practice for desalination plants to discharge the brine plume in coastal waters using an outlet. One of the main concerns regarding the outlet structure is its design requirement to minimize the environmental impact due to excessive salinity concentration being discharged at its terminus. The farther the outlet extends from the coastline, the deeper the water would be; as a result, the brine dissolves much faster. To design the outlet, there are two constraint categories. The first category is environmental constraints that regulate the elevated salinity and check whether the coastal inhabitants are able to tolerate the high salinity in the vicinity of the outlet. The second type of constraint is economic restrictions that aim to minimize the outlet length as much as possible to reduce construction and maintenance costs. These constraints can be utilized effectively to guarantee a unique solution for the optimization problem of designing the outlet length.

In order to reflect the environmental constraint of the elevated salinity near the outlet location, the state of California's 10% regulation has been applied to formulate the constraint for the optimization problem of designing the outlet length. This regulation accepts the salinity change of 10% above the ambient salinity. The economic constraint has been considered as the objective function. Therefore, the non-linear constrained optimization problem will be:

Minimize l

Subjected to $C_r < 1.1 \times C_a$

where l is the outlet length, C_r is the resulting concentration after brine discharge at the distance of 100 meters, and C_a is the ambient salinity which typically is around 32PSU.

Despite the fact that the objective function and constraint are both linear functions, the optimization problem is still classified as a non-linear optimization problem. The constraints vary non-linearly with respect to the design variables. In order to solve this nonlinear optimization problem, Sequential Quadratic Programming (SQP) Toolbox in MATLAB, which is an appropriate method for solving non-linear optimization problems, has been applied. Fig. 4-5 shows the 12 steps of the optimization procedure to converge to the optimum solution for the Persian Gulf Kish Island desalination plant outlet. The initial guess for the outlet length is set at zero. Therefore, Part 1 shows the resulting concentration without any outlet structure. As a result the salinity constraint is violated. The outlet length then was increased gradually to reduce the constraint's violation. Since the concentration constraint has been violated, the optimization algorithm continues to the next steps with updated outlet length. This

process continues until the salinity constraint is satisfied. Parts 2 through 12 show the optimization steps to the optimum point. Part 12 is the final step which represents the situation without any violation of the constraint. In Part 12, the outlet is long enough to discharge the brine in a safe location, deep enough to dilute the brine quickly and not increase the excessive salinity more than 10% of the ambient water salinity. For the Kish Island desalination plant with a SY number of 0.16, the minimum outlet length to satisfy the 10% rule is calculated to be 423 meters. Part 12 shows the brine dispersion contour with optimum outlet length of 423 meters, and all the constraints are satisfied.

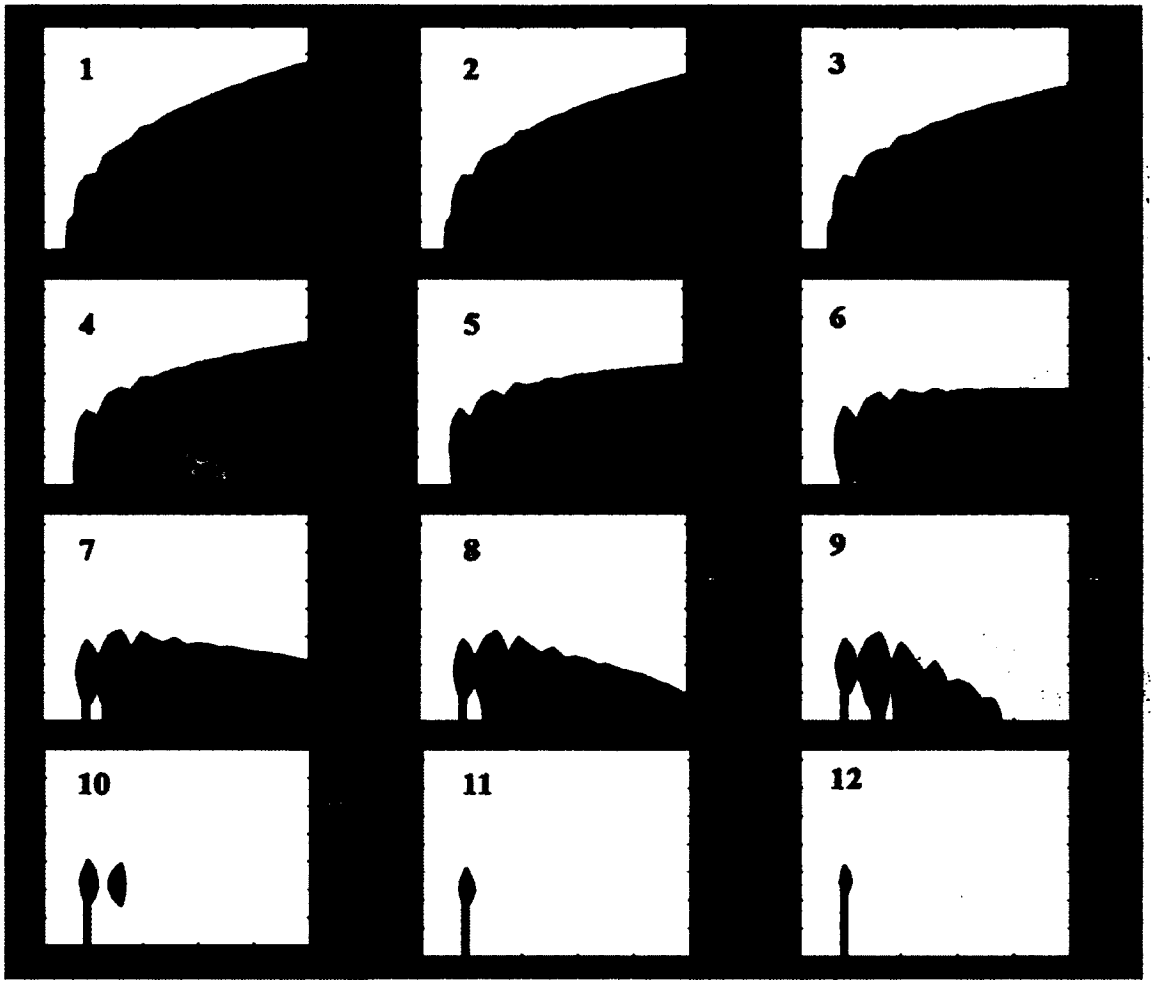

Fig. 4-5. Brine Dispersion with Different Outlet Lengths; 12 Steps to Solve Kish Island Outlet Optimization Problem with SY Number of 0.16

4-6- Design Charts

The SY number is a very powerful and practical tool for describing the mixing characteristic of coastal areas. In this section, four nomographs have been developed for design purposes by representing outlet length as a function of the SY number and seabed slope. Since outlets usually discharge the brine in the near-field zone where the slope is

typically mild, slopes of 1 to 4% have been considered to develop these nomographs for most likely design conditions. Fig. 4-6, Fig. 4-7, Fig. 4-8, and Fig. 4-9 demonstrate the designated nomographs for 1%, 2%, 3% and 4% seabed slopes, respectively. As described earlier, the SQP optimization method and the state of California 10% salinity regulation have been applied for developing these design charts.

The blue line in each chart shows the highly advective domain with a SY number of less than zero. The red line demonstrates the advective-dispersive zone with a SY number of greater than zero and less than 0.12. The green line represents the dispersive domain with a SY number of greater than 0.12. To summarize Fig. 4-6, Fig. 4-7, Fig. 4-8, and Fig. 4-9, Table 4-7 represents the outlet length formulas as a function of SY number and seabed slope.

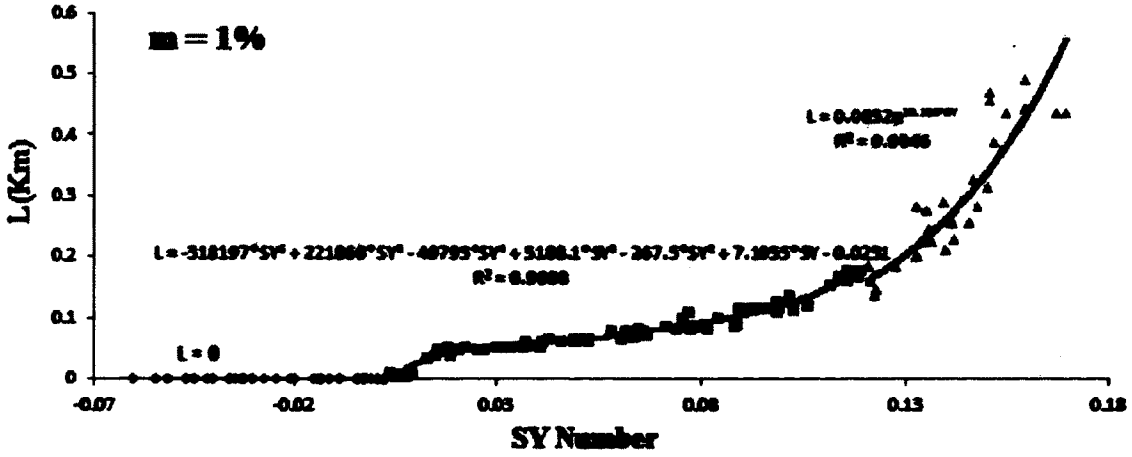

Fig. 4-6. Outlet Length as a Function of SY Number for Near Field Zone with Seabed Slope of 1%

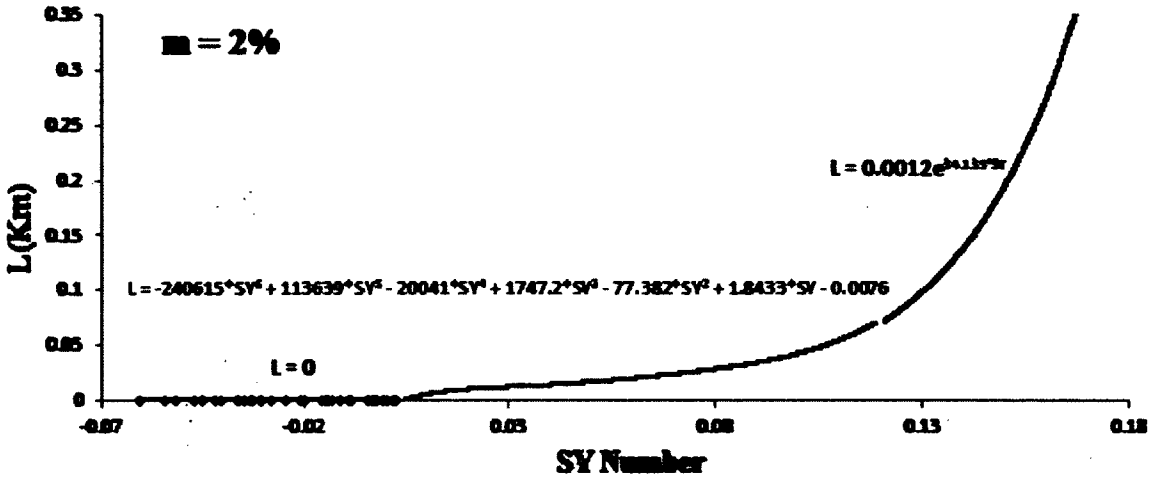

Fig. 4-7. Outlet Length as a Function of SY Number for Near Field Zone with Seabed Slope of 2%

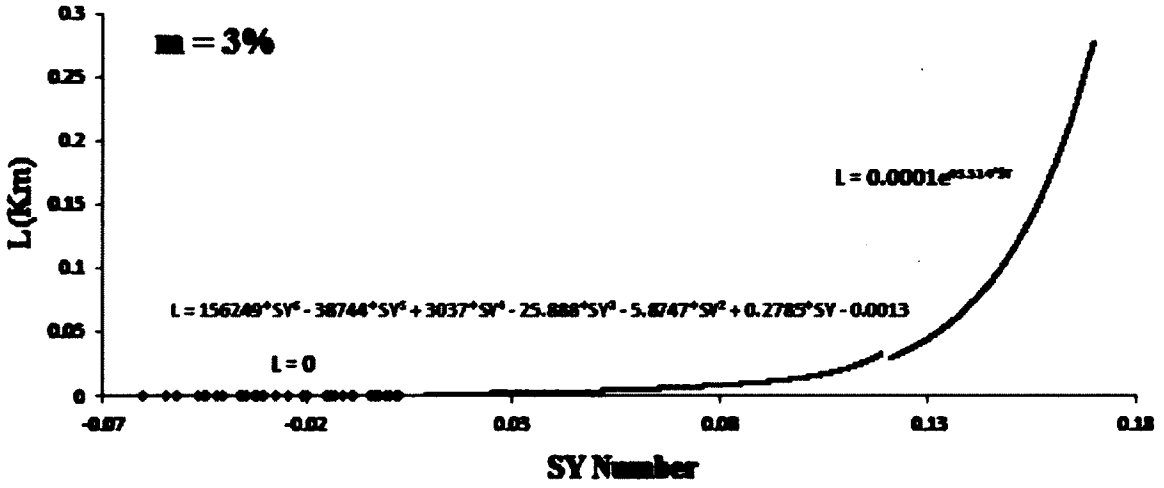

Fig. 4-8. Outlet Length as a Function of SY Number for Near Field Zone with Seabed Slope of 3%

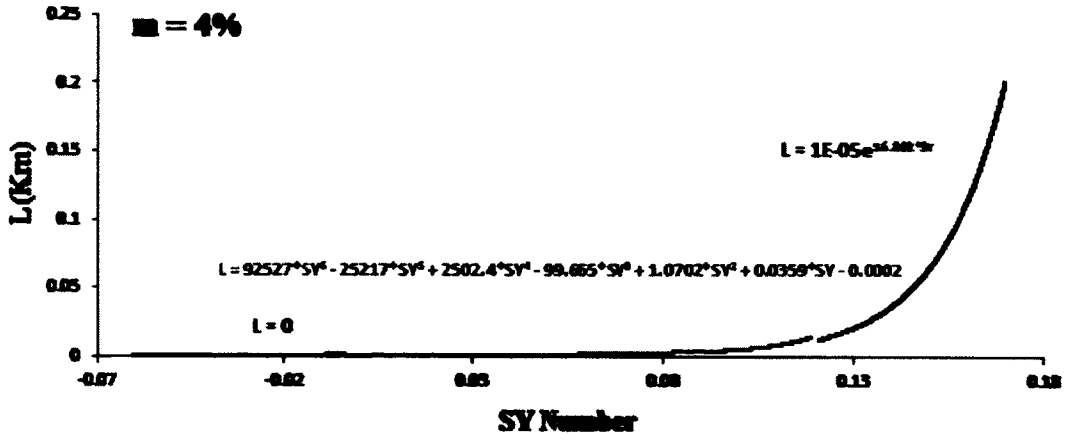

Fig. 4-9. Outlet Length as a Function of SY Number for Near Field Zone with Seabed Slope of 4%

Table 4-7. Outlet Length as a Function of SY Number and Seabed Slope

Seabed Slope / SY Range	$M = 1\%$	$M = 2\%$	$M = 3\%$	$M = 4\%$
$SY < 0$	$L = 0$	$L = 0$	$L = 0$	$L = 0$
$0 < SY < 0.12$	$L = -318197*SY^6 + 221866*SY^5 - 49793*SY^4 + 5188.1*SY^3 - 267.5*SY^2 + 7.1055*SY - 0.0251$	$L = -240615*SY^6 + 113639*SY^5 - 20041*SY^4 + 1747.2*SY^3 - 77.382*SY^2 + 1.8433*SY - 0.0076$	$L = 156249*SY^6 - 38744*SY^5 + 3037*SY^4 - 25.888*SY^3 - 5.8747*SY^2 + 0.2785*SY - 0.0013$	$L = 92527*SY^6 - 25217*SY^5 + 2502.4*SY^4 - 99.665*SY^3 + 1.0702*SY^2 + 0.0359*SY - 0.0002$
$SY > 0.12$	$L = 0.0052*e^{28.126*SY}$	$L = 0.0012e^{34.133*SY}$	$L = 0.0001e^{43.514*SY}$	$L = 1E\text{-}5e^{54.882*SY}$

CHAPTER 5

DESIGN OF OUTLET STRUCTURE USING OPTIMIZATION APPROACH AND MONTE CARLO SIMULATION

5-1- Introduction

Construction and maintenance of the outlet structure represents the main cost of the surface water discharge method. As shown in Fig. 5-1, the outlet structure costs millions of dollars, and the cost is directly proportional to the length. The cost of the outlet increases quickly with respect to the outlet length. While the outlet installation costs less than 50 million dollars for outlets less than one kilometer in length, the expenses increase to roughly 200 million dollars for outlets 4 kilometers in length. In order to minimize the environmental impacts of the concentrate in dispersive dominant coastal locations, construction of outlets thousands of meters in length is sometimes inevitable. However, since the construction of long outlet structures is extremely costly, it is necessary to identify the optimum length for the outlet structure for each location during the design phase.

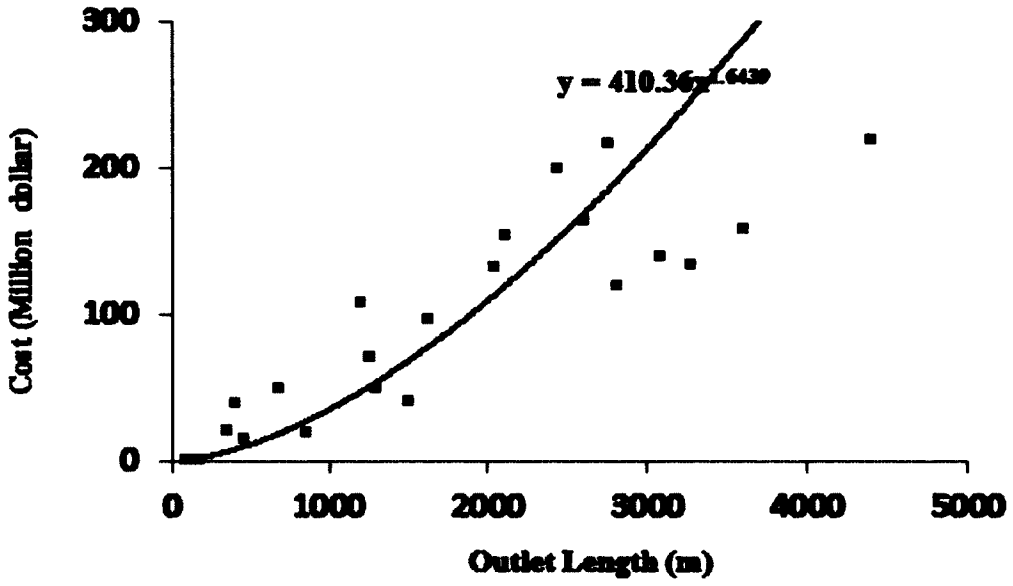

Fig. 5-1. Cost of the Outlet Structure as a Function of Outlet Length [6]

As shown in Fig. 5-1, shortening the outlet structure can save desalination projects millions of dollars. However, this process needs to be done without any environmental impact to the coastal inhabitants. Simulation of the concentrate dispersion in a coastal environment and risk analysis of water quality violations are required to identify and design the optimum outlet length. The outlet must be long enough to discharge the concentrate in a location with high dispersive capability to minimize the size of zone of initial dilution (ZID) This chapter presents a method for designing the outlet length for a seawater desalination plant based on the SY number value as the design parameter for a single discharge.

5-2- Current salinity regulations

As previously discussed in Chapter 1, there are no federal or state laws that regulate the brine discharge either in the United States or the rest of the world. However, there are some project-specific federal and state laws in some states such as California that control the brine discharge of desalination plants by creating critical and long-lasting Whole Effluent Toxicity (WET) objectives.

WET is more focused and tries to control the environmental impact of different particles in seawater excluding salinity and does not pay enough attention to salt content. Therefore, the motivation of WET is more on potential synergistic environmental impacts of the brine as a result of other constituents. However, the effect of increased salt content on the aquatic habitat in the area of the brine discharge is considered indirectly by studying the effect of total dissolved solids contained in the brine (e.g., metals, organics, and suspended solids). In other words, salinity is only a measure of the dissolved mineral (salt) content of the concentrate rather than the complex chemistry of the discharge in relationship to the receiving body of water [36].

According to current regulations in the United States, if a desalination plant discharge meets all water quality objectives defined in the applicable federal state regulations as well as acute and chronic WET objectives, then the proposed discharge does not present a threat to aquatic life regardless of what the actual salinity level of this discharge is or what increase above ambient salinity this discharge may cause because WET accounts for the salinity related environmental impacts of concentrate [29].

The California Ocean Plan establishes a daily maximum acute toxicity receiving water quality objective of 0.3 TUa (acute toxicity units). Requirement III.C.4 (b) of the California Ocean Plan designates that this 0.3 TUa objective applies to ocean waters outside the acute toxicity mixing zone. Requirement III.C.4 (b) defines the acute toxicity mixing zone as follows:

> *"The mixing zone for the acute toxicity objective shall be 10 percent (10%) of the distance from the edge of the outfall structure to the edge of the chronic mixing zone (zone of initial dilution)."*

The state of California is considering a single state wide salinity limit for all ocean discharges of 10% above ambient salinity. So far this is the only existing semi-law that regulates the concentrate discharge in California, and more or less other desalination plants around the world try to follow this rule. This rule accepts the increase of up to 10% in ambient salinity in the zone of initial dilution. The question is, should one design the outlet length based on this 10% increase law. To answer this question many studies have been done that consider this rule to be conservative. Research shows that the increase in ambient salinity can be more than 10% without any detrimental impact on coastal environments. However, the allowable time of exposure has a reverse relationship with the elevated salinity value. The more elevated the salinity, the less exposure time is allowable. In other words, the coastal water inhabitants, such as fishes, can resist higher salinities for a smaller period of time.

Fig. 5-2 shows the recent research result in the Huntington Beach desalination plant discharge with a discharge of 50 MGD and ambient salinity of 33.5 PSU. The results show that the increase of up to 20% and 50% in ambient salinity (38 PSU and 47

PSU) is only allowed for nearly 2 hours and 1 hour respectively. If the water salinity goes over 20% of the ambient salinity for more than two hours, it leads to death of the inhabitants of the coastal area. On the other hand, results show that the 10% law is conservative, and since the construction of the outlet structure is so expensive, millions of dollars can be saved by reflecting the time of exposure in the 10% law.

Since coastal waters are tidally influenced, the flow velocity starts from a maximum, slows until it reaches the zero value, and then speeds up in the opposite direction during one tidal cycle. Depending on the tidal characteristics, sometimes the velocity value reaches zero more than once in 24 hours. Dispersive capacity varies significantly as a function of current velocity during one tidal cycle. The higher the current velocity, the faster the concentrate vanishes and, consequently, the smaller the size of ZID. Whenever the velocity is fairly high, the concentrate disperses rapidly, and the resultant salinity is far below the 10% law. However, during the low velocity periods and the stagnation points, the resultant concentrate reaches its maximum value, and in some diffusive dominant environment goes above 10% law [9].

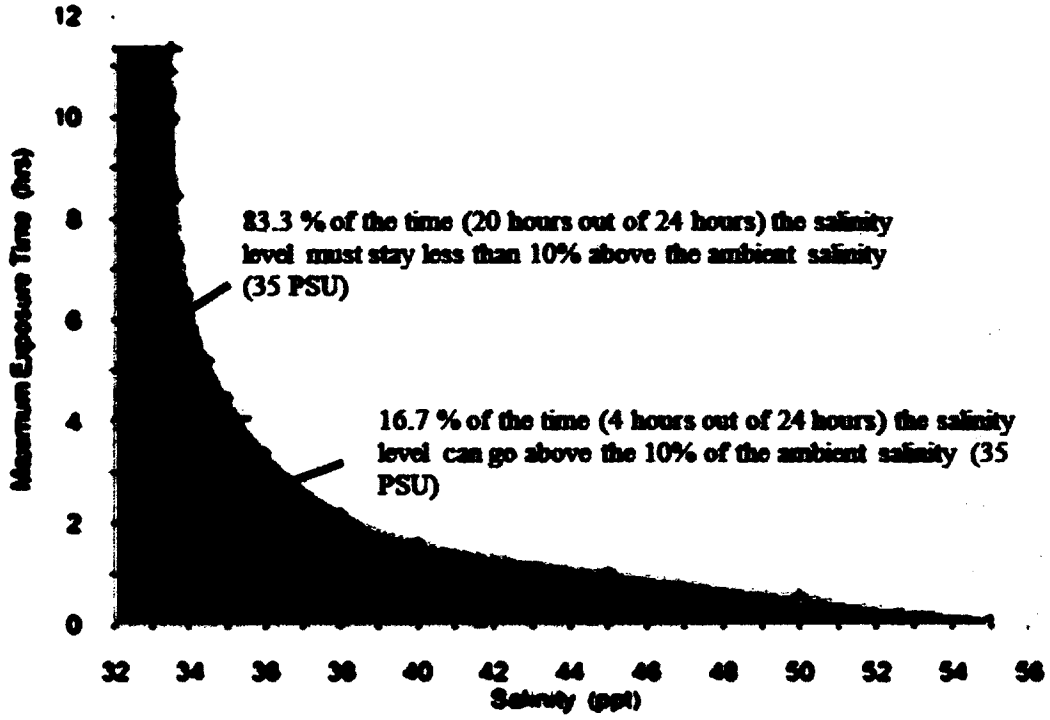

Fig. 5-2. Maximum Exposure Time of a Drifting Organism Passing Through the Discharge Plume of Concentrated Seawater from the AES Huntington Beach Outfall for Worst Case Conditions (Plant Flowrate = 50 MGD)

5-3- Outlet length optimization using Monte Carlo Simulation

As Fig. 5-2 shows, the resultant salinity can go above 10% (35 PSU) without any harmful environmental impacts. However, this increase in salinity level must be less than 4 hours during one 24 hour day. Thus, if the salinity level follows the 10% law for 20 hours out of 24 hours (83.33 percent of the time) for a certain outlet length, then the length is long enough to protect the coastal environment from the excessive salinity level. In order to obtain the optimum outlet length, the maximum capacity of the coastal environment should be considered, and the 10% law could and should be revised.

In this chapter, the 10% law has been revised in a way that firstly and most importantly determines the outlet length, to keep the coastal environment protected from excessive salinity. Secondly, optimizing the outlet length will save millions of dollars. Reflecting these two objectives simultaneously, a risk analysis is required to solve this constrained optimization problem. The current optimization problem can be formulated as follows:

Minimize L

Subjected to:

$$\begin{cases} A_0 < R_0 < A_0 + 10\% & 83.3\% \textit{ of the time} \\ R_0 > A_0 + 10\% & 16.7\% \textit{ of the time} \\ SYmin < SY < SYmax \end{cases}$$

Eq. (5.1)

where A_0 is the ambient salinity, and R_0 is the resultant salinity after brine discharge.

Monte Carlo Simulation is perfectly suited to solve this problem. Monte Carlo simulation is based on random number generation which is helpful for forecasting, design and risk analysis. A simulation calculates numerous scenarios of a model by repeatedly picking values from a user predefined probability distribution for uncertain variables and using a model; each scenario can have a forecast. For this specific model, the SY number is the uncertain parameter that needs to be defined using a probability distribution fitting, and the outlet length is the forecast.

The first step in the Monte Carlo simulation is to predefine a specific distribution for the SY number. Several statistical tests exist to conclude whether sample data comes

from a specific distribution. Kolmogorov-Smirnov and chi-square are the most common. There are also other methods such as Anderson-Darling, Lilliefors, Jacque-Bera, and Wilkes-Shapiro, which are parametric methods and require normality and, therefore, are not as common as non-parametric methods since the results of these tests are oftentimes suspect or inconsistent. In this research, Kolmogorov, Akaila, Schwartz, Anderson, and Kuiper's methods have been applied. However, the simulation has been accomplished based on the Kolmogorov-Smirnov method. Table 5-1 shows the result of distribution fitting for SY number for a coastal area in the Persian Gulf.

5-3-1- Distribution Fitting Using Kolmogorov-Smirnov

The Kolmogorov-Smirnov (KS) test is based on the empirical distribution function of a sample data set and is a nonparametric test and doesn't need the normality the sample. This nonparametric characteristic is the key to understanding the KS test, which simply means that the distribution of the KS test statistics doesn't depend on the underlying cumulative distribution function being stated. Another advantage of KS compared to Chi-square is that KS is an exact test and therefore is independent of sample size. Despite all these important advantages, KS has some limitations. KS only applies to continuous distributions and is more sensitive near the mean, and it gets less sensitive at the distribution's tails [22].

In the KS method given N ordered data points $SY_1, SY_2, \ldots SY_N$, the empirical distribution function is defined as $E_n = n_i/N$ where n_i is the number of points less than SY_i where SY_i values are ordered from the smallest to the largest value. This is a step

function that increases by $1/N$ at the value of each ordered data point. In the analysis, the null hypothesis is that the data set follows a specific distribution, and the alternative hypothesis is that the data set doesn't follow that distribution [21].

$$H_0 = \max(1 < i < N) \left| F(SY_i) - \frac{i}{N} \right|$$

Eq. (5.2)

where F is the theoretical cumulative distribution of the continuous distribution being tested that must be fully specified (i.e., the location, scale, and shape parameters cannot be estimated from the data). Since the null hypothesis is that the data set follows a specific distribution, the small p-values such as (0.1, 0.05, and 0.01) signify the fit is not a good one [22]. As shown in Table 5-1, the fitting procedure using five different methods has been presented for the Persian Gulf coastal area. All p-values for the Kolmogorov test are high which indicates a statistically good fit to the tested distribution. As shown, other methods, which are parametric tests, work with mean absolute percentage error instead of P-Values. The maximum P-Value belongs to the triangular distribution with 99.87% which represents the SY distribution perfectly. The second best fit is the Gumbel Maximum with the P-Value of 97.36% which equally represents the SY distribution well.

Table 5-1. Best Fitting Distribution Result for SY in Persian Gulf Using Five Different Methods

Best-Fitting Distributions

Rank	Kolmogorov	Akaike	Schwartz	Anderson	Kuiper's
1	Triangular	Triangular	Triangular	Beta 3	Beta 3
2	Gumbel Maximum	Beta 3	Beta 3	T	T
3	Lognormal	Beta 4	Beta 4	Rayleigh	Rayleigh
4	Normal	Gumbel Maximum	Gumbel Maximum	Chi-Square	Chi-Square
5	Logistic	Lognormal	Lognormal	Lognormal 3	Lognormal 3
Rank	P-Value	MAPE %	MAPE %	MAPE %	MAPE %
1	99.87%	0.06%	0.06%	0.19%	0.07%
2	97.36%	0.07%	0.07%	1.84%	1.84%
3	95.84%	0.07%	0.07%	1.95%	2.52%
4	93.16%	0.07%	0.07%	2.04%	2.04%
5	92.14%	0.09%	0.09%	2.09%	2.09%

P-value is not always very high. For the Persian Gulf, since the coastal water is very dispersive dominant and the tidal range is very low, the variation of the SY number during one tidal cycle is minimal. However, for some other locations the SY variation during one tidal cycle is extremely high. In these cases, the fitting process is more difficult, and the *P*-values are smaller. Table 5-2 shows the SY fitting distribution for Tampa Bay. As shown, the *P*-values are much smaller compared to the Persian Gulf since the variation of SY is significant during one tidal cycle and the coastal water is more advective dominant. Fig. 5-3, Fig. 5-4, and Fig. 5-5 show the probability distribution of the SY number for three different locations with different mixing capacity.

Table 5-2. Best Fitting Distribution Result for SY Number in Tampa Bay Using Five Different Methods

Best-Fitting Distributions:

Rank	Kolmogorov	Akaike	Schwartz	Anderson	Kuiper's
1	Gumbel Maximum	Triangular	Triangular	Beta	Beta 3
2	Parabolic	Beta 4	Beta 4	Pearson V	Pearson V
3	Lognormal	Beta 3	Beta 3	Beta 3	Beta
4	Gamma	Gumbel Maximum	Gumbel Maximum	Exponential	Exponential
5	Cosine	Pearson V	Pearson V	T	T
Rank	P-Value	MAPE %	MAPE %	MAPE %	MAPE %
1	57.75%	0.04%	0.04%	0.15%	0.06%
2	45.00%	0.06%	0.06%	0.14%	0.16%
3	41.65%	0.04%	0.04%	0.15%	0.22%
4	35.15%	0.04%	0.04%	2.14%	2.76%
5	30.08%	0.13%	0.13%	2.30%	2.30%

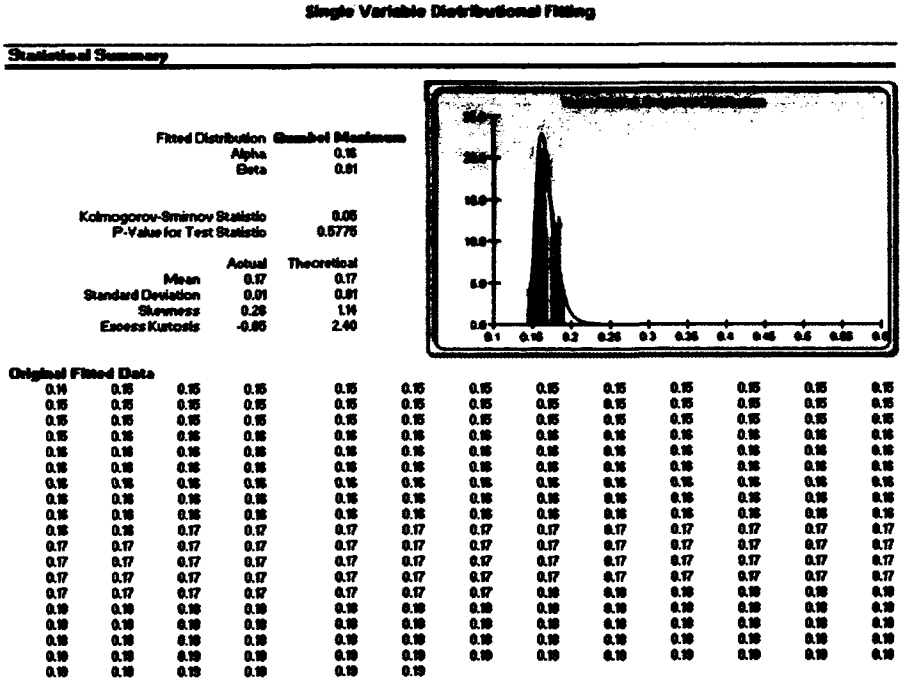

Fig. 5-3. Distribution Fitting Using Nonparametric Kolmogorov-Smirnov Method for Canary Island

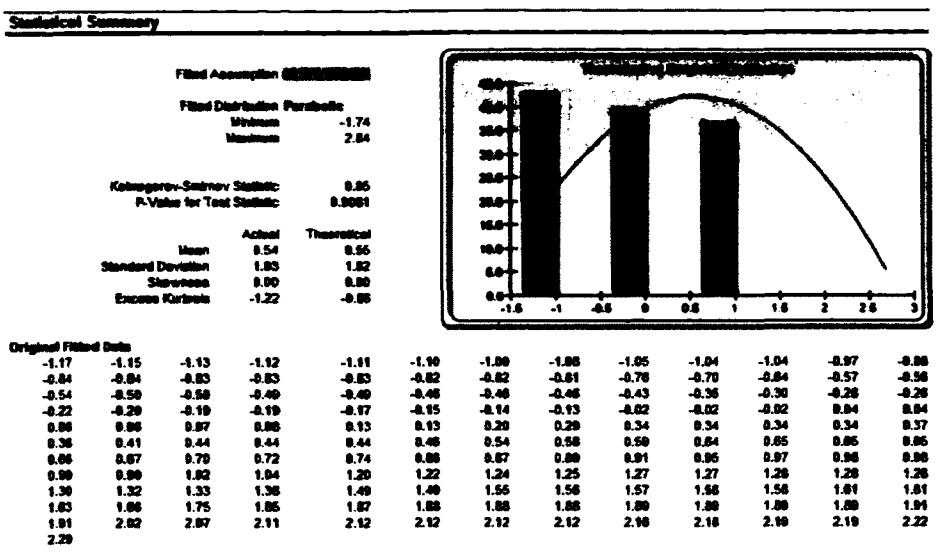

Fig. 5-4. Statistical Summary Using Nonparametric Kolmogorov-Smirnov Method for US Virgin Islands

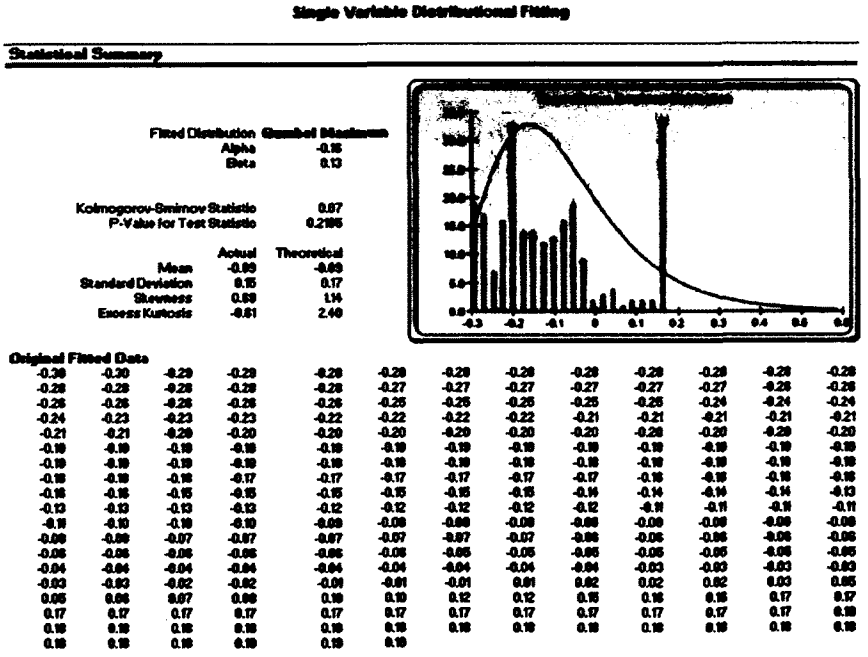

Fig. 5-5. Statistical Summary Using Nonparametric Kolmogorov-Smirnov Method for Huntington Beach

5-3-2- Monte Carlo Formulation

After defining the probability distribution for the SY number, the input variable, the next step is to formulate the outlet length as the design parameter in terms of the SY number. Fig. 5-6 and Table 5-3 show the relationship between the SY number and the outlet length(L). For instance, the outlet length for the seabed slope of 1% can be represented as follows:

$$L = \begin{cases} 0 & SY < 0 \\ -318197\,SY^6 + 221866\,SY^5 - 49793\,SY^4 + 5188.1\,SY^3 - 267.5\,SY^2 + 7.1055\,SY - 0.0251 & 0 < SY < 0.12 \\ 0.0052\,e^{28.126\,SY} & SY > 0.12 \end{cases}$$

Eq. (5.3)

The Monte Carlo Method picks up random numbers from the predefined probability distribution for the SY number which was identified and fitted to using the KS test and calculates the outlet length as shown above. The more random numbers generated, the more accurate the result will be. 5000 random numbers have been generated for this research for that purpose. These random SY numbers generate all the possible outlet lengths.

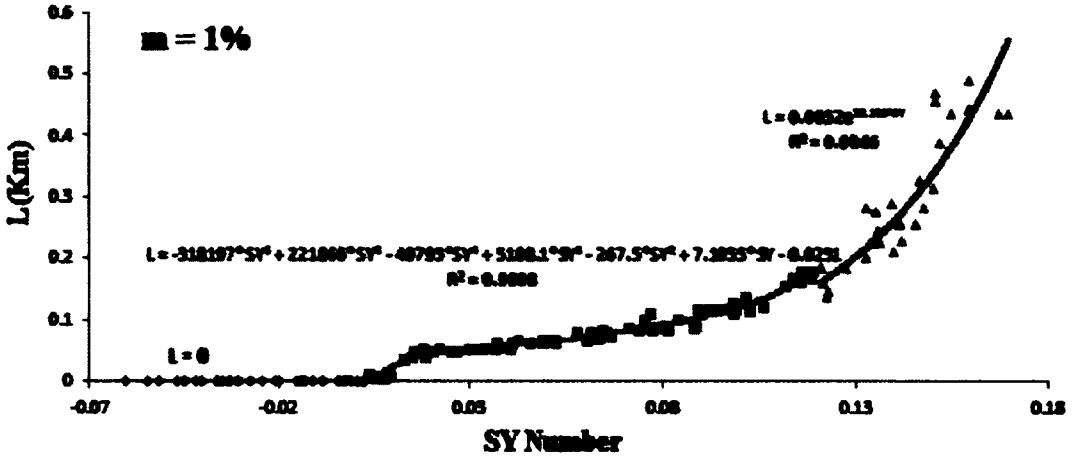

Fig. 5-6. Outlet Length as a Function of SY Number for Near Field Zone with Seabed Slope of 1%

Fig. 5-7, Fig. 5-8, and Fig. 5-9 show the results of the Monte Carlo simulation for three different locations. For example, Fig. 5-7 shows the outlet length with respect to the violation of the 10% law in Tampa Bay. In order to have an outlet with no violation of the 10% law, the outlet length should be at least 2498 meters, which is neither practical nor essential. The 10% law is conservative, and as long as the resultant salinity obeys the 10% law for 83.3% of the time during one tidal cycle then the outlet length is long enough to protect the coastal environment. Based on the results, construction of the outlet is not needed since the 10% law is already in compliance with 0 length of the outlet for 83.3% of the time.

Table 5-3. Outlet length as a Function of SY Number and Seabed Slope

Seabed Slope / SY Range	$M = 1\%$	$M = 2\%$	$M = 3\%$	$M = 4\%$
$SY < 0$	$L = 0$	$L = 0$	$L = 0$	$L = 0$
$0 < SY < 0.12$	$L = -318197*SY^6 + 221866*SY^5 - 49793*SY^4 + 5188.1*SY^3 - 267.5*SY^2 + 7.1055*SY - 0.0251$	$L = -240615*SY^6 + 113639*SY^5 - 20041*SY^4 + 1747.2*SY^3 - 77.382*SY^2 + 1.8433*SY - 0.0076$	$L = 156249*SY^6 - 38744*SY^5 + 3037*SY^4 - 25.888*SY^3 - 5.8747*SY^2 + 0.2785*SY - 0.0013$	$L = 92527*SY^6 - 25217*SY^5 + 2502.4*SY^4 - 99.665*SY^3 + 1.0702*SY^2 + 0.0359*SY - 0.0002$
$SY > 0.12$	$L = 0.0052*e^{28.128*SY}$	$L = 0.0012e^{34.133*SY}$	$L = 0.0001e^{43.514*SY}$	$L = 1E\text{-}5e^{56.882*SY}$

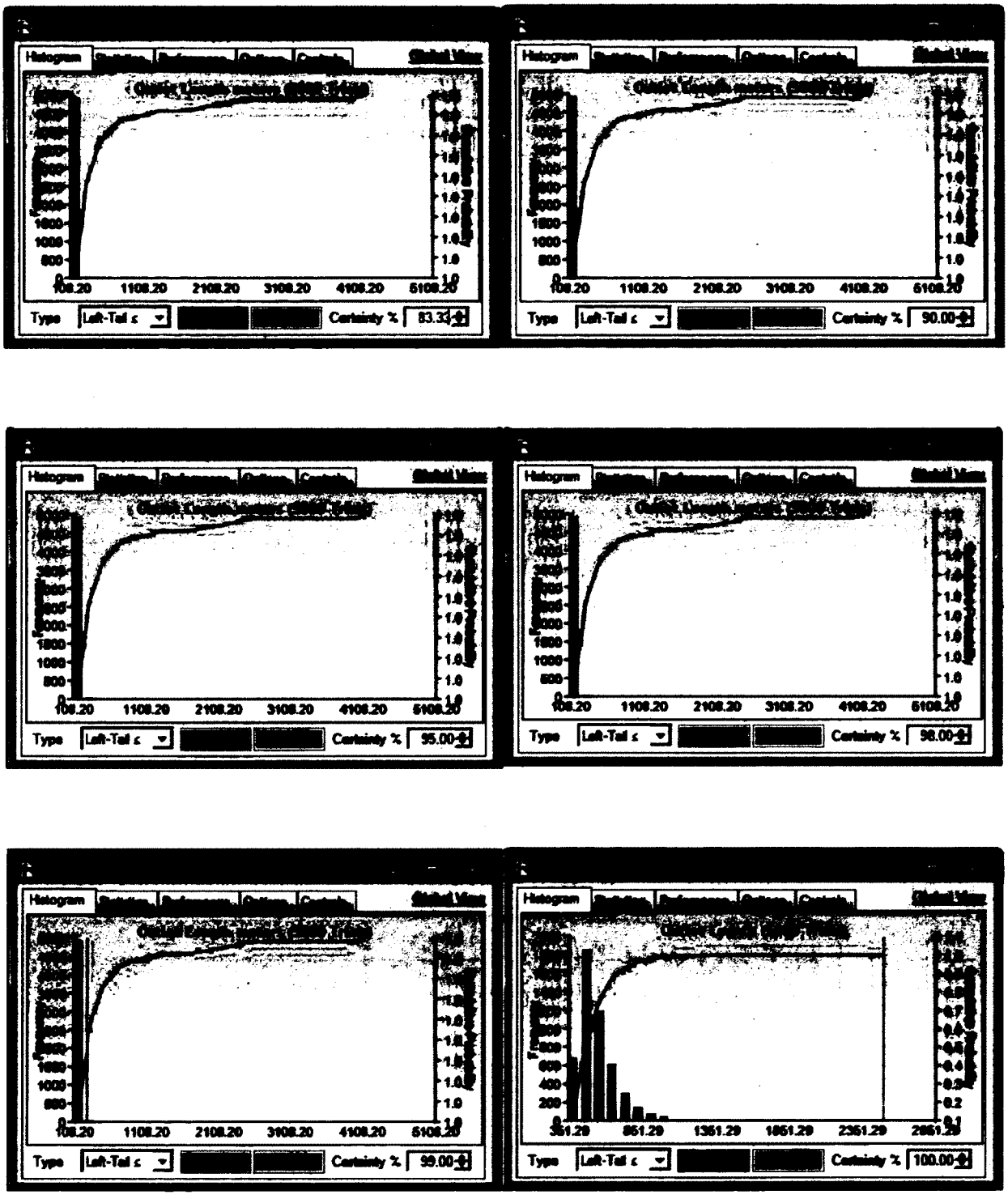

Fig. 5-7. Statistical Summary Using Nonparametric Kolmogorov-Smirnov Method for Tampa Bay

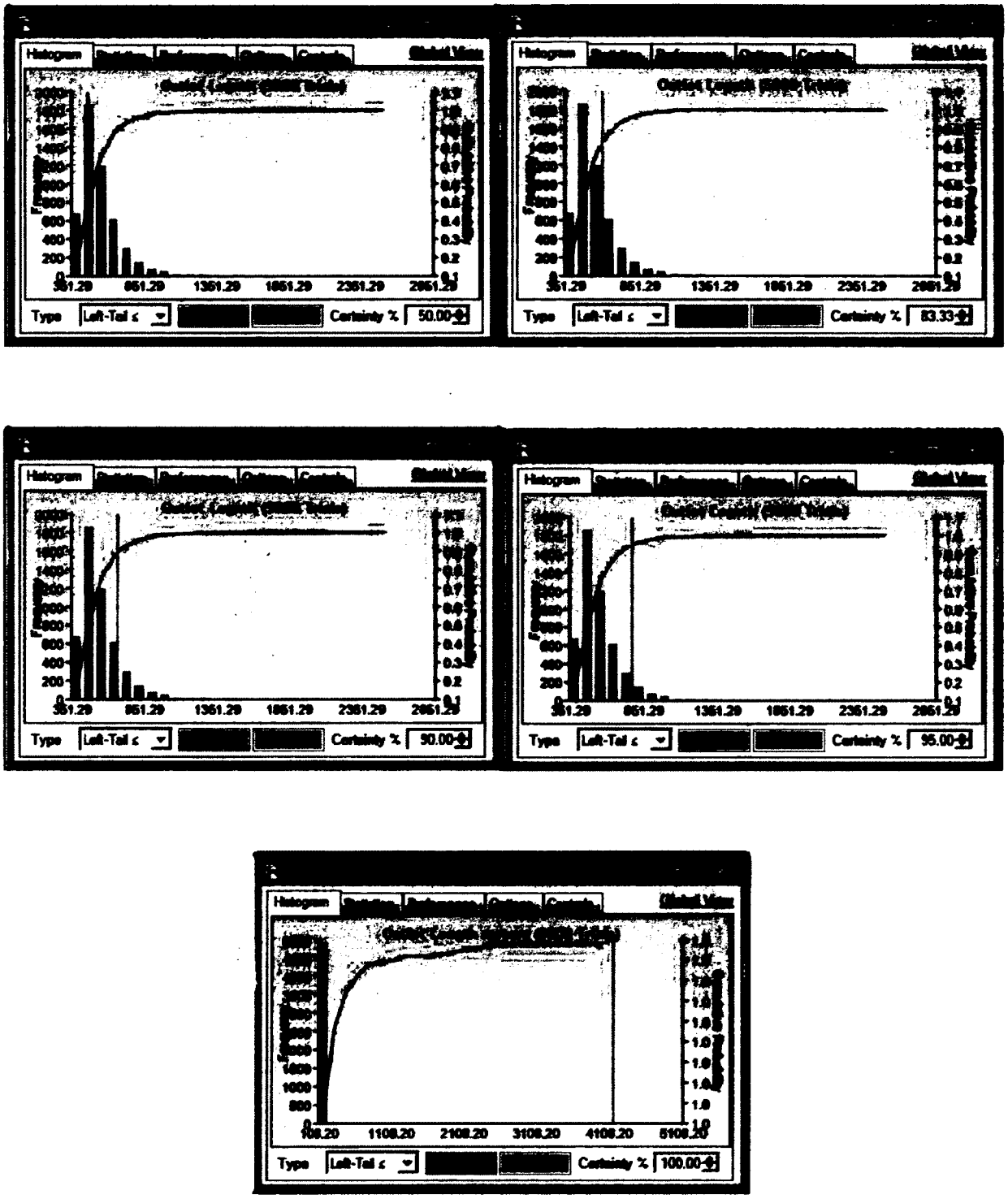

Fig. 5-8. Statistical Summary Using Nonparametric Kolmogorov-Smirnov Method for Kish Island

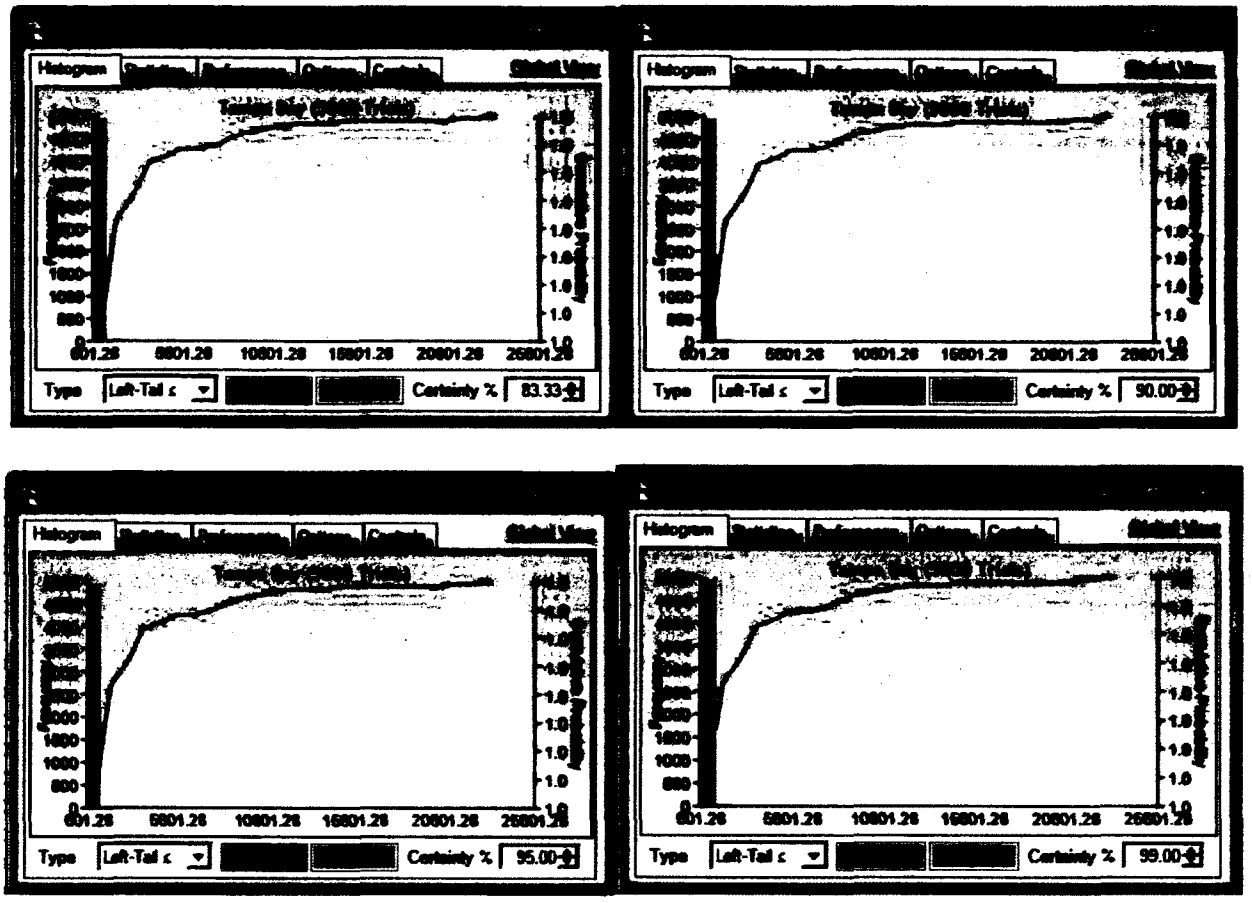

Fig. 5-9. Statistical Summary Using Nonparametric Kolmogorov-Smirnov Method for Tampa Bay (Alternative Location)

Table 5-4. Tampa Bay Risk Analysis Simulation: The Analysis Showed Based on 4 Hours Allowable Exposure Time, no Outlet is Needed.

Violation of 10% CA regulation	Violation in 24 hours	Required Outlet Length (m)
0%	0	2497
1%	0.24 hr	296
2%	0.48 hr	140
5%	1.2 hr	52
10%	2.4 hr	22
16.7%	4 hr	0

Table 5-5. Kish Island Risk Analysis Simulation: The Analysis Showed Based on 4 Hours Allowable Exposure Time an Outlet with 468 Meters length is Needed.

Violation of 10% CA regulation	Violation in 24 hours	Required Outlet Length (m)
0%	0	4161
5%	1.2 hr	778
10%	2.4 hr	674
16.7%	4 hr	607
50%	12 hr	468

Table 5-6. Tampa Bay (alternative location) Risk Analysis Simulation: The Analysis Showed Based on 4 Hours Allowable Exposure Time an Outlet with 130 Meters length is Needed.

Violation of 10% CA regulation	Violation in 24 hours	Required Outlet Length (m)
0%	0	2312
1%	0.24 hr	1417
5%	1.2 hr	360
10%	2.4 hr	200
16.7%	4 hr	130

CHAPTER 6

RESULTS, CONCLUSIONS AND RECOMMENDATIONS

6-1- Results and Conclusions

Two major methodologies, both for the purpose of system analysis and design characterization, were proposed and implemented: the Finite Segment Method (FSM) and the Analytical Method (AM). These methods were used to characterize and simulate the time-variant brine propagation and transport phenomena in estuarine and coastal environments.

AM is a very powerful method that is able to simulate transient plume dispersion with the presence of oscillating flow. It can simply simulate a single outlet of any length. Seabed topography is also reflected by being approximated with a constant slope. Although this method is very easy to use in places with simple topography, which is the case for most coastal areas, it cannot be applied in locations with a complex, locally varying seabed profile. The other disadvantage of AM is the difficulty in simulating complex loading scenarios. Although modeling of a single point load with any outlet length is not a problem in AM, simulating multiple point loads and diffusers is not an easy process and increases the complexity of the problem.

FSM is a very capable method for simulating brine dispersion in tidally influenced environments. This method is capable of simulating brine dispersion with any

complex seabed geometry. The Finite Segment discretization scheme is one of the simplest forms of discretization and does not include the topological nature of partial differential equations. FSM is easy to implement and is capable of simulating spatial and temporal brine dispersion in coastal waters. Its ability to simulate a time dependent response to the brine discharge as well as its simplicity in simulating multiple point loads and diffusers make it a very applicable method in modeling and simulating plume dispersion in coastal areas. Although FSM is a very practical method for solving very complicated plume dispersion problems with complex loading scenarios and seabed geometry, the range of its applicability and limitations must be recognized. Since this method is based on the assumption of a steady state condition and the resultant concentration vector expresses the steady state response, it is necessary to verify whether the steady state assumption is valid for its application.

The Main goal of this research was to determine the valid domain of each method. From this particular research, a new dimensionless number called Shahvari-Yoon (SY) was derived and proposed to represent the mixing characteristics of estuarine and coastal environments as a function of current velocity, dispersion coefficient and tidal characteristics. Using a SY number, applicability of the FSM or AM methods can be tested and verified beforehand to obviate confusion in selecting an appropriate, site-specific flux characterization method.

Using the SY number, the coastal regions were divided into three categories: advective, advective-dispersive and dispersive. These three categories are obtained based on the rate of reaching a steady state. The coastal area is considered advective driven if the steady state is attained in less than 5 lunar days. If the steady condition is obtained in

5 to 15 days, the study area is considered to be advective dispersive. The critical condition is when the steady state is attained in more than 15 lunar days; this describes the dispersive dominant environment. For the Maspalomas desalination plant in the Canary Islands and the Kish Island desalination plant in the Persian Gulf, the steady state was attained after 24 and 27 days. Based on these criteria, the Shahvari-Yoon (SY) number has been derived in terms of influential parameters of λ and υ.

The SY number is set to zero for the convergence time of 5 days which is assumed to be the boundary of advective and advective-dispersive driven environments. Therefore the SY number has been calculated as follows:

$$SY = -\upsilon - 0.0611 \times \lambda + 4.0981.$$

Eq. (6.1)

The SY number is completely capable of representing the mixing characteristics of coastal waters. As shown, the SY number contains both advective and dispersive aspects of mass transport phenomenon, as well as the tidal characteristics of the study area. By using the SY number, describing the mixing features of the study area becomes straightforward and succinct. The convergence time of 15 days, which separates the advective-dispersive category from dispersive driven environments, is equal to a SY number of 0.12. We categorize the three different mixing characteristics as a function of SY as follows:

$$\begin{cases} Advective\ Dominant & SY < 0 \\ Advective - Dispersive & 0 < SY < 0.12 \\ Dispersive\ Dominant & SY > 0.12 \end{cases} .$$

Eq. (6.2)

Corresponding nomographs (Fig. 6-1) for the SY number were also produced to aid the analytical methodology selection process. As shown, the SY number is proficient in describing the mixing features in a succinct and clear way. Regions with high tidal ranges have a negative or small SY number whereas as the tidal range decreases, the SY number increases. For example, in the Persian Gulf and the Mediterranean Sea, with a tidal range of 0.5 ft. and less, the SY number is greater than 0.12. The average SY number for Kish Island in the Persian Gulf with tidal range of 0.5 ft. is 0.16, which represents a highly dispersive condition.

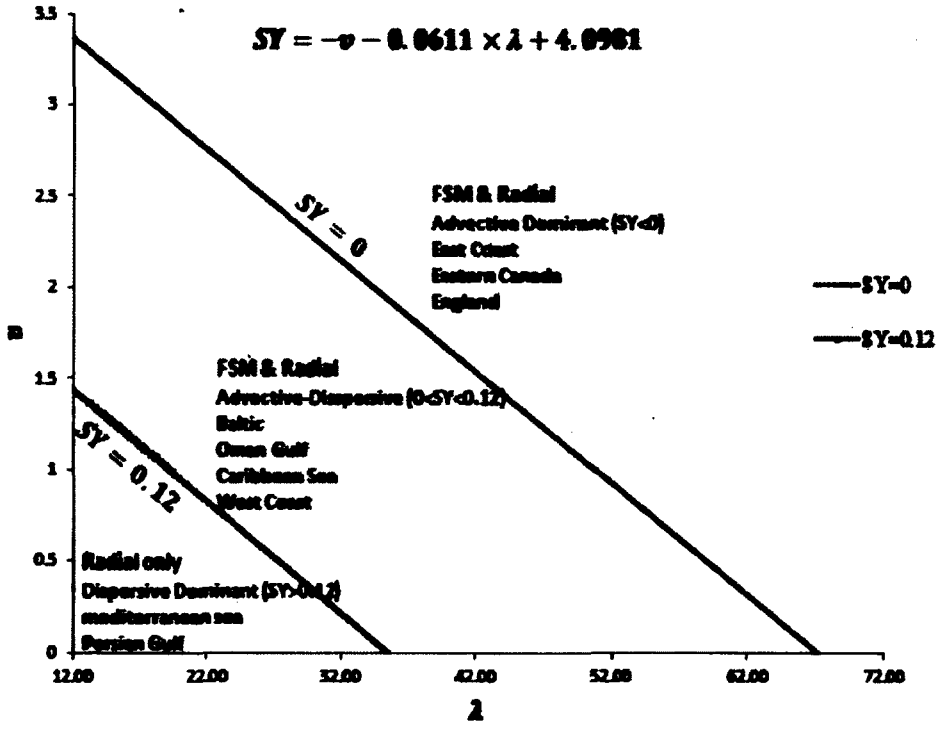

Fig. 6-1. Classification of Mixing Characteristics in Coastal Waters Using SY Number

In addition, four design charts were prepared to simplify and streamline the optimization process for estimating the minimum outlet structure length to discharge the brine plume in an environmentally safe manner jurisdicted by existing regulations for desalination plant design and operation. These charts are presented as a function of the SY number. Since outlets usually discharge the brine in the near-field zone where the slope is typically mild, slopes of 1 to 4 % have been considered when developing these nomographs. Fig. 6-2, Fig. 6-3, Fig. 6-4, and Fig. 6-5 demonstrate the designated nomographs for 1%, 2%, 3% and 4% seabed slopes, respectively. As described earlier, the SQP optimization method and the state of California 10% salinity regulation have been applied for developing these design charts.

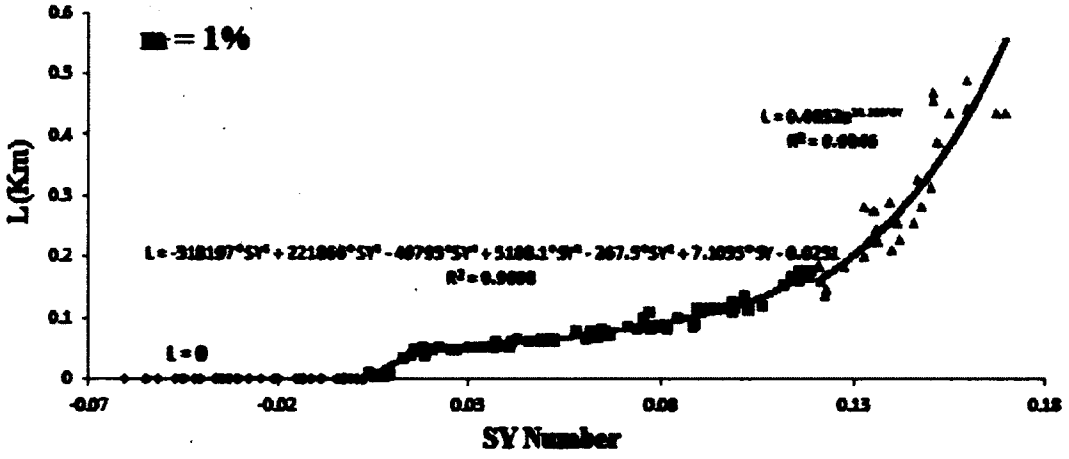

Fig. 6-2. Outlet Length as a Function of SY Number for Near Field Zone with Seabed Slope of 1%

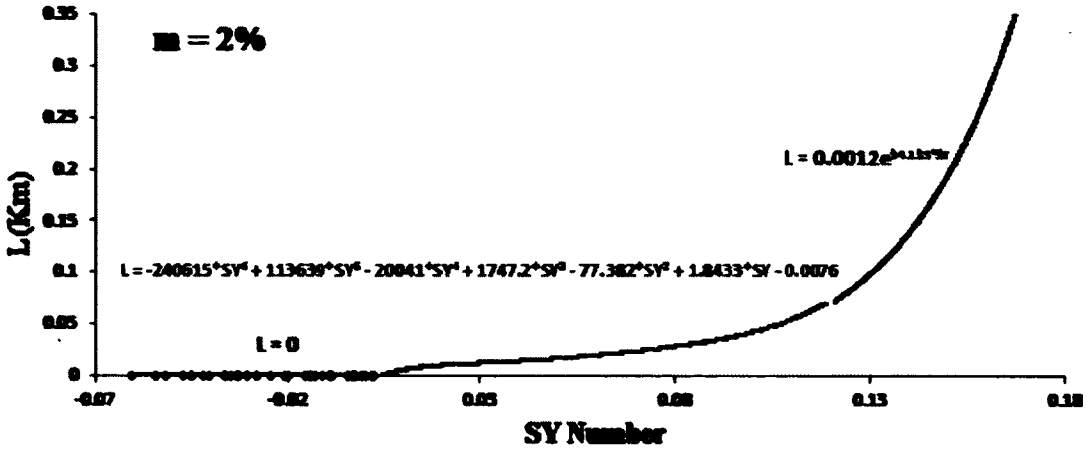

Fig. 6-3. Outlet Length as a Function of SY Number for Near Field Zone with Seabed Slope of 2%

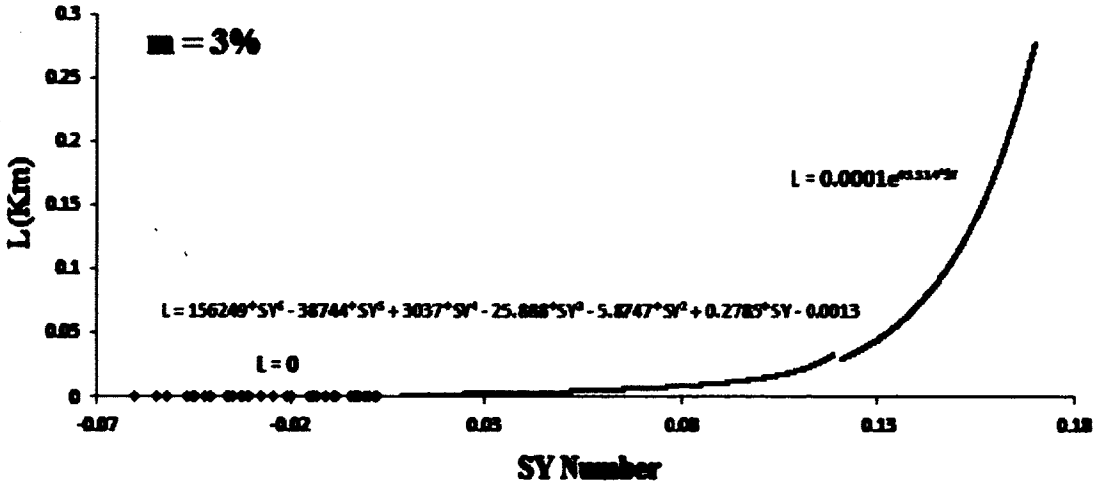

Fig. 6-4. Outlet Length as a Function of SY Number for Near Field Zone with Seabed Slope of 3%

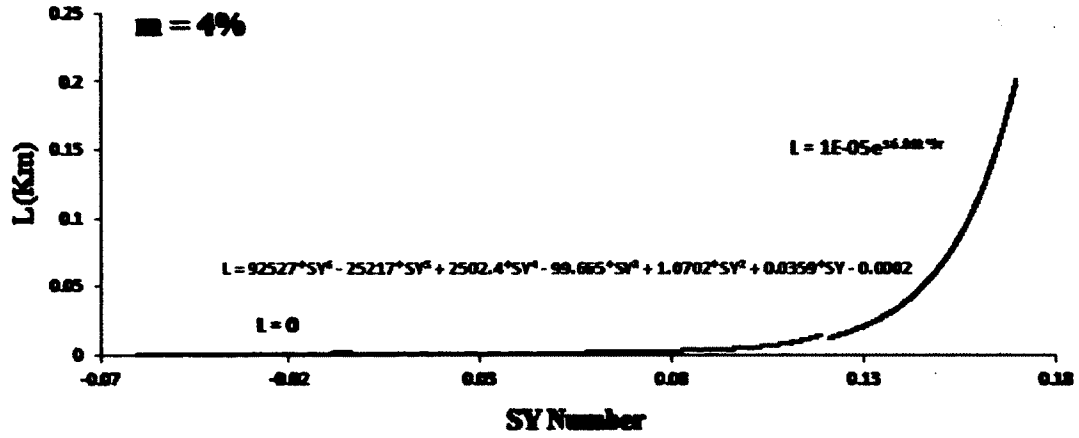

Fig. 6-5. Outlet Length as a Function of SY Number for Near Field Zone with Seabed Slope of 4%

Finally, the 10% law has been revised in a way that firstly and most importantly determines the outlet length, to keep the coastal environment protected from excessive salinity. Secondly, optimizing the outlet length will save millions of dollars. Reflecting these two objectives simultaneously, a risk analysis was performed to solve this constrained optimization problem using Monte Carlo Simulation. The Monte Carlo Simulation result indicated that the California 10% law is conservative and needs to be revised. For example, in Tampa Bay, in order to have an outlet with no violation of the 10% law, the outlet length should be at least 2498 meters which is neither practical nor essential. The 10% law is conservative, and as long as the resultant salinity obeys the 10% law for 83.3% of the time during one tidal cycle the outlet length is long enough to protect the coastal environment. Based on the simulation result, construction of the outlet

is not needed since the 10% law is already in compliance with 0 length of the outlet for 83.3% of the time.

6-2- Recommendations

The methodology represented in this research is applicable for any conservative substances. With some primary changes in governing equations and considering decay and settling terms it can be applied for non-conservative plume dispersion simulation.

A future plan for research is to expand the current conservative salinity plume into a non-conservative substance plume dispersion problem domain in tidally influenced environments. Other future plans include applying FSM and AM for analyzing and characterizing conventional impulse/step loadings from natural and anthropogenic sources to develop a dimensionless number to describe the mixing characteristic in coastal environments and developing design charts to represent the outlet length as a function of the dimensionless number for wastewater treatment plants.

References:

1. Al-Barwani, H.H., & Purnama, A. (2008). Simulating brine plumes discharged into the seawaters. Desalination, 221, 608-613.
2. Doneker, R.L., & Jirka, G.H. (2001). CORMIX-GI systems for mixing zone analysis of brine wastewater disposal. Desalination, 139, 263–274.
3. Fritzmann, C., Löwenberg, J., Wintgens, T., Melin, T. (2007). State-of-the-art of reverse osmosis desalination. Desalination, 216(1–3), 1–76.
4. Graham, J. (2004). Marine biological considerations related to the reverse osmosis desalination project at the Encina power plant, Carlsbad, CA. Submitted to Poseidon Resources.
5. Greenlee, L.F., Lawler, D.F., Freeman, B.D., Marrot, B., Moulin, P. (2009). Reverse osmosis desalination: Water sources, technology, and today's challenges. Water Res., 43(9), 2317–2348.
6. http://outfalls.ifh.uni-karlsruhe.de/database.htm, International Association for Hydro-Environment Engineering and Research (2013).
7. http://www.swrcb.ca.gov/rwqcb9/press_room/announcements/carlsbad_desalination/updates_3_13_09/item_2.pdf ,MacLaggan, Peter M. (2007) Transmittal flow, entrainment, and impingement minimization plan for the Carlsbad seawater desalination project. tech. San Diego: Poseidon Resources Corporation.
8. Iso, S., & Suizu, S., & Maejima, A., (1994). The lethal effect of hypertonic solutions and avoidance of marine organisms in relation to discharged brine from a desalination plant. Desalination 97, 389-399.

18. McConnell, R. (2009), .Tampa Bay seawater desalination Facility. Environmental impact monitoring. Proceedings of 2009 Annual WateReuse Symposium, Seattle, WA, September.

19. Mickley, M. (2009). Treatment of concentrate. Desalination and water purification research and development program report No.155. U.S. Department of the Interior, Bureau of Reclamation, Denver.

20. Miller, E.G., (1960). An introduction to the calculus of Finite Differences and difference equations, Henry Holt, New York.

21. Mooney, C. Z. (1997). Monte carlo simulation. SAGE publications.

22. Mun, J. (2006). Modeling risk, applying Monte Carlo Simulation, real options analysis, forecasting, and optimization techniques. (1st ed.). John Wiley & Sons, Inc.

23. Pedley, T. J. (1975). A thermal boundary layer in a reversing flow. Journal of Fluid Mechanics, 67, 209-250.

24. Pillard, D. A., Dufresne, L. D., Tietge, J. E., & Evans, J. M. (1999). Response of mysid shrimp (mysidopsis bahia), sheepshead minnow. Environmental Toxicology and Chemistry, 18, 430-435.

25. Purnama, A., Al-Barwani, H.H. (2004). Some criteria to minimize the impact of brine discharges into the sea, Desalination, 171, 167–172.

26. Purnama, A., Al-Barwani, H.H. (2006). Spreading of brine waste discharges into the Gulf of Oman. Desalination, 195, 26-31.

27. Purnama, A., et al. (2003). Modeling dispersion of brine waste discharges from a coastal desalination plant. Desalination, 155, 41-47.

28. Purnama, A., Kay, A. (1999). Effluent discharges into tidal waters: optimal or economic strategy. Environmetrics, 10, 601–624.

29. Reynolds, T. et al. (2007) Desalination on San Francisco Bay; Results from the MMWD SWRO pilot program.

30. Shao, D. D., Law, A. W. K., & Li, H. Y. (2008). Brine discharges into shallow coastal waters with mean and oscillatory tidal currents. Journal of Hydro-environment Research, 2, 91-97.

31. Smith, R. 1976 Longitudinal dispersion of a buoyant contaminant in a shallow channel. Journal of Fluid Mechanics, 78, 677-688.

32. Thomann, R. V., (1973). Time variable water quality models, estuaries, harbors and off-Shore waters; in Mathematical Modeling of Natural Systems, Summer Institute in Water Pollution Control, Manhattan College.

33. Thomann, R. V., (1983). Finite Difference approach to estuary water quality analysis, in Quality Models of Natural Water Systems, Twenty-Eighth Summer Institute in Water Pollution Control, Manhattan College.

34. Thomann, R., & Mueller, J. A. (1997). Principles of surface water quality modeling and control.

35. Voutchkov, N., Sommariva, C., Pankratz, T., Tonner, J. (2010). Desalination process technology, in Desalination Technology—Health and Environmental Impacts. CRC Press, Boca Raton.

36. Younos, T. (2005). Environmental issues of desalination. Journal of Contemporary Water Research & Education. 132(1), 11–18.

VITA

Alireza Shahvari, Ph.D.

Old Dominion University, Norfolk, VA
Ph.D. Civil/Environmental Engineering
December 2013
Major: Civil/Environmental Engineering
Dimensionless Criteria for Selecting Tidally-Influenced Advective-Dispersive Desalination Brine Mixing Plume Characterization Models

Shiraz University (Pahlavi University), Shiraz, Iran
M.S. Civil Engineering
June 2007
Major: Civil Engineering (Design of Hydraulic Structures)
Thesis Topic: Pumping Optimization of "Abadeh-Tashk" Coastal Aquifer with Genetic Algorithm

Shiraz University (Pahlavi University), Shiraz, Iran
B.S. Civil Engineering
May 2004
Major: Civil Engineering